

University of Windsor

Scholarship at UWindor

Electronic Theses and Dissertations

Theses, Dissertations, and Major Papers

1-1-1983

STUDIES ON HUMAN ERYTHROCYTE MEMBRANE SURFACE CARBOHYDRATES.

DANTE JAMES CAPALDI
University of Windsor

Follow this and additional works at: <https://scholar.uwindsor.ca/etd>

Recommended Citation

CAPALDI, DANTE JAMES, "STUDIES ON HUMAN ERYTHROCYTE MEMBRANE SURFACE CARBOHYDRATES." (1983). *Electronic Theses and Dissertations*. 7191.
<https://scholar.uwindsor.ca/etd/7191>

This online database contains the full-text of PhD dissertations and Masters' theses of University of Windsor students from 1954 forward. These documents are made available for personal study and research purposes only, in accordance with the Canadian Copyright Act and the Creative Commons license—CC BY-NC-ND (Attribution, Non-Commercial, No Derivative Works). Under this license, works must always be attributed to the copyright holder (original author), cannot be used for any commercial purposes, and may not be altered. Any other use would require the permission of the copyright holder. Students may inquire about withdrawing their dissertation and/or thesis from this database. For additional inquiries, please contact the repository administrator via email (scholarship@uwindsor.ca) or by telephone at 519-253-3000ext. 3208.

CANADIAN THESES ON MICROFICHE

I.S.B.N.

THESES CANADIENNES SUR MICROFICHE



National Library of Canada
Collections Development Branch

Canadian Theses on
Microfiche Service

Ottawa, Canada
K1A 0N4

Bibliothèque nationale du Canada
Direction du développement des collections

Service des thèses canadiennes
sur microfiche

NOTICE

The quality of this microfiche is heavily dependent upon the quality of the original thesis submitted for microfilming. Every effort has been made to ensure the highest quality of reproduction possible.

If pages are missing, contact the university which granted the degree.

Some pages may have indistinct print especially if the original pages were typed with a poor typewriter ribbon or if the university sent us a poor photocopy.

Previously copyrighted materials (journal articles, published tests, etc.) are not filmed.

Reproduction in full or in part of this film is governed by the Canadian Copyright Act, R.S.C. 1970, c. C-30. Please read the authorization forms which accompany this thesis.

THIS DISSERTATION
HAS BEEN MICROFILMED
EXACTLY AS RECEIVED

AVIS

La qualité de cette microfiche dépend grandement de la qualité de la thèse soumise au microfilmage. Nous avons tout fait pour assurer une qualité supérieure de reproduction.

S'il manque des pages, veuillez communiquer avec l'université qui a conféré le grade.

La qualité d'impression de certaines pages peut laisser à désirer, surtout si les pages originales ont été dactylographiées à l'aide d'un ruban usé ou si l'université nous a fait parvenir une photocopie de mauvaise qualité.

Les documents qui font déjà l'objet d'un droit d'auteur (articles de revue, examens publiés, etc.) ne sont pas microfilmés.

La reproduction, même partielle, de ce microfilm est soumise à la Loi canadienne sur le droit d'auteur, SRC 1970, c. C-30. Veuillez prendre connaissance des formules d'autorisation qui accompagnent cette thèse.

LA THÈSE A ÉTÉ
MICROFILMÉE TELLE QUE
NOUS L'AVONS REÇUE



National Library of Canada

Bibliothèque nationale du Canada

CANADIAN THESES ON MICROFICHE

THÈSES CANADIENNES SUR MICROFICHE

2001

NAME OF AUTHOR/NOM DE L'AUTEUR Dante James Capaldi

TITLE OF THESIS/TITRE DE LA THÈSE Studies on human erythrocyte membrane surface carbohydrates

UNIVERSITY/UNIVERSITÉ University of Windsor, Windsor, Ontario

DEGREE FOR WHICH THESIS WAS PRESENTED/GRADÉ POUR LEQUEL CETTE THÈSE FUT PRÉSENTÉE Ph.D.

YEAR THIS DEGREE CONFERRED/ANNÉE D'OBTENTION DE CE GRADE Fall, 1983

NAME OF SUPERVISOR/NOM DU DIRECTEUR DE THÈSE Dr. Keith E. Taylor

Permission is hereby granted to the NATIONAL LIBRARY OF CANADA to microfilm this thesis and to lend or sell copies of the film. *L'autorisation est, par la présente, accordée à la BIBLIOTHÈQUE NATIONALE DU CANADA de microfilmer cette thèse et de prêter ou de vendre des exemplaires du film.*

The author reserves other publication rights, and neither the thesis nor extensive extracts from it may be printed or otherwise reproduced without the author's written permission. *L'auteur se réserve les autres droits de publication; ni la thèse ni de longs extraits de celle-ci ne doivent être imprimés ou autrement reproduits sans l'autorisation écrite de l'auteur.*

DATED/DATÉ 7 July 1983 SIGNED/SIGNÉ Dante J. Capaldi

PERMANENT ADDRESS/RÉSIDENCE FIXE _____

STUDIES ON HUMAN ERYTHROCYTE MEMBRANE
SURFACE CARBOHYDRATES

by
Dante James Capaldi

A Dissertation
Submitted to the Faculty of Graduate Studies through the
Department of Chemistry in Partial Fulfillment
of the requirements for the Degree of
Doctor of Philosophy at the
University of Windsor

Windsor, Ontario, Canada
1983

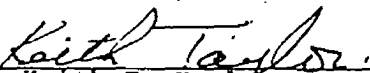
© Dante James Capaldi 1983
All rights reserved

790241

This dissertation has been examined and approved by



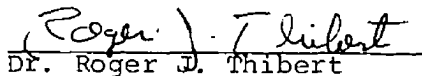
Dr. Mark W. C. Hatton
External Examiner
McMaster University



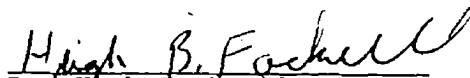
Dr. Keith E. Taylor
Chairman



Dr. Bulent Mutus



Dr. Roger J. Thibert



Dr. Hugh B. Fackrell
Department of Biology

DEDICATION

To my dear parents and fiancée Vilma for their
love and understanding.

ABSTRACT

Studies on Human Erythrocyte Membrane
Surface Carbohydrates

by
Dante James Capaldi

A novel heterobifunctional photolabile crosslinking reagent specific for periodate- or galactose oxidase-generated cell surface aldehydes is presented. The reagent N-(2-nitro-4-azidophenyl)- β -alanine hydrazide had an electronic spectrum consisting of maxima at 255 nm ($\epsilon = 8.5 \text{ mM}^{-1} \text{ cm}^{-1}$) and 465 nm ($\epsilon = 3.0 \text{ mM}^{-1} \text{ cm}^{-1}$) in aqueous solution. The long wavelength maximum was useful for quantitating incorporation into cell surface aldehydes via hydrazone formation.

Sialyl-derivatized membranes in the presence of wheat germ agglutinin, a sialic acid binding lectin, showed no apparent photocrosslinking of sialoglycoproteins with the lectin. However, galactosyl-derivatized membranes in the presence of galactose binding lectins namely, jequity bean (Abrus precatorius) lectin or castor bean (Ricinus communis) lectins type 60 and type 120 or the sialic acid binding lectin wheat germ (Triticum vulgare) agglutinin yielded high molecular weight protein conjugates in sodium dodecyl sulfate polyacrylamide gels suggesting photocrosslinking.

Membrane-bound sialic acid may be quantitated by the colorimetric determination of formaldehyde released upon mild periodate oxidation. In the presence of washed erythrocyte membranes at 20% suspension colorimetry based on 3-methyl-2-benzothiazolinone hydrazone has an extinction coefficient of $68.5 \pm 0.1 \text{ mM}^{-1} \text{ cm}^{-1}$. With intact erythrocytes large losses in color yield are experienced with suspensions in excess of 2% (2×10^8 cells/ml).

Hydrogen peroxide in the presence of horseradish peroxidase effects the oxidative coupling of 3-methyl-2-benzothiazolinone hydrazone with its formaldehyde azine to form a tetraazapentamethine dye. The blue chromophore, when formed at pH 3.5 and quenched with acetone or 1N hydrochloric acid, has an extinction coefficient of 69 ± 2 or $55 \pm 2 \text{ mM}^{-1} \text{ cm}^{-1}$, respectively. This chromogen system has been adapted for enzymatic determinations of hydrogen peroxide and of glucose in the 10 to 45 nanomole range, choline in the 5 to 20 nanomole range and galactose in the 63 to 250 nanomole range.

ACKNOWLEDGEMENTS

I wish to express my sincere gratitude to my advisor Dr. Keith E. Taylor for his ever-continuing patience, professional advice, direction and guidance throughout my stay in the Department of Chemistry. The many discussions and consultations with him has facilitated a broader and deeper understanding of biochemistry not only as a science but as an art.

A special thanks and sincere debt of gratitude to Dr. Hugh B. Fackrell for his helpful discussions on cell surface biochemistry.

I would also like to express my appreciation to Drs. Bulent Mutus, Roger J. Thibert and Norman F. Taylor for their positive and encouraging contributions towards my study of biochemistry.

I wish to acknowledge and express my sincere thanks to the University of Windsor for their financial support provided in the form of a Post-Graduate Scholarship and Teaching Assistantship.

The present study was supported by operating grants from the Natural Sciences and Engineering Research Council of Canada.

TABLE OF CONTENTS

| | |
|---|-----|
| DEDICATION. | iv |
| ABSTRACT. | v |
| ACKNOWLEDGEMENTS. | vii |
| LIST OF FIGURES | xi |
| LIST OF TABLES. | xiv |
| ABBREVIATIONS | xv |
| CHAPTER | |
| I. INTRODUCTION. | 1 |
| The Historical Development of the Fluid Mosaic Model of the Plasma Membrane. | 1 |
| Lipid and Protein Arrangement in the Human Erythrocyte Membrane | 8 |
| Glycophorin-A: Structure and Function. | 14 |
| Chemical Techniques in N-Acetylneuraminic Acid Determination | 28 |
| Characterization of Glycophorin-A by Assorted Techniques. | 33 |
| Potential Use of Peroxidase Color Reactions in the Determination of Cell Surface Carbohydrates via Hydrogen Peroxide. | 40 |
| Usefulness of Macromolecules Including Plant Lectins in Investigating Cell Surface Receptor Function. | 46 |
| Application of Photoaffinity Labeling in Biological Systems | 50 |
| Approaches Taken in the Present Study | 62 |
| II. EXPERIMENTAL. | 64 |
| Materials and Apparatus. | 67 |
| Reagents | 67 |
| Procedures | 70 |
| Standard Procedure (a) for Formaldehyde | 70 |
| Standard Procedure (b) for Formaldehyde | 70 |
| Periodate-treated Erythrocytes. | 70 |
| Erythrocyte Hemolysate. | 71 |
| Periodate-treated Erythrocyte Ghosts. | 71 |
| Formaldehyde-treated Erythrocytes or Ghosts. | 72 |

| | |
|--|-----|
| Determination of Optimal Enzyme Activity, and Incubation Time for Enzymatic Determination of Hydrogen Peroxide, Glucose, Galactose and Choline. | 72 |
| Standard Procedure (a) for Hydrogen Peroxide | 73 |
| Standard Procedure (b) for Hydrogen Peroxide | 74 |
| Standard Procedure for Glucose. | 74 |
| Standard Procedure for Galactose. | 74 |
| Standard Procedure for Choline. | 75 |
| Galactose Oxidase Treatment of Cell Surface Carbohydrates. | 75 |
| Neuraminidase Treatment of Cell Surface Carbohydrates. | 76 |
| Hemagglutination Assays | 76 |
| Synthesis of 2-nitro-4-azidofluorobenzene (F-NAP). | 76 |
| Synthesis of N-(2-nitro-4-azidophenyl)- β -alanine (NAPBA). | 76 |
| Synthesis of N-(2-nitro-4-azidophenyl)- β -alanine methyl ester (NAPBAME) | 77 |
| Synthesis of N-(2-nitro-4-azidophenyl)- β -alanine hydrazide (NAPBAH) | 77 |
| Incorporation of N-(2-nitro-4-azidophenyl)- β -alanine hydrazide into Cell Surface Periodate- and Galactose Oxidase-Generated Aldehydic Groups | 78 |
| Photolysis Experiments. | 79 |
| Polyacrylamide Gel Electrophoresis. | 82 |
| III. RESULTS AND DISCUSSION. | 84 |
| A New Peroxidase Color Reaction. | 84 |
| A simplified Procedure for the Determination of Cell Surface Sialic Acid | 121 |
| Preparation of a Novel Photolabile Heterobifunctional Crosslinking Reagent and its Biological Application | 134 |
| IV. CONCLUSIONS | 178 |

| | |
|-------------------------|-----|
| APPENDIX. | 181 |
| REFERENCES. | 183 |
| VITA AUCTORIS | 197 |

LIST OF FIGURES

| <u>Figure</u> | | <u>Page</u> |
|---------------|--|-------------|
| 1. | The Fluid Mosaic Model of the Plasma Membrane Lipid Bilayer. | 3 |
| 2. | Arrangement of Integral and Peripheral Proteins in the Lipid Bilayer. | 7 |
| 3. | Erythrocyte Membrane Organization. | 11 |
| 4. | Electrophoretic Distribution of Human Erythrocyte Membrane Sialoglycoproteins . | 13 |
| 5. | The Primary Structure of Glycophorin-A | 17 |
| 6. | N- and O- Carbohydrate-Peptide Linkages in Glycoproteins. | 20 |
| 7. | Carbohydrate Sequence of the O-Glycosidically Linked Tetrasaccharides on Glycophorin-A. | 22 |
| 8. | Carbohydrate Sequence of the Complex N-Glycosidically Linked Oligosaccharide on Glycophorin-A. | 24 |
| 9. | Schematic Illustration of Glycophorin-A Arrangement in the Human Erythrocyte Membrane. | 27 |
| 10. | Sodium Metaperiodate Oxidation of Erythrocyte Surface N-Acetylneuraminic Acid. | 32 |
| 11. | Tritium Labeling of Cell Surface Sialyl Residues. | 35 |
| 12. | Tritium Labeling of Cell Surface Galactosyl Residues | 42 |
| 13. | Galactose Oxidase Treatment of Erythrocyte Surface Galactosyl Residues | 44 |
| 14. | Typical Precursors Generating Highly Reactive Electrophilic Intermediates. . . | 57 |

| <u>Figure</u> | <u>Page</u> |
|--|-------------|
| 15. Possible Reactions Involving Nitrenes. . . . | 60 |
| 16. Photolysis Vessel. | 81 |
| 17. Oxidative Coupling of 3-Methyl-2-Benzo- thiazolinone Hydrazone with its Azine Generating the Blue Chromophore | 86 |
| 18. Spectra of the Quenched Reaction Mixtures. . | 89 |
| 19. Influence of pH on Chromophore Formation . . | 91 |
| 20. Influence of Peroxidase Concentration on Chromophore Formation and Stability . . . | 96 |
| 21. Standard Curve for Hydrogen Peroxide | 101 |
| 22. Glucose Oxidase Treatment of D-Glucose . . . | 104 |
| 23. Influence of Glucose Oxidase Concentration on Chromophore Formation and Stability in the Coupled Glucose Oxidase- Peroxidase System | 106 |
| 24. Standard Curve for Glucose | 110 |
| 25. Choline Oxidase Treatment of Choline | 113 |
| 26. Chromophore Formation in the Stepwise Choline Oxidase-Peroxidase Reaction . . . | 115 |
| 27. Chromophore Formation and Stability in the Stepwise Choline Oxidase-Peroxidase System. | 117 |
| 28. Standard Curve for Choline | 119 |
| 29. Chromophore Development in the Stepwise Galactose Oxidase-Peroxidase System . . . | 123 |
| 30. Chromophore Development and Stability in the Stepwise Galactose Oxidase- Peroxidase System | 125 |
| 31. Standard Curve for Galactose | 127 |

| <u>Figure</u> | <u>Page</u> |
|---|-------------|
| 32. Formaldehyde Determination Using the MBTH Test. | 130 |
| 33. Syntheses of Azido-containing Reagents. . . | 136 |
| 34. Photolysis of N-(2-Nitro-4-Azidophenyl)- β -Alanine Hydrazide in Methanol. | 138 |
| 35. Photolysis of N-(2-Nitro-4-Azidophenyl)- β -Alanine Hydrazide in Aqueous Buffer. . . | 140 |
| 36. Incorporation of N-(2-Nitro-4-Azidophenyl)- β -Alanine Hydrazide Onto Erythrocyte Membrane Surface Sialyl Residues | 144 |
| 37. Incorporation of N-(2-Nitro-4-Azidophenyl)- β -Alanine Hydrazide Onto Erythrocyte Membrane Surface Galactosyl or N-Acetylgalactosaminyl Residues. | 146 |
| 38. Hydrolysis of Glycoconjugate-containing Sialyl Residues with Neuraminidase . . . | 150 |
| 39. Spectrum of Reagent-Derivatized Erythrocyte Ghosts Solubilized in Sodium Dodecyl Sulfate. | 153 |
| 40. Protein and Glycoprotein Stained Gel Via the Silver Stain | 166 |
| 41. Proteins Stained Via Coomassie Blue | 168 |
| 42. Proposed Route of Photoincorporation of D-Galactosyl-Derivatized Glycoproteins Into Galactose Binding Lectins | 171 |
| 43. Sialoglycoproteins Stained Via Dansyl Hydrazine | 175 |

LIST OF TABLES

| <u>Table</u> | | <u>Page</u> |
|--------------|--|-------------|
| 1. | Color Yield for Coupling of MBTH and its Azine as a Function of Reagent Concentration and Ratio. | 92 |
| 2. | Influence of Peroxidase Concentration on Chromophore Formation. | 98 |
| 3. | Standard Curve Data for Hydrogen Peroxide | 99 |
| 4. | Extent of Reagent Incorporation onto Erythrocyte Membrane Surfaces of Various Chemical or Enzymic Treatment. . | 147 |
| 5. | Extent of Membrane-Bound Reagent Released by Nucleophiles. | 154 |
| 6. | Theoretical and Observed Apparent Molecular Weights of the Membrane-Lectin Conjugates . | 172 |

ABBREVIATIONS

| | |
|---------------|---|
| A | absorbance |
| Å | angstrom |
| BSA | bovine serum albumin |
| cm | centimeter |
| DMSO | dimethylsulfoxide |
| esr | electron spin resonance |
| FITC | fluorescein isothiocyanate |
| F-NAP | 4-azido-2-nitrofluorobenzene |
| g | gravitational force ($9.8 \text{ m}\cdot\text{s}^{-2}$) |
| HDCBS | 2-hydroxy-3, 5-dichlorobenzene sulfonate |
| IR | infrared |
| ϵ | extinction coefficient at maximum absorption |
| μM | micromolar |
| mg | milligram |
| mM | millimolar |
| NAP | 2-nitro-4-azidophenyl |
| NAPBA | N-(2-nitro-4-azidophenyl)- β -alanine |
| NAPBAME | N-(2-nitro-4-azidophenyl)- β -alanine methyl ester |
| NAPBAH | N-(2-nitro-4-azidophenyl)- β -alanine hydrazide |
| nm | nanometer |
| NMR | nuclear magnetic resonance |
| PAS | periodic acid Schiff |
| PBS | phosphate buffered saline |

rpm revolutions per minute

RCA₆₀ Ricinus communis agglutinin type II

RCA₁₂₀ Ricinus communis agglutinin Type I

SDS sodium dodecyl sulfate

SDS-PAGE sodium dodecyl sulfate polyacrylamide gel
 electrophoresis

UV ultraviolet

Ours is a strange profession
We who trap the cells where life beats
And strike them on a diamond
Transmuting them to flakes of gold and silver
Which sparkle as they float upon the water
And we coarse fishermen
Catch them in our little nets

We speak to them by hurling at them
Elemental particles
And they answer in a language
That we can only vaguely understand. . .

- D. L. Ringo

STUDIES ON HUMAN ERYTHROCYTE MEMBRANE
SURFACE CARBOHYDRATES

CHAPTER I

INTRODUCTION

The Historical Development of the Fluid Mosaic Model of the Plasma Membrane

The living cell is contained by a membrane which provides a number of important functions. The membrane acts as a structural barrier maintaining the integrity of the cell. Further, it allows for the passage of molecules into and out of the cell. The advancement of the study of membranes is attributable to the development of model bilayer membrane systems formed by dispersing phospholipids or other amphipathic lipids in an aqueous medium. Insertion of proteins into these lipid bilayers allows further study of the protein-lipid-membrane complex. The most commonly cited hypothesis is the fluid mosaic model proposed by Singer and Nicolson (1) shown in Figure 1. However, the first significant attempt to illustrate the organization of membranes on a molecular level was in 1935 by Danielli and Davson (2). Their model of membrane structure showed two layers of phospholipid molecules with the hydrophobic non-polar acyl chains facing each other

Figure 1

The Fluid Mosaic Model of the Plasma
Membrane Lipid Bilayer

Legend

Schematic three-dimensional view of the lipid-globular protein mosaic model as proposed by Singer and Nicolson (1). The large irregular bodies present within the lipid matrix are globular integral proteins. Drawing from Clark and Switzer (3).

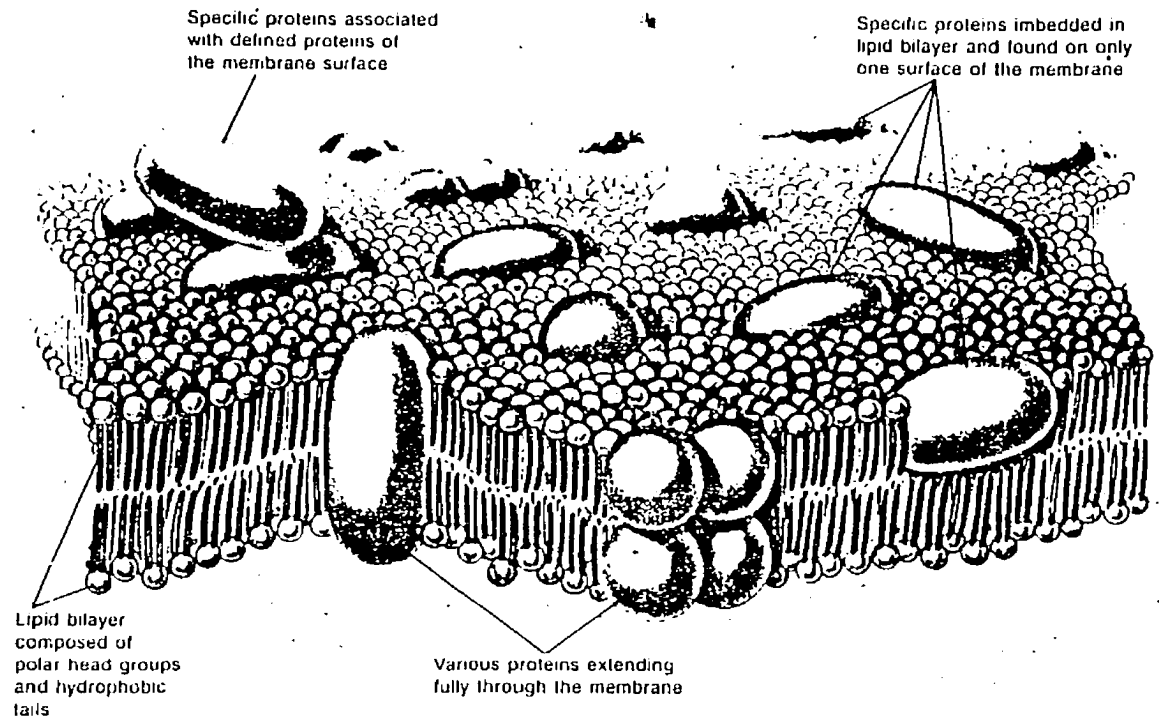


Figure 1

inside the membrane. At the surface of this bilayer consisting of the hydrophilic polar phosphate-containing heads are found globular proteins which were thought to be electrostatically associated with the phospholipids. This membrane model was constructed on the foundation of lipid function and to a lesser degree on protein behaviour. With the advent of electron microscopy Robertson studied cellular membranes and proposed a three-layered membrane of 75 Å thickness (4). He extended the studies of Danielli and Davson providing a more elaborate and detailed structure of the unit membrane model which retained the lipid bilayer and included a single layer of protein molecules arranged in a β -sheet formation associated with both surfaces of the bilayer as opposed to their existence in globular form.

Increased skepticism and objections to this model ranging from gross malpreparation of cells to insufficient information accounting for differential extraction of membrane proteins from lipid components led others, such as Singer and Nicolson and Green and Capaldi (5,6) to reexamine lipid-protein, lipid-lipid and protein-protein interactions. Their investigations provided new models in illustrating that protein molecules are dynamic and were arranged non-uniformly in the lipid matrix contrary to the postulation of Robertson. The fluid mosaic model as described by

Singer and Nicolson (1) illustrates the significance of the lipid bilayer in maintaining the framework of the membrane. Further, proteins which are embedded or attached to the bilayer (see Figure 1) are capable of interacting with each other and with lipid, and are capable of moving laterally in the lipid phase. They also postulated that protein-protein, lipid-protein and lipid-lipid interactions account for membrane structure and dynamics. In contrast, Green and Capaldi suggested that the predominant interactions contributing to membrane integrity are the protein-protein interactions.

Singer and Nicolson (1) discussed two types of non-covalent interactions (hydrophilic and hydrophobic) and stressed their importance in maintaining a stable conformation in a minimum free-energy state. The integral proteins are believed to be held in place by strong hydrophobic and/or hydrophilic interactions and thus are more difficult to remove from the bilayer than peripheral proteins (Figure 2). It was further postulated that no protein is completely embedded within the lipid matrix.

The erythrocyte membrane is one of the most exploited and well understood membrane systems (7-9) and thus provides a defined model system for further study of cell surface glycoprotein function. This dissertation takes

Figure 2

Arrangement of Integral and Peripheral
Proteins in the Lipid Bilayer

Legend

Schematic representation of the arrangement of trans-
membrane and peripheral polypeptides in the bilayer.

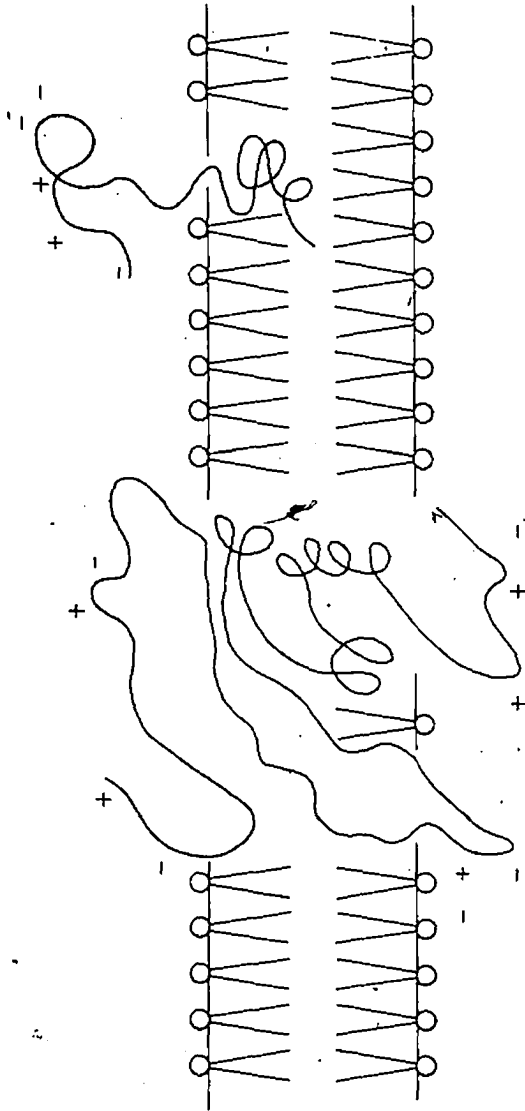


Figure 2

advantage of this well understood system and focuses on the further characterization of erythrocyte glycoproteins. In the following pages a review of relevant erythrocyte membrane components is given in order to introduce the problem addressed by this dissertation.

Lipid and Protein Arrangement in the Human Erythrocyte Membrane

Contained in the lipid bilayer are the phospholipids, phosphatidyl-choline, -ethanolamine, and -serine and the sphingolipid, sphingomyelin. Studies with specific phospholipases (10,11) and other reagents (12-14) have shown that these phospholipids are distributed asymmetrically in specific halves of the membrane bilayer. The outer half of the human erythrocyte membrane contains 65-75% of the total phosphatidylcholine and 80-85% of the total sphingomyelin while 80-90% of the total phosphatidyl-ethanolamine and -serine are found in the inner portion of the lipid bilayer. Cholesterol also exists in the lipid bilayer in equimolar amounts with phospholipids distributed throughout both halves of the bilayer (15), however, its arrangement in erythrocyte membrane remains to be determined (16).

The normal human erythrocyte membrane also contains at least one hundred different asymmetrically organized polypeptides (17). The best characterized proteins are depicted

in Figure 3. Exposed at the cell surface are glycoproteins and they, along with glycolipids, have antigenic properties which confer blood group specificity. Since membrane proteins have a tendency to become denatured or aggregated it is sometimes difficult to isolate and study them apart from the membranes. One technique, used for molecular weight determination, consists of solubilization of the whole membrane in sodium dodecyl sulfate followed by polyacrylamide gel electrophoresis (SDS-PAGE) (18). The respective groups or bands of proteins detected by Coomassie blue stain are denoted according to the classification of Fairbanks et al. (19) shown in Figure 4a. In this procedure molecular weight is empirically correlated with electrophoretic mobility. The utilization of SDS-PAGE on plasma membrane proteins (suspended in SDS) yields six prominent bands and at least thirty-five less intense bands ranging in molecular weight from 10,000-300,000 (20). In Figure 3, the most prominent proteins are diagrammatically shown with respect to their position in the membrane. Here the polypeptides sialoglycoprotein (PAS 1) and glycoprotein (band 3) are known as intrinsic or integral proteins because they are embedded within the membrane (21). The network of proteins which aid in the lamination of the cytoplasmic side of the membrane to form the cytoskeleton include spectrin (bands 1 and 2,

Figure 3

Erythrocyte Membrane Organization

Legend

The major transmembrane protein band 3, a heterogeneous array of glycoproteins, may exist as a dimer or tetramer. This group of proteins is thought to be involved in anion transport (11). A particular group of glycoproteins PAS(1)₂ known as glycophorin exists as a dimer and has been extensively characterized (9,12). At the cytoplasmic surface these glycoproteins are associated with other proteins such as band 2.1 (ankyrin) and band 6 (glyceraldehyde 3-phosphate dehydrogenase). The primary point of attachment of the cytoskeletal proteins, bands 1 and 2, occurs at band 2.1. These spectrin tetramers are joined together forming a mesh framework by short filaments of F-actin (band 5) and another protein band 4.1. Diagram reproduced from Mueller and Morrison (22).

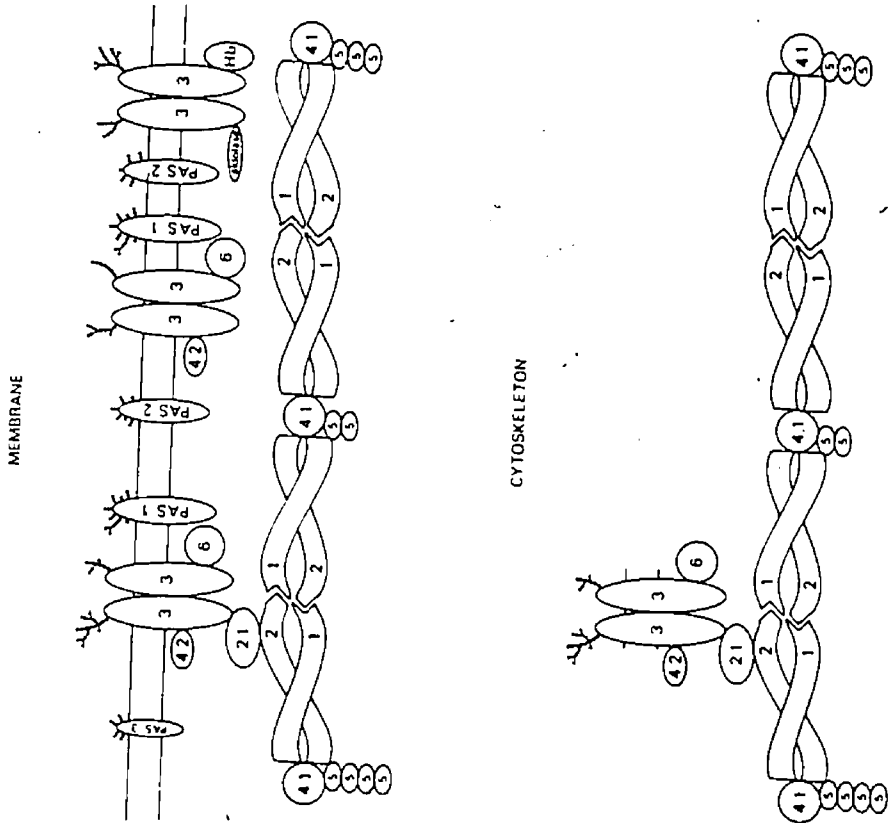


Figure 3

Figure 4

Electrophoretic Distribution of Human Erythrocyte
Membrane Sialoglycoproteins

Legend

^a Coomassie blue staining of solubilized erythrocyte membranes on a 7.5-15% linear gradient of acrylamide (24).

^b Periodic acid Schiff staining of solubilized erythrocyte membranes on a linear 12-20% gradient of acrylamide reveals the presence of three different sialoglycopeptides PAS 1, 2, and 3. Both PAS 1 and 3 occur as dimers (PAS(1)₂ and PAS(3)₂, respectively. A complex consisting of PAS 1 and 3 also occurs (22).

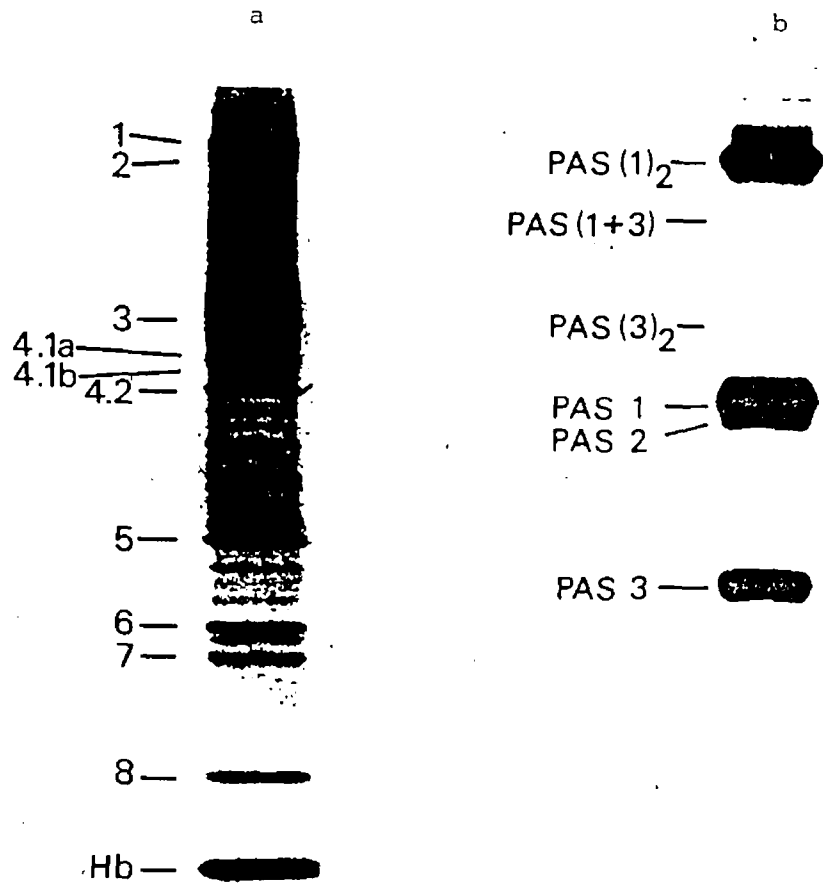


Figure 4

together comprise spectrin) which exist as tetramers with apparent molecular weights of 240,000 and 215,000, respectively, F-actin (band 5) with a molecular weight of 43,000 and band 4.1 with a molecular weight of 80,000. According to Marchesi (23) and Clarke (24) these major polypeptides are removed from the membrane by aqueous solutions containing chelating and reducing agents. The integral or hydrophobic transmembrane proteins are clearly distinct from the cytoskeletal polypeptides.

Glycophorin-A: Structure and Function

The human erythrocyte membrane glycoproteins are divided into two classes distinguished by the amounts of sialic acid present in the carbohydrate fraction. The major membrane protein band 3, which constitutes one group of glycoproteins in the 90,000 molecular weight range contains little or no sialic acid (17). This group of polypeptides has been shown to be involved in anion transport (25). The carbohydrate portion on band 3 has primarily terminal galactosyl residues (26,27) as opposed to the sialoglycoproteins, which have N-acetylneuraminic acid as their terminal carbohydrate (28). It was initially believed that the group of sialoglycoproteins was homogeneous, i.e., comprised of a single polypeptide as described by Winzler (29) and Marchesi (30). These sialoglycoproteins, which can be identified using the classical periodic acid Schiff (PAS) staining procedure (31), are

composed of several minor polypeptides (PAS 2, 2' and 3) and a major polypeptide (PAS 1) (32-34), also known as glycophorin-A, which contains 60% of the total erythrocyte sialic acid (34) (Figure 4b). Glycophorin-A migrates on SDS-PAGE gels both as a monomer PAS 1 and as a dimer $PAS(1)_2$ with an apparent molecular weight of 85,000 (34,35). PAS band 2 has been recently described, identified and named glycoconnectin (22) as it appears to interact with the cytoskeletal core (36). The other two minor sialoglycoproteins PAS bands 2' and 3, which together contain 10% of the total erythrocyte sialic acid, require further characterization, however, they have been tentatively named glycophorin-C and -B, respectively. PAS band 3 also migrates as a monomer PAS 3 and as a dimer $PAS(3)_2$ in SDS-PAGE gels, whereas, PAS bands 2' and 2, which migrate identically, exist as monomers. Another complex, a heterodimer, $PAS(1+3)$, composed of both PAS 1 and PAS 3 has also been observed.

Glycophorin-A, as a monomer, contains one hundred and thirty-one amino acids and sixteen oligosaccharide side chains as illustrated in Figure 5. It is the most characterized of the integral membrane proteins in the human erythrocyte membrane with a molecular weight of 31,000 (8), 60% of which is carbohydrate (28,30,37). Fifteen carbohydrate side chains are O-glycosidically linked and one is N-glycosi-

Figure 5

The Primary Structure of Glycophorin-A

Legend

The amino acid sequence of the major sialoglycoprotein of the human erythrocyte membrane is presented. Each of the fifteen serine or threonine residues are linked to a tetrasaccharide. Linked to the asparagine residue is a complex undecasaccharide (23).

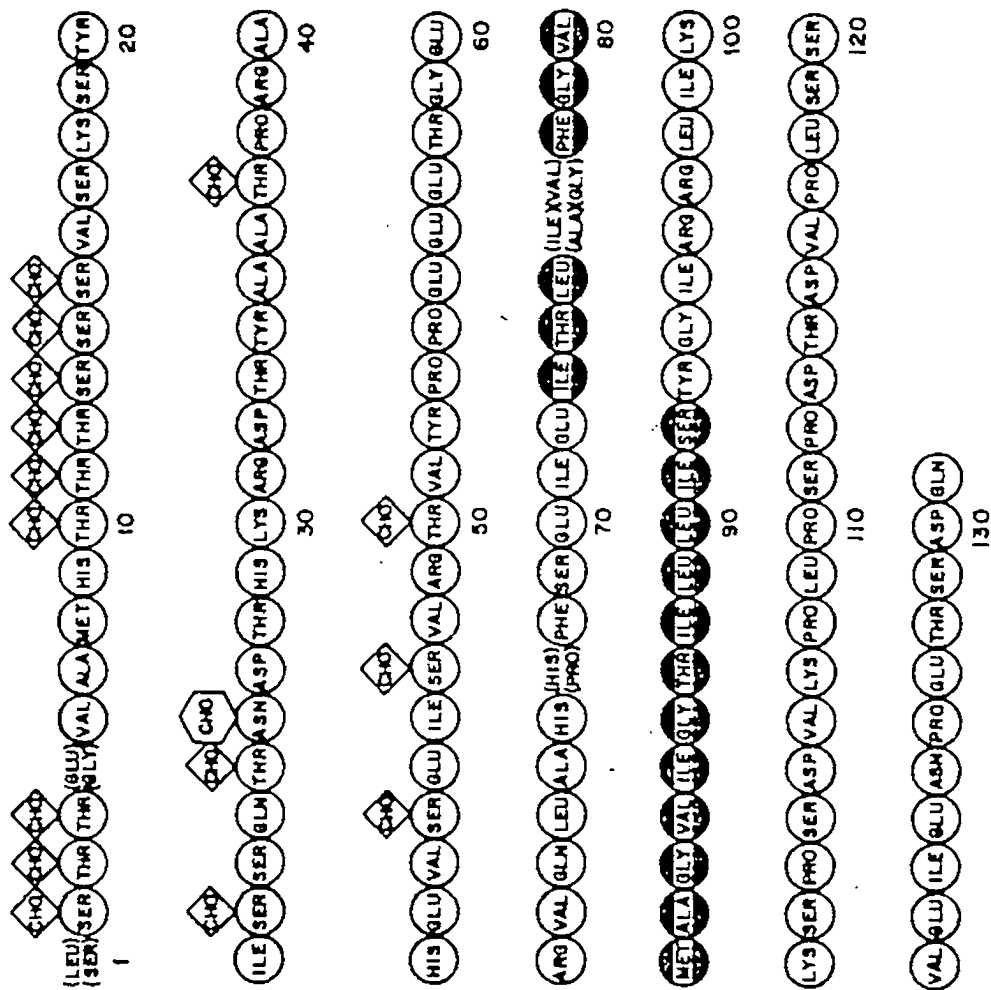


Figure 5

dically attached (8) as shown in Figures 6-8. The carbohydrate portion, which accounts for a large proportion of the total membrane sialic acid, is confined to the amino terminus which is exposed on the external face of the erythrocyte membrane. This particular exofacial carbohydrate segment has been implicated in M- and N-blood group specificity (27,38,39), according to the Landsteiner nomenclature (40,41). A substitution of the terminal serine residue and glycine residue in the five position in the N-active species by leucine and glutamic acid, respectively, accounts for the M^c-active species (33,39,42). This segment of glycophorin-A consists of seventy amino acids which contain twenty-two serine and threonine residues. Fifteen of these hydroxyamino acids participate in O-glycosidic saccharide-linkages. Also contained in this hydrophilic segment is a N-glycosidic saccharide-linkage of a more complex oligosaccharide side chain. The carboxyl terminus of the polypeptide, also hydrophilic, residues 96 through 131, extends into the cytoplasm (47,48) and is involved in interactions with cytoplasmic peripheral membrane proteins, such as spectrin. The presence of a large proportion of charged and polar amino acids accounts for the hydrophilicity of the carboxyl and amino termini of glycophorin. In contrast the central segment, residues 75 through 95, is highly hydrophobic. This hydrophobic domain which spans the membrane is arranged

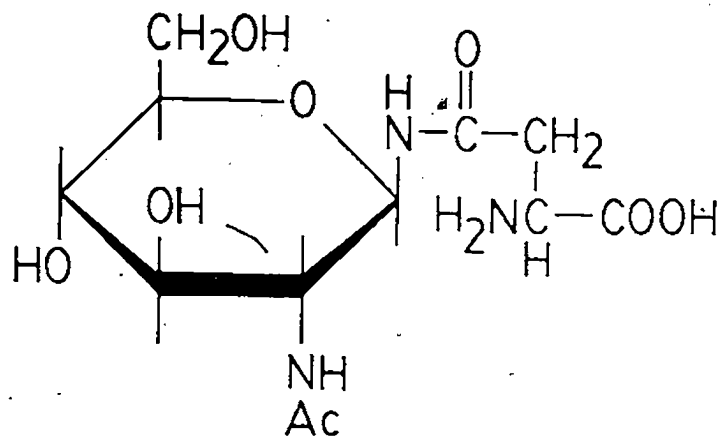
Figure 6

N- and O- Carbohydrate-Peptide
Linkages in Glycoproteins

Legend

Two typical carbohydrate-peptide linkages present in sialoglycopeptides are presented. The N-glycosidic linkage consists of β -N-acetylglucosamine attached to asparagine and the O-glycosidic linkage consists of α -N-acetylgalactosamine attached to serine or threonine.

N - GLYCOSIDIC



O - GLYCOSIDIC

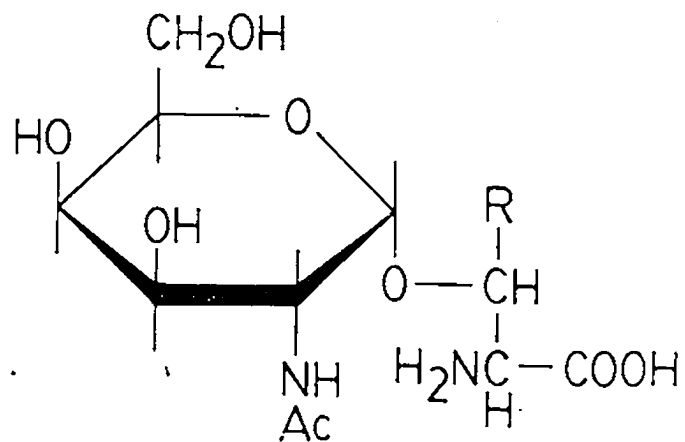


Figure 6

Figure 7

Carbohydrate Sequence of the O-Glycosidically
Linked Tetrasaccharides on Glycophorin-A

Legend

The monomer of glycophorin-A contains fifteen of these tetrasaccharides O-linked to threonine or serine residues (43-46).

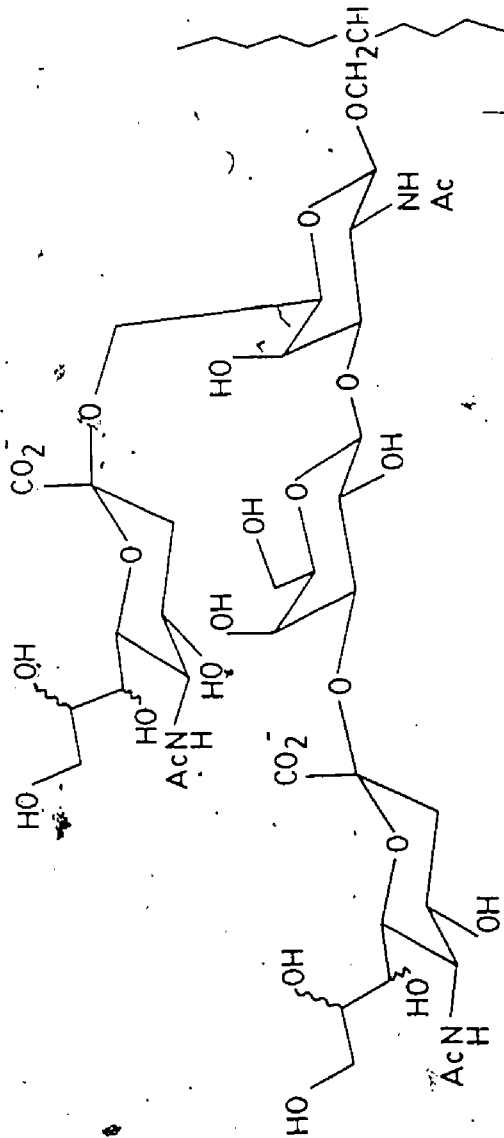


Figure 7

Figure 8

- Carbohydrate Sequence of the Complex N-Glycosidically Linked Oligosaccharide on Glycophorin-A

Legend

The monomer of glycophorin-A contains one complex oligosaccharide N-linked to asparagine residues (43-46).

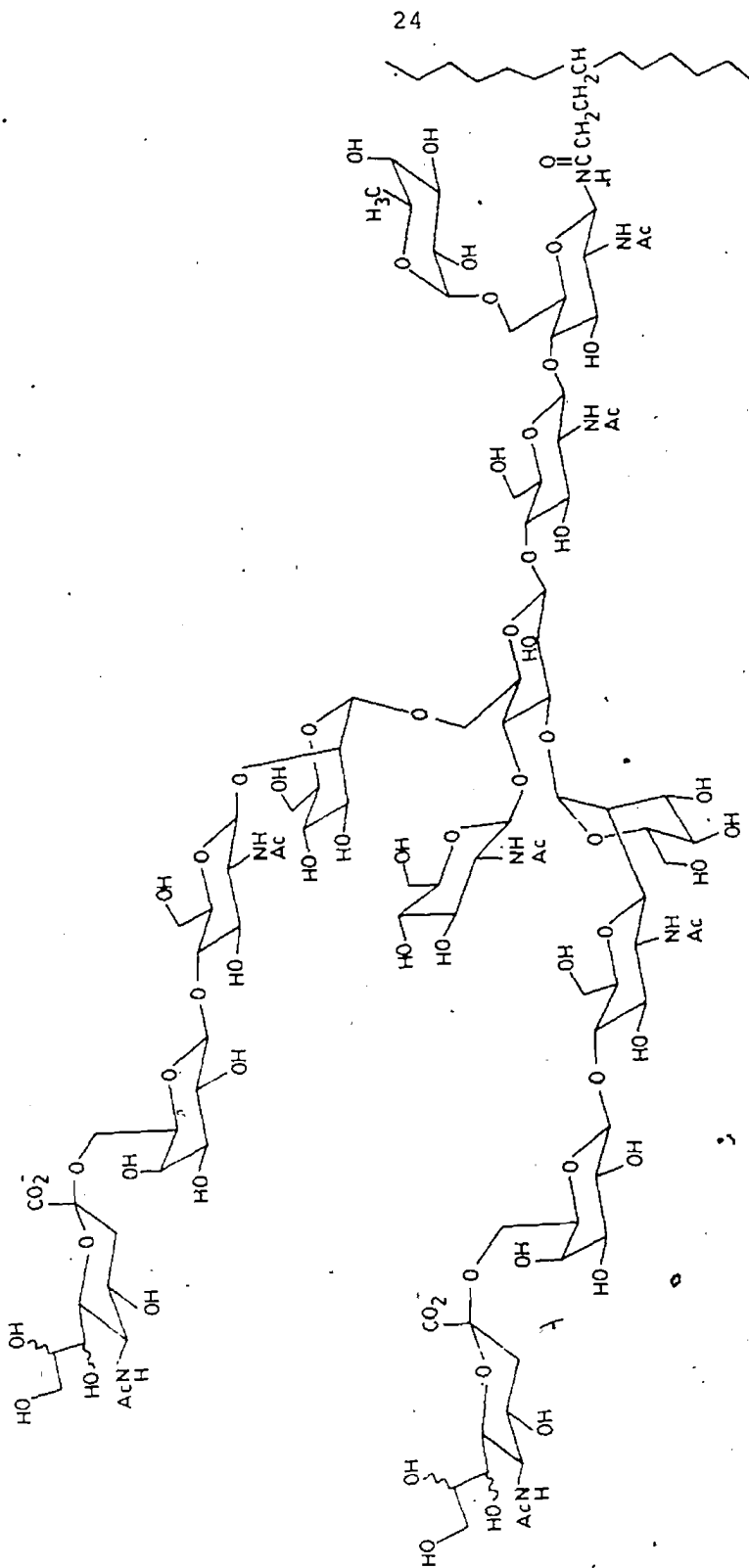


Figure 8

in the form of an α -helix and participates in interactions with the hydrocarbon tails of phospholipids (37). These strong interactions maintain glycophorin within the sea of lipids in the erythrocyte membrane (8,49,50) as shown in Figure 9.

Glycophorin with its unique tripartite orientation across the erythrocyte membrane serves as an attractive model for the study of structural-functional relationships in membranes. Many aspects of the complex structure of glycophorin-A still remain unknown even though its primary structure has been outlined. Very little information is available for the individual oligosaccharide chains attached to the fifteen serine or threonine residues and one asparagine residue. Earlier studies on the erythrocyte cell surface glycophorin-A O-linked oligosaccharides which were prepared from isolated sialoglycopeptides of erythrocyte membranes with alkaline borohydride revealed the presence of tetrasaccharides and trisaccharides. These tetrasaccharides (and complex oligosaccharide) in Figures 7 and 8, were first proposed by Thomas and Winzler (43) and confirmed by Lisowska et al. (51). As for the trisaccharides, a similar structure is suggested with the absence of one sialic acid residue (8).

Recently, it has been shown that there exist abnormal erythrocytes which contain unusual sialic acid-rich sialo-

Figure 9

Schematic Illustration of Glycophorin-A Arrangement
in the Human Erythrocyte Membrane

Legend

The orientation of the glycophorin-A molecule in
lipid bilayer is presented (37).

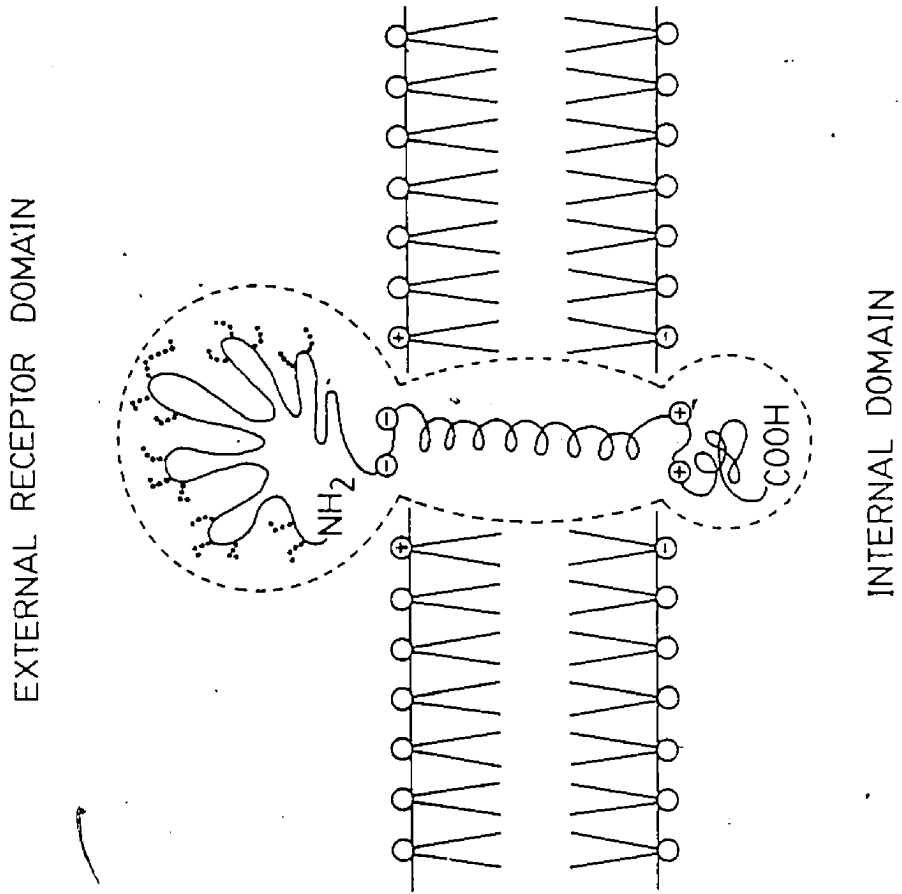


Figure 9

glycoproteins (38,52) and those which lack glycophorin-A, En (a⁻) erythrocytes, retaining normal amounts of sialic acid distributed on other glycoproteins (53-56). Current studies have illustrated the architecture of the membrane lipids and proteins in these En (a⁻) erythrocytes by electron spin resonance (esr) techniques (57). Further, these studies have attempted to identify the functional defects which could explain the absence of glycophorin-A. With the use of lipid specific spin labels (doxyl derivatives of stearic acid) and protein thiol specific labels (nitroxide derivatives of maleimide) it was shown that these abnormal erythrocyte membranes contained a hydrophobic bilayer allowing greater fluidity and less mobile proteins than in normal erythrocytes. Earlier, affinity labels designed to measure phospholipid distribution such as trinitrobenzenesulfonate which efficiently labeled phosphatidylethanolamine indicated an alteration in the phospholipid bilayer (57,58). Later, with the use of non-penetrating phospholipases, it was observed that phospholipid localization in En (a⁻) erythrocyte membranes remain unchanged as compared to normal erythrocytes (59).

Chemical Techniques in N-Acetylneuraminic Acid Determination

This negatively charged carbohydrate has been implicated in many membrane-associated processes such as cellular fusion, contact inhibition, and hormone, neurotransmitter and lectin

binding. Further, sialic acid is associated with immuno-chemical and tumorigenic properties (22). Present evidence suggests a possible role of cell surface sialic acid in erythrocyte sequestration. The sequestration of senescent mammalian erythrocytes by macrophagic spleen or liver cells has been of immense interest in the past several years (60-63). It has been suggested that a 10-15% loss in glycopeptide sialic acid may account for the removal of red cells from circulation. This desialylation exposes galactosyl residues which is thought to be the signal for macrophagic adhesion (63).

N-acetylneuraminic acid, better known as sialic acid, may be characterized by several techniques (64). The nine-carbon sugar is present in all higher animals and less frequent in some bacteria as the neuraminic acid or conjugated with other neuraminic acid derivatives (65). Sialic acid generally does not occur in its free form in biological fluids. The acetylated sugar is found as a glycosidic component of glycoconjugates such as glycolipids, oligosaccharides, homo- and heteropolysaccharides and glycoproteins (66). The bond between the glycosidic hydroxyl group of sialic acid and other monosaccharide residues such as galactose, glucose, N-acetylglucosamine and sialic acid is an α -linkage (67). Sialic acid can be

isolated as the free sugar by initial mild hydrolysis of the glycosidic linkage by acids or enzymatically by neuraminidases with subsequent separation by dialysis (68).

Procedures have been reported for the determination of bound or free sialic acid spectrophotometrically (69-71) and fluorimetrically (77) using thiobarbituric acid. A recently developed enzymatic method employed peroxidase for generation of the final chromophore (73). Moreover a new fluorimetric procedure was recently adopted by Shukla and Schauer (74) for the determination of free or glycosidically bound sialic acid. This procedure is a modification of a standard fluorimetric assay for formaldehyde first described by Belman (75). Conventional procedures require an initial metaperiodate oxidation of cell surface carbohydrates generating free formaldehyde (32) as shown in Figure 10. The formaldehyde is then measured by a coupling reaction with acetylacetone in the presence of ammonium acetate based on the 'Hantzsch' reaction generating a sensitive chromophore (76) 3,5-diacetyl-1,4-dihydro-2,6-dimethylpyridine illustrated in the scheme below:

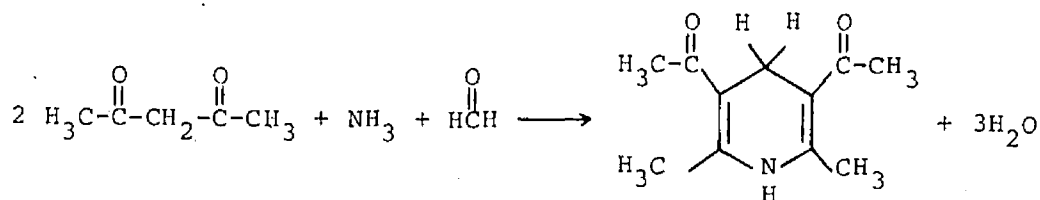


Figure 10

Sodium Metaperiodate Oxidation of Erythrocyte
Surface N-Acetylneuraminic Acid

Legend

Under defined conditions cell surface sialyl residues can be oxidized by sodium metaperiodate. The bond between carbons 7, 8 and 9, containing vicinal hydroxyls, is cleaved releasing one equivalent each of formaldehyde, formic acid and sialyl aldehyde (32).

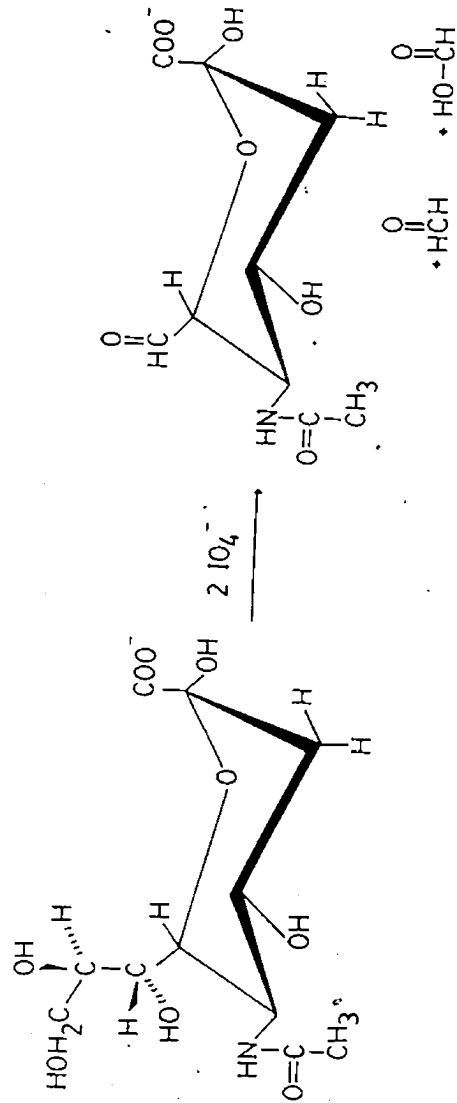


Figure 10

Alternatively, the aldehyde reagent 3-methyl-2-benzothiazoline hydrazone (MBTH) was used to estimate erythrocyte sialic acid content (77). In this procedure the formaldehyde liberated upon mild periodate treatment (32) was captured as the MBTH azine and oxidatively coupled with a second molecule of MBTH to form the tetraazapentamethine dye. We have recently shown (78) that the same dye is formed in the presence of peroxidase plus hydrogen peroxide and thus may be used to estimate the latter.

Characterization of Glycophorin-A by Assorted Techniques

In recent years interest in elucidating the role and importance of glycoproteins, particularly human erythrocyte glycophorin, as potential membrane surface recognition sites by means of chemical probes has grown immensely (30,32,79-88). For example, sialyl residues at the non-reducing termini of many cell surface oligosaccharides have been labeled by consecutive periodate oxidation and [³H]-borohydride reduction, Figure 11 (89), under defined conditions (32,40). Periodate cleaves the two carbon-carbon bonds containing vicinal hydroxyl groups on the sialic acid residue, giving rise to the products formaldehyde and formic acid in addition to protein bound sialyl aldehyde. However, this labeling procedure often leads to extensive non-specific labeling. An adaptation of the labeling procedure allows

Figure 11

Tritium Labeling of Cell Surface
Sialyl Residues

Legend

Glycoconjugate sialic acid residues are radiolabeled by [^3H]-borohydride reduction of periodate-generated sialyl groups (40).

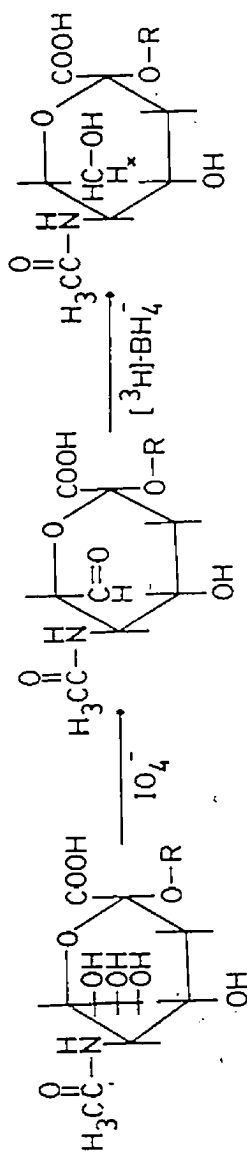
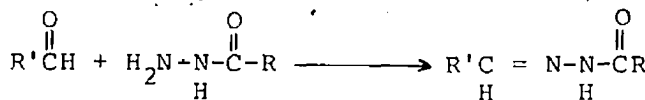


Figure 11

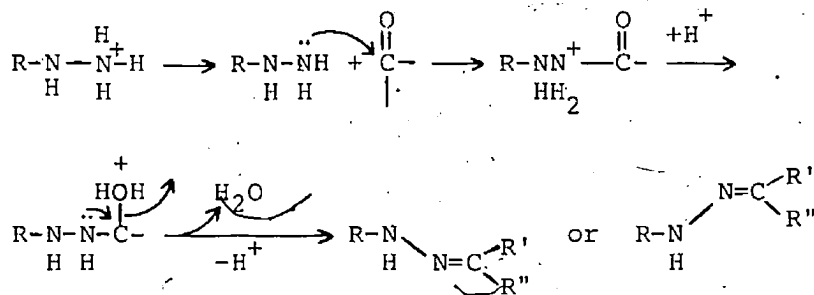
a more reliable identification of this glycoprotein (90).

Recently, Feix et al. (91) used spin labeling techniques to shed some light on the conformational properties of the cell surface glycoprotein when acted upon by carbohydrate specific lectins such as wheat germ agglutinin and phytohaemagglutinin. In this study, glycoprotein-bound sialic acid was derivatized with nitroxide spin labels, 2,2,6,6-tetramethyl-4-aminopiperidine-1-oxyl and 2,2,6,6-tetramethyl-4-maleimidopiperidine-1-oxyl. From the esr spectra it was concluded that the behaviour of the lectin receptor on the erythrocyte membrane was dependent on the type of lectin used and is unique to each lectin-glycoprotein system. The characterization of these events could lead to a further explanation of carbohydrate-mediated cellular recognition.

Acyl hydrazides are currently being used in further elucidating the carbohydrate distribution in erythrocyte membrane glycoproteins (92-94) and platelet membrane glycoproteins (95). An acyl hydrazide, in fact any hydrazide, undergoes a condensation reaction with available aldehydes as shown below to give a relatively stable hydrazone:

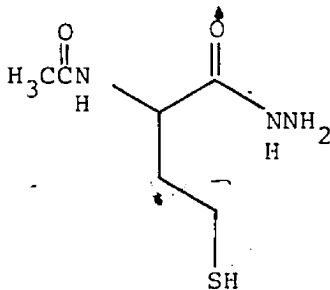


This hydrazone bond (Schiff base) can be further reduced to the amine with sodium borohydride or sodium cyanoborohydride (96). As Itaya *et al.* (97) have illustrated reactions between hydrazides and carbonyl groups involve a rapid nucleophilic attack on the R-NH₂ group towards the electrophilic carbon center of the aldehyde carbonyl as outlined below:



They suggested that in the presence of manganese (Mn⁺⁺) this reaction proceeds more efficiently at room temperature under physiological conditions.

Recently, our laboratory reported the preparation and use of 2-acetamido-4-mercaptobutyric acid hydrazone as a potential thiolation reagent for cell surface carbohydrates (92).



This heterobifunctional reagent, containing a carbon-14 label in the acetyl group, allows for a convenient and facile introduction of a thiol 'handle' onto periodate-generated aldehyde-containing glycoconjugates present on erythrocyte cell surfaces.

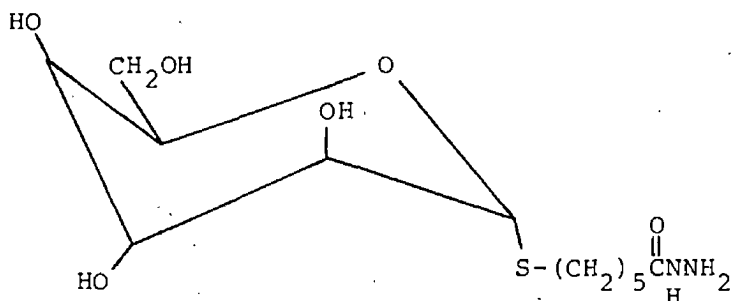
The development of fluorescence labeling techniques has enabled others to specifically label sialyl or galactosyl residues with fluorescent primary amines (95) via Schiff base formation with periodate- or galactose oxidase-generated aldehydic groups (32,98). This particular study concluded that specific labeling of carbohydrates with fluorophores is attained irrespective of the heterogeneity of the protein composition. Recently, Wilchek *et al.* (98) described the preparation of rhodamine and fluoresceine hydrazides for labeling membrane-bound and soluble glycoproteins and glycolipids. Taking advantage of intense chromophoric capability of fluorescent markers they were able to stain membrane glycoproteins on polyacrylamide gels. Further exploitation of these fluorophores enabled Low *et al.* (99) to provide evidence for restricted oligosaccharide mobility on glycophorin at the surface of the erythrocyte membrane.

Other acylhydrazides have been prepared including biotinyl hydrazide and dinitrophenyl hydrazide in studying

cellular recognition processes and cell-cell interactions in lymphocyte stimulation (100,101). Human platelet membrane glycoprotein organization has been studied with other phenyl hydrazides (95). For electron microscopy use of an electron-dense material such as ferritin hydrazide which labels biological glycoconjugates has been reported (102). More recently, sialic acids on membrane-bound glycolipids and glycoproteins could be distinguished with an adaptation of the biotin hydrazide modification procedure (103) used in topographical derivatization of terminal sialyl or galactosyl residues. In that study biotinylated cell surfaces were subsequently exposed to a ferritin-conjugated avidin system. Electron microscopy has revealed that glycolipids contain carbohydrate residues which are closer to the membrane surface than those of glycoproteins. This specific localization of cell surface carbohydrates has allowed the discerning of particular glycoconjugate head-group dynamics on the cell surface (99,104-106).

Earlier, sugar-containing acyl hydrazides were used to demonstrate the roles of cell surface carbohydrates as ligands in mediated cellular recognition (107). For example, derivatization of bovine erythrocyte cell surfaces with 6-(1'- α -D-thiomannosyl) hexanoyl hydrazide led to the agglutination by concanavalin-A, a plant lectin. Under

native conditions these cells are not agglutinated by concanavalin-A (108).



Potential Use of Peroxidase Color Reactions in the
Determination of Cell Surface Carbohydrates via
Hydrogen Peroxide

Cell surface glycoconjugates contain to a large degree galactosyl and N-acetylgalactosaminyl residues which are substrates for galactose oxidase (109). These cell surface glycoconjugates have been labeled using galactose oxidase followed by sodium borotritiide (110,111) (Figure 12). This enzyme catalyzes the oxidation of the primary alcohol group of free (112) or terminal non-reducing galactose units when glycosidically linked (113,114) liberating stoichiometric hydrogen peroxide (112) illustrated in Figure 13. By exploiting the properties of hydrogen peroxide quantitative determination of galactose might be obtained through the use of peroxidase-catalyzed chromogen systems (115-119).

Figure 12

Tritium Labeling of Cell Surface
Galactosyl Residues

Legend

Glycoconjugate galactose residues are radiolabeled by borotritiide reduction of galactose oxidase-generated galactosyl aldehyde groups (98).

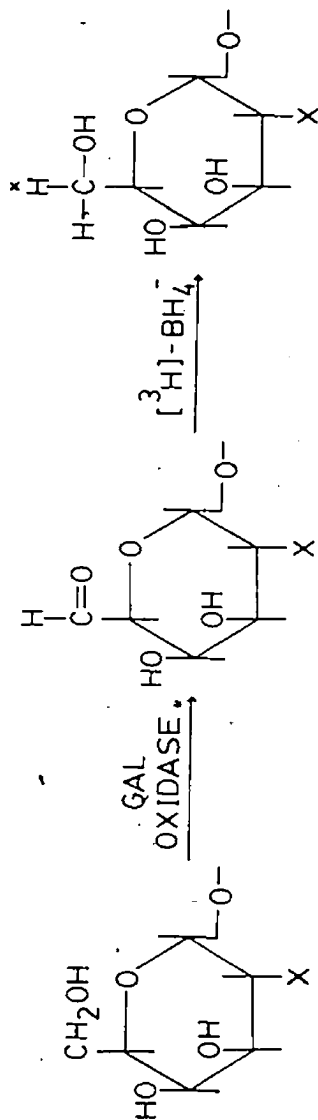


Figure 12

Figure 13

Galactose Oxidase Treatment of Erythrocyte
Surface Galactosyl Residues

Legend

Cell surface galactosyl and N-acetylgalactosaminyl residues are oxidized by galactose oxidase at the primary alcohol group under defined conditions (113,114).

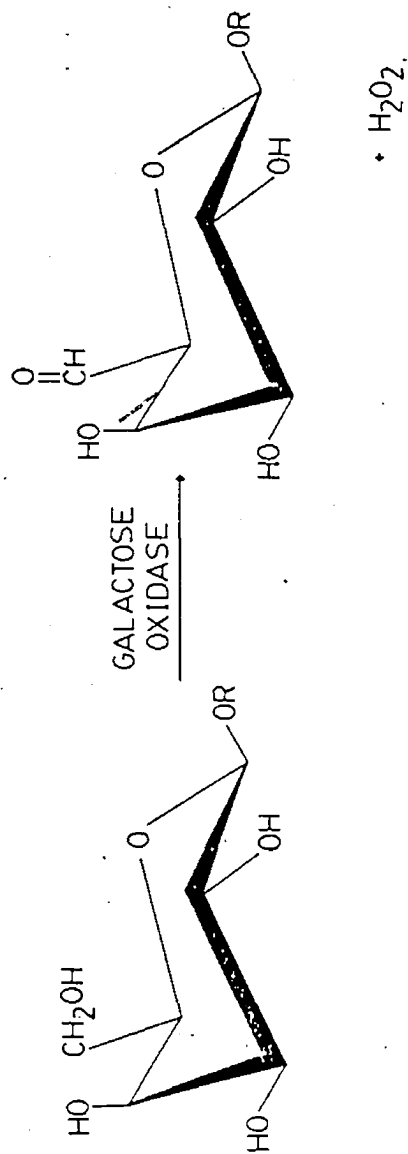
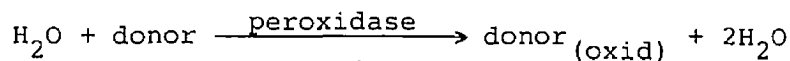


Figure 13

The many substrates for peroxidase-catalyzed hydrogen peroxide oxidations which have been studied (120) can be classified into two main reaction types: oxidation of redox indicators such as 2,2'-azino-di-(3-methylbenzothiazolin)-6-sulfonate (119) and *o*-dianisidine (120) or oxidative coupling of an amino aromatic with another aryl compound. In the latter class, for example, 4-aminoantipyrine oxidatively coupled to phenol or substituted phenol (120, 121) such as 2-hydroxy-3,5-dichlorobenzene sulfonic acid (HDCBS) were used in many instances. Alternately, 3-methyl-2-benzothiazolinone hydrazone (MBTH) has been previously reported to be a co-substrate with N,N'-dimethylaniline (122,123), HDCBS (120), or 3-(dimethylamino)benzoic acid (124) and recently with the azine of MBTH for determining hydrogen peroxide (78).

Typically, the enzymic reaction described below operates in the development of the final chromophore:



Usefulness of Macromolecules Including Plant Lectins in
Investigating Cell Surface Receptor Function

The human erythrocyte has the capacity to interact with many different biological molecules in very small concentrations by virtue of many different 'receptors' on the membrane surface for viruses, toxins, antibodies and lectins (125,126), prostaglandins (127), acetylcholine (128), β -adrenergic agents and growth hormone (129), and insulin (130). These sites, glycolipids or glycoproteins, provide an important function when occupied by these key effectors. A spontaneous trans-membrane signal could be transmitted from the external portion of the cell to the cytoplasmic face upon adhesion. It is obligatory that an estimate be made on the number of potentially available receptors, especially high affinity receptors (131). Numerous studies have resulted in further illustrating the existence of these types of receptors. For instance, the use of spin-labels (80) and fluorescent molecules (132) have enabled the detection of slight perturbations localized in the membrane upon binding of the aforementioned effectors even at the level of a few molecules per cell.

The study of carbohydrate-bearing receptors has benefitted greatly from the availability of lectins (also known as agglutinins, phytohaemagglutinins, phytoagglutinins and protectins). The term lectin is derived from the Latin

word legere: to choose. Lectins are a group of sugar-binding proteins or glycoproteins of non-immune origin (133). This diverse group of substances contain at least two carbohydrate-binding sites, agglutinate animal and plant cells, (most commonly normal or enzyme-treated erythrocytes) and/or precipitate polysaccharides, glycoproteins and glycolipids. The definition of lectin specificity is in terms of monosaccharide(s) or simple oligosaccharide(s) inhibition of lectin-mediated agglutination reactions. Lectins may be soluble proteins such as concanavalin-A or membrane-bound such as rabbit or rat hepatocyte lectins (134).

Lectins serve as powerful probes in the elucidation of the behaviour, structure and organization of membrane glycoproteins. These plant and bacterial proteins specifically bind and crosslink sugars contained in oligosaccharide portions of glycoproteins (49,135,136). These interactions with carbohydrate-containing cells resemble those of antibodies (137). The property of specific carbohydrate binding by the lectins sometimes promotes recognition events at a cellular level. For instance there is an induction of lectin production which promotes cell to cell adhesion when sialic acid-containing cell membranes bind to influenza virus possessing a hemagglutinin (134,138). The role of lectins

}

in the plant or bacterium is not fully understood, however, an hypothesis is that lectins act as receptor sites for pathogens (139) or symbionts (140). The cytotoxic properties of lectins when present in certain seeds at high concentrations may serve as a defense mechanism against seed-eating herbivores (141).

Lectins have been characterized for virtually all of the sugars occurring in cell surface oligosaccharides. For example, the list includes lectins for N-acetylneuraminic acid (142), galactose (143), mannose (144), N-acetylglucosamine (145) and N-acetylgalactosamine (146). Wheat germ agglutinin (Triticum vulgare) (147), comprised of two identical subunits of molecular weight 17,500, has not been thoroughly characterized since the complete amino acid sequence still remains to be determined. However, x-ray crystallography of this glycoprotein recently led to a greater understanding of the binding mode of several saccharides (148,149) such as N-acetyl-D-glucosamine, $\beta(1\rightarrow4)$ -linked N-acetyl-D-glucosamine oligomers, N-acetyl-D-galactosamine and N-acetyl-D-neuraminic acid, the former being a more potent inhibitor of erythrocyte agglutination (142,150) suggesting that wheat germ agglutinin association with cell surface carbohydrates is complex (149-151). It was determined that the binding of the lectin could be

impaired (i.e., higher concentrations of lectin required for agglutination) by enzymatically hydrolyzing N-acetylneuraminic acid (142, 152) from defined oligosaccharides.

There are only a few lectins in existence which have specificity for N-acetylneuraminic acid residues. Limulin and carcinoscorpín have been isolated and purified from American horseshoe crab (Limulus polyphemus) (153) and the Indian horseshoe crab (Carcinoscorpus rotunda cauda) (154). Another two sialic acid specific lectins recently have been isolated on a Sepharose-colominic acid affinity column from the hemolymph of the American lobster (Homarus americanus) (155) and the other from the slug (Limax flavus) (156).

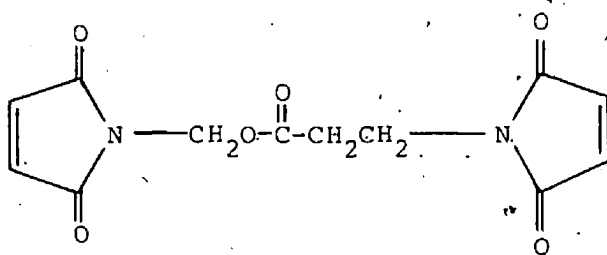
Many lectins have been shown to agglutinate erythrocytes^o by binding to specific carbohydrates on the cell surface (134). Some D-galactose binding lectins include Ricinus communis agglutinin (castor bean lectin) (157), Abrus precatorius agglutinin (jequirty bean lectin) (158), Sophora japonica agglutinin (Japanese pagoda tree lectin) (159) and Arachis hypogaea (peanut lectin) (160).

The specific arrangement of the aforementioned sugars on carbohydrate moieties of glycoproteins influences the effect of the cognate ligands (161). A recent survey by Goldstein and Hayes (134) clearly outlines the importance and roles of these lectins. The exploitation of their

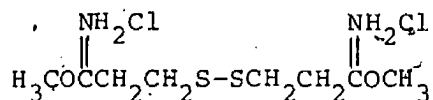
binding properties has led to the use of lectins in purification of cell membrane glycoproteins (162) via affinity chromatography.

Application of Photoaffinity Labeling in Biological Systems

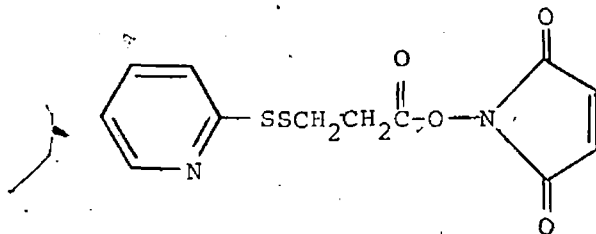
Bifunctional crosslinking reagents, hetero- and homo-bifunctional, are being developed to further elucidate macromolecular interactions in biochemical processes. This family of reagents contains two different classes, chemical crosslinking and photo-crosslinking reagents. Crosslinking of the former class requires that specific nucleophiles be present at the site of interaction and on the probe molecule (163). Included in this class of bifunctional reagents are maleimido-methyl- β -maleimido propionate (164).



and dimethyl-3,3-dithiobispropionimidate (165), both cleavable



homobifunctional reagents. Also included in this class are heterobifunctional reagents, such as N-succinimidyl 3-(2-pyridyldithio) propionate (166)



and N-(maleimidobenzoyloxy) succinimides (167) which have been used in membrane protein modifications to clarify their interactions in intact cells.

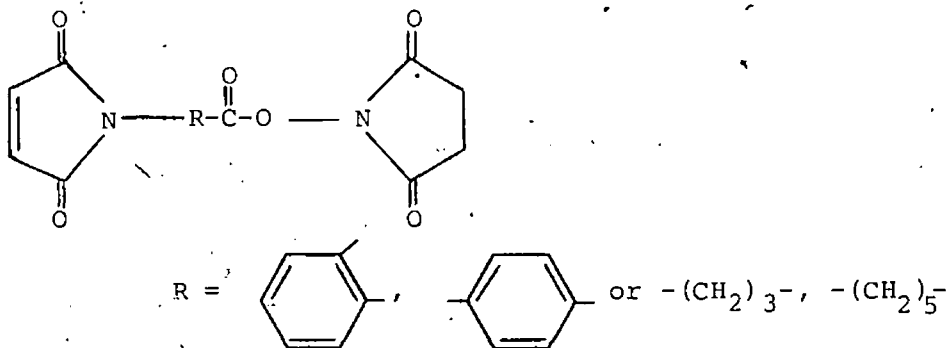
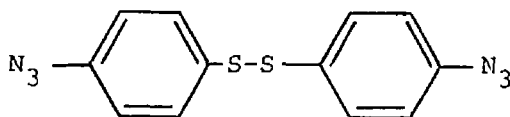
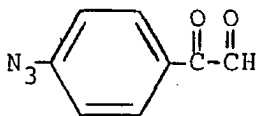


Photo-crosslinking reagents, however, do not rely on the presence of these nucleophiles on the probe molecule (168). A representative homobifunctional photo-crosslinking reagent is 4,4'-dithiobisphenylazide (169,170) which has been used

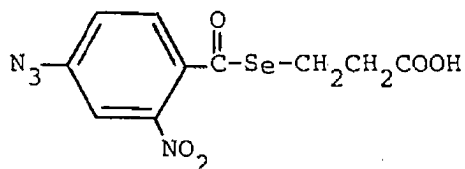


in probing membrane structure. This reagent is easily cleaved by disulfide reduction with mercaptoethanol.

The availability of heterobifunctional reagents provides a further advantage by allowing an initial chemical incorporation of the label into the particular site with the subsequent irreversible insertion upon photolysis.² Included in this group of reagents are para-azidophenylglyoxal (171), which reacts initially with



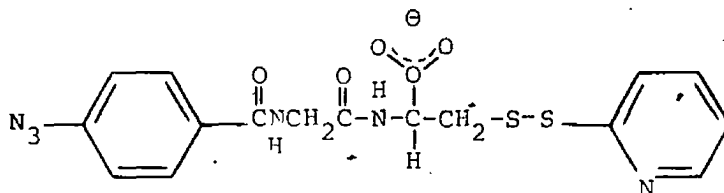
arginine residues on proteins through the phenyl-glyoxal moiety and 3-(4-azido-2-nitrobenzoylseleno) propionic acid (172), designed to primarily react with sulfhydryl residues



on macromolecules with the elimination of the selenal ester function.

A variety of biological receptor systems and their molecular interactions have been examined by means of affinity labeling the corresponding receptor binding sites

(173,174). In particular, photolabeling (175) shows much promise in minimizing non-specific labeling. For instance, a photosensitive probe N-(4-azidobenzoylglycyl)-S-(2-thiopyridyl)-cysteine was observed to become attached to protein sulfhydryl groups through the cysteine side chains of the reagent via a disulfide bridge liberating 2-thiopyridone (176).



Photolabeling techniques are advantageous as compared to the standard practice of affinity labeling since reagent incorporation is independent of nucleophilic reactivity (i.e., in the absence of nucleophilic residues on the macromolecule) which often requires defined pH, temperature or concentration. However, the extent of reagent incorporation and the degree of specificity is dictated by its inherent properties such as reactivity, binding site selectivity and orientation.

Prior to the examination of the effectiveness of a particular reagent three important points should be fulfilled: (i) the architecture of the reagent must allow

preferential binding to the receptor (i.e., the reagent must closely mimic the geometry of the natural ligand or macromolecule); (ii) the reagent must be chemically inert in the absence of light allowing reversible binding to the biological system; and (iii) the reagent (or activated intermediate) should not be a generally reactive electrophile as is the case in many classes of affinity reagents.

In general, photoinduced incorporation of a reagent follows transformation of a photosensitive substituent on the reagent into a highly reactive intermediate upon irradiation. This process must be very rapid to avoid escape of the reagent from the active site upon photolysis. Ideally, the highly reactive species (carbene or nitrene) should be generated (i) at the particular interacting site; (ii) in a conformation facilitating irreversible modification through covalent insertion; (iii) and at wavelengths distantly removed from the absorption maxima of the macromolecules so as not to damage the biological system in question (177). Furthermore, the highly reactive species should be short-lived and should not undergo intramolecular rearrangement to a less reactive (and longer-lived) compound (173,175).

Two of the most useful groups of photolabile compounds for photoaffinity labeling are the diazo- and azido-containing reagents. Upon photolysis these light-sensitive groups become highly reactive carbenes and nitrenes,

respectively (Figure 14). The advantage of these types of reagents is that the highly reactive species attacks not only functional groups of a nucleophilic nature but rather many types of amino acid residues including aliphatic amino acids.

The reactive carbene or nitrene which is generated upon irradiation by light will rapidly undergo at least four different reactions: (i) coordination with nucleophilic centers to give carbanions; (ii) addition to double and triple bonds; (iii) insertion into single bonds; and (iv) abstraction of hydrogen to generate two free radicals (172). The carbene or nitrene precursor must not contain a hydrogen atom on the carbon atom adjacent to the carbene carbon. Upon carbene generation the proton will migrate to the carbene terminus giving rise to an unreactive intermediate. This is also observed when a carbonyl group is present in the same position. The derived carbene then becomes susceptible to an intramolecular Wolff rearrangement to ketones as shown below:

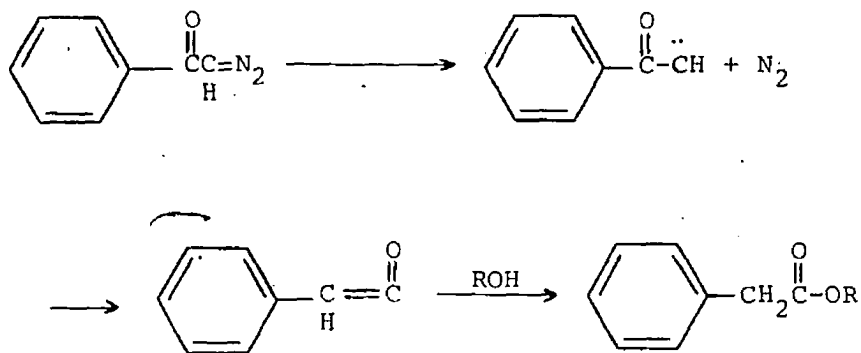


Figure 14

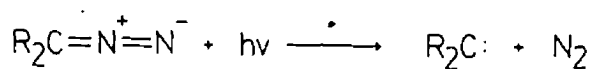
Typical Precursors Generating Highly Reactive
Electrophilic Intermediates

Legend

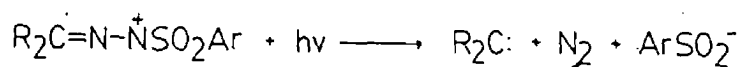
Typical photolabile reagents capable of transformation into highly reactive species in the presence of light are presented.

CARBENES AND CARBENE PRECURSORS

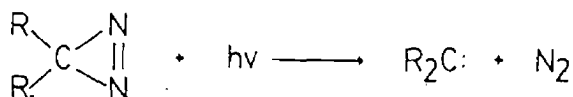
Diazoalkanes



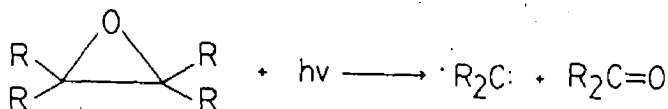
Sulfonylhydrazone salts



Diazirines



Epoxides



NITRENES AND NITRENE PRECURSORS

Azides



Figure 14

A characteristic feature of aryl azide photochemical reagents is the presence of a trisubstituted phenyl ring consisting of at least the azido and nitro substituents including attachment to the corresponding ligand. The addition of an electron-withdrawing substituent such as nitro group to the aromatic ring provides a more reactive and electrophilic nitrene (173) and also shifts the absorption maxima to longer wavelengths. Aryl azides, the most frequently used nitrene precursor, undergo several reactions in the presence of light as shown in Figure 15.

It has been recently suggested that aryl azide photolabels probably do not insert predominantly into C—H bonds as previously thought (178). Nitrenes, however, are currently being extensively used as photolabels and have been shown to be potent tools in photoaffinity labeling, especially the aryl nitrenes (173,179). The primary advantage of using this photolabel is its facile manner of preparation by well-established methods. Also, aryl azides substituted with appropriate electron-withdrawing substituents such as nitro-substitution absorb incident light in the near ultraviolet region with propitious extinction coefficients. A favorable consequence of this photochemical behaviour is negligible radiation damage on the macromolecule or biological system. The presence of electron-withdrawing

Figure 15

Possible Reactions Involving Nitrenes

Legend

Nitrenes can potentially undergo a series of reactions namely: (i,iii) non-productive reactions producing primary amines; (ii) non-productive reactions producing azobenzenes; (iv) reactions producing azepines; (v) reactions producing aziridines; and (vi) reactions producing secondary aryl amines.

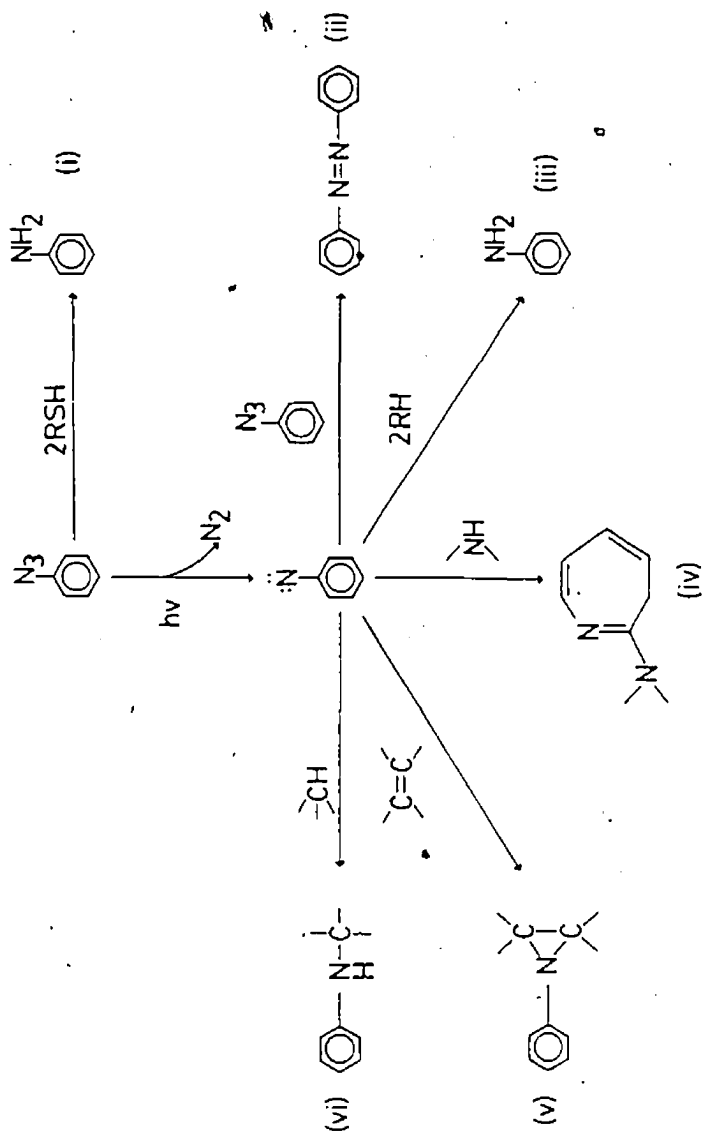
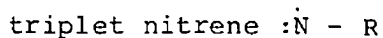
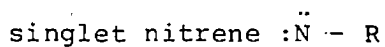


Figure 15

groups causes a shorter lifetime (173) for the highly reactive nitrene upon photolysis (180,181). The absorption of ultraviolet or visible light by azido-containing compounds generate two excited electronic states of the nitrene species which are electron deficient: (i) a singlet state where the electron spins are paired, (ii) and a triplet state where the electron spins are unpaired.



The singlet species of nitrenes are involved in intramolecular bond reorganizations leading to several forms of covalent bonds as seen in Figure 15. Singlet nitrenes are of particular interest as opposed to the triplet species as their mode of insertion into nucleophiles is much superior. In this process an electron pair is taken from the nucleophile through a single reaction, namely, a concerted electrophilic reaction generating a covalent attachment. The triplet species, however, requires a two-step reaction for covalent bond formation between the nitrene and macromolecule. Potential loss in yield of nitrene incorporation could result because of a prior paired intermediate which is capable of dissociation. Recent reviews by Staros

(178) and Brunner (182) and more recently a photochemical study of aryl azides (183) strongly indicate that indiscriminate insertion reactions involving triplet nitrenes is insignificant as the prominent reactions of aryl azides proceed through singlet nitrenes.

Approaches Taken in the Present Study

The objective of the present study was to further characterize cell surface sialoglycoprotein organization with in situ light-dependent crosslinking. The approach taken involves the conventional sodium metaperiodate (32) or galactose oxidase (97) treatment of erythrocyte membrane surface carbohydrates followed by N-(2-nitro-4-azidophenyl)- β -alanine hydrazide derivatization of the periodate- or galactose oxidase-generated aldehydic group functions. Subsequent photolysis in the presence of sialic acid-specific wheat germ agglutinin (150) or galactose-specific lectins such as castor bean lectins (157) or jequirty bean lectin (158) could reveal important information regarding cellular recognition events.

Further, as we have been concerned with chemical modification of cell surface sialic acid residues via periodate oxidation followed by hydrazone formation with various acyl hydrazides (92) we sought a method for rapid determination of periodate-generated sialyl aldehyde content

on cell suspensions of high density, 20% packed volume or greater, and were attracted by the potential of MBTH. In this dissertation a simplified MBTH procedure is presented and demonstrate its application to determination of erythrocyte membrane sialic acid (184). Furthermore, this report focuses on the extension of this new chromogen to galactose oxidase-peroxidase, glucose oxidase-peroxidase and choline oxidase-peroxidase systems (78).

CHAPTER II

EXPERIMENTAL

Materials and Apparatus

Human erythrocytes were obtained from the Canadian Red Cross Society, Windsor Branch and London Regional Centre. The 3-methyl-2-benzothiazolinone hydrazone hydrochloride hydrate (MBTH), silver nitrate, ammonium hydroxide, sodium hydroxide, cupric sulfate, acrylamide, and N,N'-methylenebisacrylamide was purchased from Aldrich Chemical Company, Inc., Milwaukee, WI. Formaldehyde solution, 37% w/w, A.C.S., ferric chloride, sodium periodate, sodium borohydride, anhydrous dextrose (D-glucose), D-galactose, sucrose, reagent grade sodium peroxide, 30% potassium iodide, sodium thiosulfate, mercuric iodide, ammonium molybdate, trichloroacetic acid, copper sulfate pentahydrate, potassium tartrate, sodium hydroxide, sodium carbonate, Folin-Ciocalteu phenol reagent and buffer salts were from Fisher Scientific Company, Fair Lawn, N.J. 5-dimethylaminonaphthylsulfonyl hydrazine (dansyl hydrazine) was from Pierce Chemical Company, Rockford, IL. 5,5-dimethyl-1,3-cyclohexanedione (dimedone) was purchased from Eastman Kodak Company, Rochester, N.Y.

Acetone, A.C.S. and citric acid was purchased from BDH Chemicals, Toronto, Ontario. Glucose test kits, bovine serum albumin, chicken egg albumin, myoglobin, hemoglobin, ribonuclease-A, dithioerythritol, N-acetyl-D-glucosamine, N-acetyl-D-neuraminic acid, sodium dodecyl sulfate, sodium deoxycholate, sodium persulfate, pyronin-G dye, Coomassie brilliant blue G, and basic fuchsin were obtained from Sigma Chemical Company, St. Louis, MO. N,N,N',N'-tetramethylethylenediamine was from Bio-Rad Laboratories, Richmond, CA.

Peroxidase (horseradish), (donor: hydrogen peroxide oxidoreductase; EC 1.1.1.17) was from Boehringer Mannheim Canada, Ltd., Dorval, Que. One unit of enzyme activity is the amount which will catalyze the oxidation of 1 μ mole of guaiacol, by H_2O_2 per minute at 25°C, pH 7.0.

Glucose oxidase (Aspergillus niger), (β -D-glucose: oxygen 1-oxidoreductase; EC 1.1.3.4) was from Sigma Chemical Company, St. Louis, MO. One unit of enzyme activity is the amount which will oxidize 1 μ mole of β -D-glucose to D-gluconic acid and H_2O_2 per-minute at 35°C, pH 5.1.

Galactose oxidase (Dactylium dendroides), (D-galactose: oxygen 6-oxidoreductase; EC 1.1.3.9) was from Sigma. One unit of enzyme activity is the amount which will produce an absorbance (425nm) of 1.0 per minute at 25°C, pH 6.0,

in a peroxidase and o-toluidine system.

Choline oxidase (Alcaligenes species), (choline: oxygen 1-oxidoreductase; EC 1.1.3.17) was from Sigma. One unit of enzyme activity is the amount which will form 1 μ mole of H_2O_2 from choline and H_2O per minute at 30°C, pH 8.0.

Neuraminidase (Clostridium perfringens), (acyl-neuraminy l hydrolase; EC 3.2.1.18) was from Sigma. One unit of enzyme activity is the amount which will liberate 1 μ mole of N-acetylneuraminic acid per minute at 37°C, pH 5.0.

Wheat germ agglutinin (Triticum vulgare), jequirty bean agglutinin (Abrus precatorius), castor bean agglutinins types 60 and 120 (Ricinus communis) were from Sigma and horseshoe crab agglutinin (Limulus polyphemus) from Bethesda Research Laboratories, Inc., Bethesda, MD. Fluorescein isothiocyanate (FITC) labeled castor bean lectins (RCA₆₀ and RCA₁₂₀) and wheat germ agglutinin were from E-Y Laboratories, Inc., San Mateo, CA.

pH of buffer solutions was determined at room temperature using a Radiometer Model 26 instrument equipped with a Radiometer semi-micro combination electrode number Gk 2301-C. Buffer solutions of pH 7.0 and pH 4.0 from Fisher Scientific were used in standardizing the pH meter.

All infrared spectra were made on Perkin Elmer 180 Recorder console or Beckman IR 12 spectrometers. Samples

at 0.5 percent concentrations were pelleted with dry KBr.

The nuclear magnetic resonance spectra were recorded on an EM 360 NMR spectrometer from Varian Instrument Division.

Absorbances and visible and ultraviolet spectra of solutions were measured with a Beckman 35 spectrophotometer, Beckman Instruments, Inc., Fullerton, CA using quartz semi-micro cuvettes (1 cm and 0.5 cm path length and 1 ml volume).

Centrifugation was carried out with a Sorval RC-2B instrument and SS-34 rotor. Whole cell sedimentation was at 6,000 rpm (4,340 x g) for 1 minute while ghosts were packed at 12,000 rpm (17,300 x g) for 5 minutes.

Reagents

Distilled deionized water was used for all solutions below. The enzyme stock solutions were stable for at least one week when stored at 4°C in the dark.

Stock hydrogen peroxide: 30% hydrogen peroxide was diluted 1000-fold with water to approximately 10 mM, standardized according to Kolthoff et al. (185), and further diluted 10-fold with H₂O.

All solutions of MBTH (as the hydrochloride) and formaldehyde, either separately or together, were made up in water. Formaldehyde stock solutions were standardized by the method of Frisell et al. (186).

Premixed solutions of MBTH and formaldehyde were made

on the day of the experiment to contain 0.85 mM MBTH and 0.83 mM formaldehyde, respectively, or 3.40 mM and 3.32 mM of the two respective reagents. These solutions were allowed to stand at room temperature for at least 30 minutes prior to use. The less concentrated solution was stable for several days while the more concentrated solution often began crystallizing after six hours.

Separate solutions of MBTH were stable for at least two days while the formaldehyde stock solutions were stable for months when stored at room temperature in the dark.

Ferric chloride solutions, 9.25 and 37.0 mM and sodium periodate solution, 20 mM, were prepared daily and kept at room temperature in the dark.

The following buffers were used: sodium acetate (0.2 M, pH's 3.44, 4.10, 4.40, 5.00 and 5.60), sodium phosphate (5 mM, pH 7.8, 10 mM, pH 7.0 and 1.0 M, pH 7.4), potassium acid phthalate-HCl (0.2 M, pH's 2.50, 3.00 and 3.50), phosphate-buffered saline (PBS; 5 mM sodium phosphate, 150 mM sodium chloride, pH 7.4), wash buffer (5 mM sodium phosphate, 15 mM sodium chloride, 0.1 mM ethylenediaminetetraacetic acid, pH 7.4), lysis buffer (0.5 mM tris(hydroxymethyl) aminomethane hydrochloride, 0.1 mM ethylenediaminetetraacetic acid, pH 7.4), Tris-NaCl-CaCl₂ buffer (50 mM tris(hydroxymethyl) aminomethane hydrochloride, 150 mM sodium chloride,

10 mM calcium chloride, pH 8.0), Tris-HCl buffers (1.5 M, pH 8.8 and 0.5 M, pH 6.8), bicarbonate buffered saline (150 mM sodium chloride, 5 mM calcium chloride, 4 mM sodium bicarbonate, pH 6.5), Tris-acetate-EDTA electrode buffer (40 mM tris (hydroxymethyl) aminomethane hydrochloride, 20 mM sodium acetate, 2 mM ethylenediaminetetraacetic acid, 0.2% sodium dodecyl sulfate, pH 7.4) and Tris-glycine electrode buffer (50 mM tris (hydroxymethyl) aminomethane hydrochloride, 0.4 M glycine, pH 8.3).

Glucose solution, 0.8 mM, and galactose solution, 10 mM, were allowed to stand for 24 hours at room temperature to allow complete mutarotation of the sugar. Choline chloride solution, 0.4 mM, was prepared daily.

Peroxidase solution was prepared to contain, 1U, 0.5U or 0.25U peroxidase per 50 μ l of sodium acetate buffer at pH 3.44 unless noted otherwise. Glucose oxidase solution was prepared to contain 10U glucose oxidase in 50 μ l of the same sodium acetate buffer. Glucose oxidase - peroxidase solution was prepared to contain 0.5U and 5U or 15U of peroxidase and glucose oxidase, respectively, in 50 μ l of sodium acetate buffer. Choline oxidase solution was prepared to contain 0.6U choline oxidase in 50 μ l of sodium phosphate buffer pH 7.8. Galactose oxidase solution was prepared to contain 5U or 10U galactose oxidase in 50 μ l of sodium phosphate buffer pH 7.0. Neuraminidase solution was prepared to contain 0.2U in 0.5 ml

of bicarbonate-buffered saline pH 6.5.

Procedures

Standard Procedure (a) for Estimation of Formaldehyde

To a 50 μ l aliquot of 17.4 mM MBTH and a 50 μ l formaldehyde standard or sample (2 to 25 nmoles) which was incubated for 30 minutes at room temperature, 200 μ l of 9.25 mM ferric chloride was added. The reaction was quenched with 700 μ l of acetone after 5 minutes at room temperature and the absorbance at 670 nm was measured.

Standard Procedure (b) for Estimation of Formaldehyde

To a 50 μ l aliquot of 17.4 mM MBTH and a 200 μ l formaldehyde standard or sample, which was incubated for 30 minutes at room temperature, 50 μ l of 37.0 mM ferric chloride was added. The reaction was quenched with 700 μ l of acetone after 5 minutes and the absorbance at 670 nm was measured.

Periodate Treatment of Erythrocytes

Whole cells were washed in PBS as described by Fairbanks et al. (19). Washing was judged complete when glucose was not detected in the wash supernatant either by (a) using a serum glucose kit based on a glucose oxidase-peroxidase coupled system, or (b) treating an aliquot with periodate (see below) and then subjecting it to the MBTH test for

formaldehyde (see above). After washing the erythrocytes were resuspended to the original volume of whole blood taken. Coulter Counter determination (performed at Windsor Salvation Army Hospital, Windsor, Ontario by M. Goodwin) on such suspensions typically showed 2.5×10^9 cells per ml (21% hematocrit, 7.4% hemoglobin).

One ml aliquots of the above suspension were treated with 50 μ l of 20 mM periodate for 10 minutes at 0°C in the dark (32) before centrifugation for one minute. Quadruplicate aliquots of the supernatant, 50 or 200 μ l, were removed and tested for formaldehyde using the standard procedure.

Hemolysis of Erythrocytes

Washed erythrocytes at 21% hematocrit were centrifuged and the supernatant was replaced by lysis buffer. Centrifugation yielded a hemolysate considered to be 74 mg/ml in hemoglobin, based on 7.4g% hemoglobin in the initial suspension (see above). Serial dilutions of this stock were prepared with PBS.

Periodate Treatment of Erythrocyte Ghosts

Ghosts were prepared by hypotonic lysis as described by Fairbanks et al. (19) and finally suspended in PBS to correspond to a packed cell volume of 20%. Protein concentration (187) at this stage was 0.86 mg per ml.

Periodate oxidation was carried out on one ml aliquots as for the intact cells, above, and the supernatants were likewise tested for formaldehyde.

Formaldehyde Treatment of Erythrocytes or Ghosts

Whole cell or ghost suspensions in PBS as above, 1 ml aliquots of 20% suspensions except as noted, were mixed with 40 to 500 nmoles formaldehyde in 50 μ l. The mixtures were incubated for 10 minutes at 0°C, centrifuged, and quadruplicate 50 μ l aliquots of the supernatants were tested for formaldehyde. At 2×10^8 cells/ml 2 ml suspensions were taken and quadruplicate 200 μ l aliquots of the supernatants were tested for formaldehyde.

Determination of Optimal Enzyme Activity, and Incubation Time for Enzymatic Determination of Hydrogen Peroxide, Glucose, Galactose and Choline

In the procedures detailed below units of enzyme activity are given based on the respective manufacturer's unit definition and nominal specific activity. Due to the wide variation in conditions for enzyme specific activity determination we have elected to determine optimal levels of enzyme activity empirically as follows. The range of substrate concentrations comprising the standard curve was tested with a range of enzyme concentrations. Since the procedures given below involve quenching of the enzymic

reaction by 3.3-fold dilution with acetone (or aqueous acid) these trial runs were formulated with the concentrations existing in the enzymic reactions prior to quenching. To cover approximately the same range of substrate concentration the higher absorbances in these undiluted solutions were determined in 0.5 cm pathlength cuvettes. The wavelength chosen was 630 nm, the maximum for the tetraazapentamethine dye in aqueous solution (188). Absorbance versus time curves were recorded and that enzyme activity furnishing the highest absorbance and the greatest stability of that absorbance across the range of substrate concentrations was selected as optimal. The incubation times given prior to quenching were determined from the same sets of progress curves.

Standard Procedure (a) for Hydrogen Peroxide

To a 200 μ l aliquot of reagent solution containing 0.85 mM MBTH and 0.83 mM formaldehyde was added 50 μ l of H_2O_2 sample or standard solution. The reagent blank contained H_2O rather than H_2O_2 . The reaction was then initiated at room temperature by adding 50 μ l (0.5U) of peroxidase solution and was quenched with 700 μ l of acetone (or 1N HCl) 45-120 seconds after starting. The absorbance at 670 (or 630) nm was measured 15-30 minutes after quenching.

Standard Procedure (b) for Hydrogen Peroxide

To a 50 μl aliquot of reagent solution containing 3.4 mM MBTH and 3.32 mM formaldehyde was added 200 μl of H_2O_2 sample or standard solution. The reagent blank contained H_2O rather than H_2O_2 . The reaction was initiated at room temperature by adding 50 μl (0.5U) of peroxidase solution and was quenched with 700 μl of acetone (or 1N HCl 45-120 seconds after starting). The absorbance at 670 (or 630) nm was measured 15-30 minutes after quenching.

Standard Procedure for Glucose

To a 200 μl aliquot of reagent solution containing 0.85 mM MBTH and 0.83 mM formaldehyde was added 50 μl of a mixture of peroxidase (0.5U) and glucose oxidase (5U). Subsequently, 50 μl of standard glucose solution was added. The reagent blank contained H_2O rather than glucose. This reaction was quenched with 700 μl of acetone 5-7 minutes after starting and the absorbance measured at 670 nm 15-30 minutes after quenching.

Standard Procedure for Galactose

Equal volumes (25 μl) of the standard serial dilutions of galactose and galactose oxidase (5U) were allowed to react. After 2.5-3.5 minutes each of these solutions was diluted with a 200 μl aliquot of the reagent solution.

containing 0.85 mM MBTH and 0.83 mM formaldehyde and 50 μ l of peroxidase solution (0.25U). The reagent blank contained H₂O rather than galactose. The reaction was quenched with 700 μ l of acetone 15-45 seconds after starting and the absorbance measured at 670 nm 15-30 minutes after quenching.

Standard Procedure for Choline

Equal volumes (25 μ l) of the standard serial dilutions of choline chloride and choline oxidase (0.3U) were allowed to react. After 3.5-5.0 minutes each of these solutions was diluted with a 200 μ l aliquot of the reagent solution containing 0.85 mM MBTH and 0.83 mM formaldehyde and 50 μ l of peroxidase solution (0.25U). The reagent blank contained H₂O rather than choline chloride. The reaction was quenched with 700 μ l of acetone 50-120 seconds after starting and the absorbance measured at 670 nm 15-30 minutes after quenching.

Galactose Oxidase Treatment of Cell Surface

Carbohydrates

Membranes were warmed 15 minutes at 37°C to restore their discoid shape (189). Then to 500 μ l packed erythrocyte ghosts was added 10U galactose oxidase in sodium phosphate buffer, pH 7.0, for 1 hour. The suspension was washed twice with 0.2M galactose in phosphate wash buffer.

and twice further in excess phosphate wash buffer.

Neuraminidase Treatment of Cell Surface Carbohydrates

After warming membranes for 15 minutes at 37°C (189), 0.2U neuraminidase in saline bicarbonate buffer, pH 6.5, was added to 500 μ l packed erythrocyte ghosts (190) for 1 hour. The ghosts were then washed thrice in excess phosphate wash buffer.

Hemagglutination Assays

Washed human erythrocytes or ghosts, regardless of blood type, at 2% cell suspension in PBS was used in all the hemagglutination tests unless noted otherwise. These tests were done by the double dilution technique in micro-titer plates (191).

Synthesis of 2-nitro-4-azidofluorobenzene (F-NAP)

2-nitro-4-azidofluorobenzene was prepared by the method of Fleet et al. (192).

Synthesis of N-(2-nitro-4-azidophenyl)- β -alanine (NAPBA)

N-(2-nitro-4-azidophenyl)- β -alanine was prepared according to the procedure of Jeng and Guillory (193) as modified by Hosang et al. (194).

Synthesis of N-(2-nitro-4-azidophenyl)- β -alanine
methyl ester (NAPBAME)

400 mg NAPBA was dissolved in 20 ml methanol. To it was slowly added 2-3 drops of concentrated sulfuric acid. This solution was heated under stirring at 50-60°C for 6 hours, the volume reduced to 2 ml and cooled to room temperature. Excess sulfuric acid was neutralized by adding dropwise 1M sodium bicarbonate to pH 8.3. The solution was extracted with five 80 ml portions diethyl ether. The ethereal solution was evaporated to dryness and the residue recrystallized from hot methanol-water (1:2.5). Dark red crystals were obtained in 95% yield. IR revealed absorption bands at 2200, 1750, 1550, 1435 and 1350, 1270 and 1200 cm^{-1} while NMR ($\text{d}_4\text{-CH}_3\text{OH}$) showed triplets at 3.1 and 4.0 ppm, singlet at 4.0 ppm and doublets at 7.5 and 8.0 ppm. This compound melted at 58-59°C. Elemental analysis (Galbraith Laboratories, Knoxville, TN) calculated for $\text{C}_{10}\text{H}_{11}\text{N}_5\text{O}_4 \cdot \text{CH}_3\text{OH}$:
C = 44.44%, H = 5.05%, N = 23.57%, found: C = 44.07%,
H = 4.36%, N = 24.94%.

Synthesis of N-(2-nitro-4-azidophenyl)- β -alanine
hydrazide (NAPBAH)

250 mg of NAPBAME was dissolved in 30 ml hot methanol. To this solution was added 5 mmoles anhydrous hydrazine. The solution was stirred under heating at 60°C for 16 hours. Thin

layer chromatography of the solution at this stage showed only one spot corresponding to the hydrazide. The mixture was evaporated to dryness and recrystallized in hot methanol-water (1:2) to obtain dark red crystals in quantitative yield. NMR (d_6 -DMSO) revealed singlets at 4.4 and 8.3 ppm, doublets at 7.3 and 7.8 ppm and triplets at 2.4 and 3.5 ppm. IR showed absorptions at 2140, 1650, 1540, 1360 and 1450, 1420 and 1270 cm^{-1} . This compound melted at 110-113°C. UV(H_2O)-255 nm ($\epsilon = 8.5 \times 10^3$) and 465 nm ($\epsilon = 3.0 \times 10^3$) and UV(CH_3OH)-255 nm ($\epsilon = 1.5 \times 10^4$) and 450 nm ($\epsilon = 4.5 \times 10^3$). Elemental analysis (Galbraith Laboratories, Knoxville, TN) calculated for $C_9H_{11}N_7O_3 \cdot H_2O$: C = 38.16% H = 4.59%, N = 34.63% found: C = 38.57%, H = 4.60%, N = 27.01%.

Incorporation of N-(2-nitro-4-azidophenyl)- β -alanine hydrazide into Cell Surface Periodate- and Galactose Oxidase-Generated Aldehydic Groups

Two milliliters of a 50% cell suspension were oxidized with 100 μ l of 20 mM sodium periodate for 10 minutes at 0°C in the dark (32) or treated with 20U of galactose oxidase for 1 hour at 37°C (99). The cells were washed thrice in excess phosphate wash buffer 9,000 rpm (9,750 x g) for 3 minutes and sedimented. To the pellet was added 2 ml of 700 μ M N-(2-nitro-4-azidophenyl)- β -alanine hydrazide

thoroughly mixed and let stand for 4 hours at room temperature in the dark, with periodic mixing of the solution. The cells were washed and sedimented as above. To this was added 10% SDS to a final 1.0% and the absorbance of the solution monitored as a function of wavelength.

Photolysis Experiments

A Rayonet photochemical reactor model RPR-100 equipped with RPR-3500A lamps was used for photolysis experiments. These lamps give a broad band of radiation between 300-420 nm. All experiments were done at room temperature in a photolysis vessel shown in Figure 16. The solutions of N-(2-nitro-4-azidophenyl)- β -alanine hydrazide and erythrocyte ghost suspensions were contained in tube A, (inside diameter 1.4 cm). Rod B (outside diameter 1.1 cm), was inserted to facilitate photolysis of a narrow film of solution (0.1 to 0.2 cm) and was slowly rotated to thoroughly mix the solutions.

Agglutinated derivatized erythrocyte ghosts at 2 and 4 percent suspensions were photolyzed for 5 minutes at room temperature. After photolysis, ghost suspensions were poured into 15 mm x 80 mm centrifuge tubes. The residue on Rod B was rinsed thrice with phosphate wash buffer and collected in the same tube. Ghost suspensions were sedimented at 9,000 rpm (9,750 x g) for 3 minutes and the pellet was washed twice in excess

Figure 16

Photolysis Vessel

Legend

To a quartz tube (A), 25 cm x 1.4 cm, was added 8 ml. sample. To reduce the path length (0.2 - 0.1 cm) for the incident light a Pyrex rod (B), 39 cm x 1.1 cm, was inserted. In a Rayonet Photochemical Reactor (RPR 100) the samples were irradiated with sixteen RPR 3500A lamps at a distance of 12 cm.

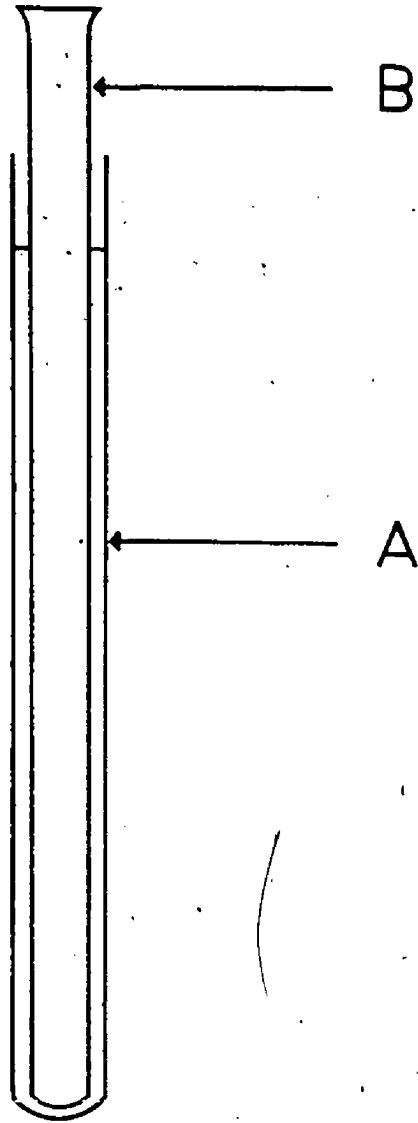


Figure 16

phosphate wash buffer containing 200 mM galactose or 200 mM N-acetyl-D-glucosamine to remove unbound lectin and twice in excess phosphate wash buffer. The pellet was collected and prepared for sodium dodecyl sulfate polyacrylamide gel electrophoresis.

Photolysis of aqueous and methanolic solutions of N-(2-nitro-4-azidophenyl)- β -alanine hydrazide was performed for various times. Aliquots were removed and their corresponding visible and ultraviolet spectra recorded.

Polyacrylamide Gel Electrophoresis

5.6% polyacrylamide tube gels, 6 mm x 160 mm, were prepared using the sodium dodecyl sulfate (SDS) system of Fairbanks *et al.* (19) or 8.0% and 7.0% polyacrylamide slab gels, 1 mm x 11 cm x 15 cm, using the SDS system of Laemmli (195). The membrane sample (in phosphate wash buffer) was mixed with an equal volume of solubilizing, reducing solution (19) and boiled 5 minutes.

Using the electrophoresis procedure of Fairbanks *et al.* (19), approximately 100 μ l samples (containing 150 μ g of membrane protein) were applied to the gel. Total membrane protein was determined by the method of Peterson (187) on a portion of the membrane sample prior to solubilization. Electrophoresis was performed on a Bio-Rad Model 500 Gel Electrophoresis Power supply at an initial current of 2.0 mA/gel until the tracking dye had sufficiently penetrated

the gel then at a constant current of 10 mA/gel for about 3 hours. After electrophoresis, the dye front was marked and the gels were stained for protein for 16 hours in a solution of 0.1% Coomassie Brilliant Blue-R, 25% 2-propanol and 10% glacial acetic acid. The latter was observed not to be important in protein fixing and was omitted in subsequent experiments. The gels were destained in 10% 2-propanol and 10% glacial acetic acid solution for 16 hours and repeated once. Gels were stored in 10% acetic acid.

Sialoglycoproteins were identified using the classical periodic acid Schiff (PAS) staining procedure (19,31).

Using the electrophoresis system of Laemmli (195) approximately 10 μ l samples (containing 30 μ g of membrane protein) were deposited in a 3 mm-wide slot. An initial current of 2.5 mA/lane which was used during the stacking of the membrane sample was changed to a constant current of 8 mA/lane for about 1.5 hours. After electrophoresis the gels were stained for protein or glycoproteins using an ultrasensitive procedure employing a silver stain (195,197). Proteins were also stained with Coomassie Brilliant Blue-R as described above.

Gels were then scanned and the absorbance of the stained proteins measured on an Ortec 4310 densitometer at 560 nm.

CHAPTER III

RESULTS AND DISCUSSION

A New Peroxidase Color Reaction

The chromogen 3-methyl-2-benzothiazolinone hydrazone was first used to measure minute quantities of aldehyde in solution (198,199) and air (200) via initial Schiff-base formation. In these non-enzymic reactions a blue cationic tetraazapentamethine dye forms, Figure 17. The azine is formed by the condensation of formaldehyde and MBTH. Subsequent formation of the blue chromophore occurs by oxidative coupling of MBTH with the azine in a four-electron process. Hünig has suggested that reactions of this type proceed via the diazenium ion of MBTH (188). The extinction coefficients for this colored cationic dye in 100% acetone, 70% acetone and water have been reported to be 70,000 (201), 65,000 (198) and 66,000 (199), respectively. Subsequently, MBTH was shown to have a broad range of applicability including the determination of soluble and insoluble carbohydrates (202,204). Its sensitivity has led us to investigate the potential for peroxidase-catalyzed oxidative coupling of MBTH and the azine as a means of

Figure 17

Oxidative Coupling of 3-Methyl-2-Benzothiazolinone
Hydrazone with its Azine Generating the
Blue Chromophore

Legend

Schematic illustration of the oxidation of the chromogen (MBTH) and its corresponding azine forming the final blue tetraazapentamethine dye. The absorbance of the chromophore is measured at 635 or 670 nm.

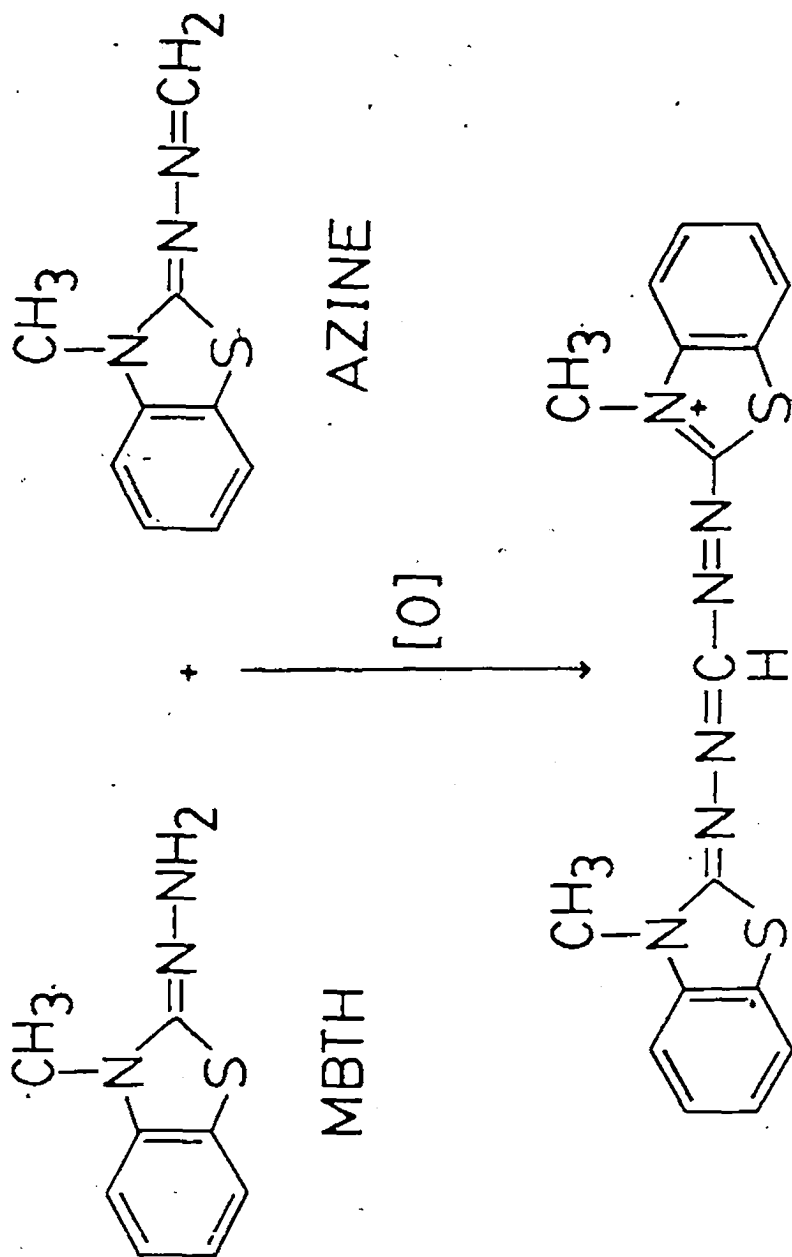


Figure 17

measuring limiting hydrogen peroxide.

Initial studies showed that hydrogen peroxide in the presence of peroxidase was indeed capable of oxidatively coupling MBTH with the azine to give the same cationic tetraazapentamethine dye (198). Figure 18 shows spectra of the reaction mixture quenched in aqueous acid solution and in aqueous acetone (70% acetone, by volume). Prior to quenching the stability of the chromophore generated has been found to be dependent on peroxidase activity and pH (199). With respect to the latter parameter it was observed that the chromophore was comparatively stable at pH's in the neighbourhood of 3.0 - 3.5 as shown in Figure 19.

The mixture of MBTH and its azine was formed by incubating formaldehyde with excess MBTH. In choosing the final concentrations of MBTH (0.57 mM) and formaldehyde (0.55 mM) we examined concentrations ranging from 9.13 mM and 8.67 mM, respectively, to 0.052 mM and 0.048 mM, respectively. Data are presented in Table 1. For these experiments MBTH and formaldehyde were not pre-mixed, as for the standard procedure, but were removed from separate stock solutions and added to each test. The mixture of these two stock solutions (200 μ l) was allowed to stand for 30 minutes at room temperature to allow for azine formation before peroxide and peroxidase were added. Two aspects

Figure 18

Spectra of the Quenched Reaction Mixtures

Legend

The standard procedure (a) for hydrogen peroxide was carried out with 44 nmoles of hydrogen peroxide. Spectra of the quenched reaction mixtures were recorded directly against their respective blanks. Upper curve, quenched with acetone; lower curve, quenched with 1N HCl.

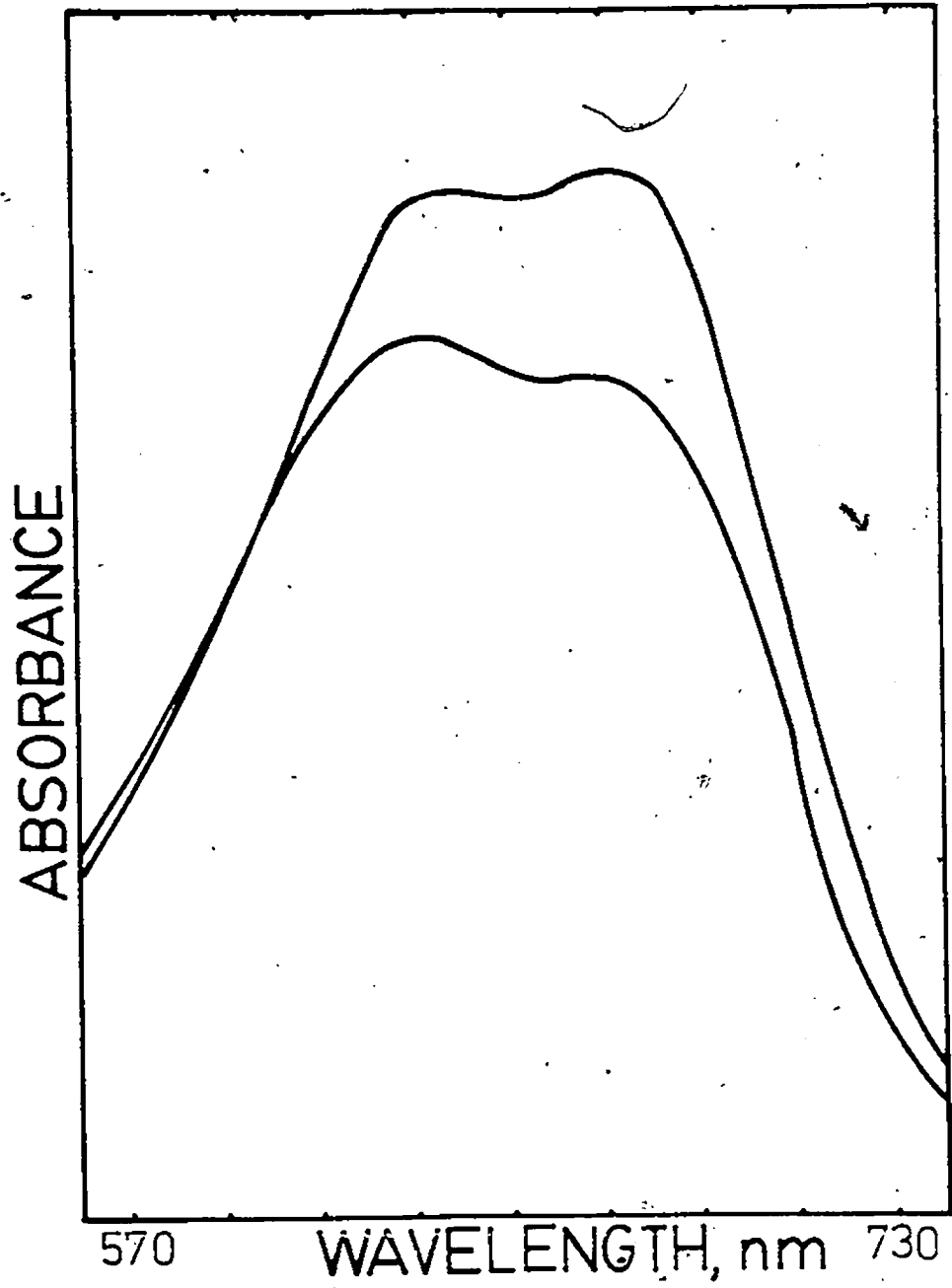


Figure 18

Figure 19

Influence of pH on Chromophore Formation

Legend

Runs were formulated as in the standard procedure (a) for hydrogen peroxide with hydrogen peroxide at 151 μ M except that the reactions were carried out at different pH's using acetate and phthalate-HCl buffers. Reactions were not quenched, but the maximum absorbance of these runs were determined by monitoring A_{630} as a function of time. At pH 3.50 two similar reactions using both buffers were monitored and similar maxima at A_{630} were obtained.

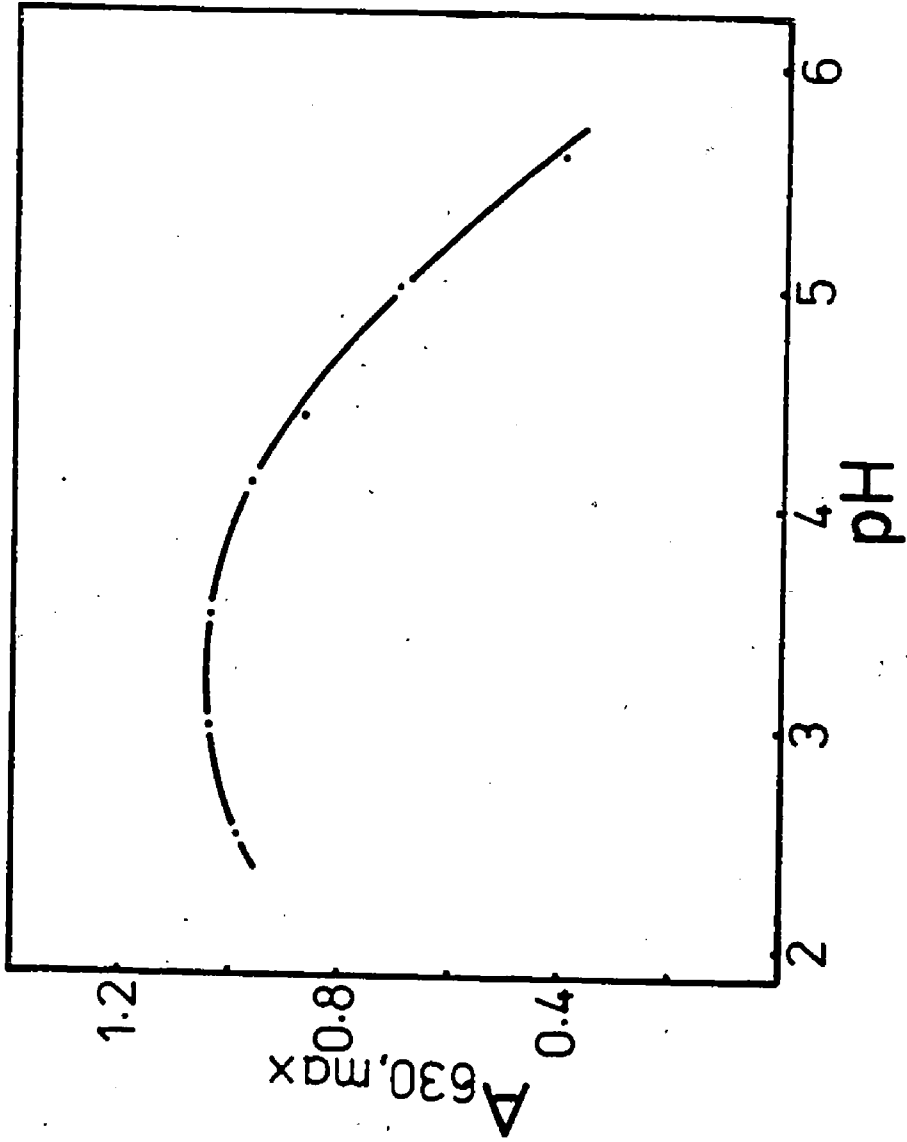


Figure 19

TABLE 1

Color Yield for Coupling of MBTH and its
Azine as a Function of Reagent
Concentration and Ratio^a

| Experiment | [MBTH] (mM) | [HCHO] (mM) | [H ₂ O ₂] (mM) | A _{630,max} |
|------------|----------------|----------------|--|-----------------------|
| 1 | 0.567 | 0.533 | 0.150 ^b | 2 (1.70) ^c |
| 2 | 9.130 | 8.670 | 0.030 | 0.30 |
| 3 | 4.570 | 4.330 | 0.030 | 0.60 |
| 4 | 1.030 | 1.000 | 0.045 | 1.06 |
| 5 | 0.173 | 0.167 | 0.045 | 1.06 |
| 6 | 0.567 | 0.433 | 0.030 | 0.60 |
| 7 | 0.173 | 0.130 | 0.045 | 0.98 |
| 8 | 0.142 | 0.043 | 0.030 | 0.30 |
| 9 | 0.567 | 0.567 | 0.150 ^b | 2 (1.56) |
| 10 | 0.052 | 0.048 | 0.045 | 0.72 |

^aReactions were formulated at pH 3.44 and room temperature with the reagent concentrations noted plus peroxidase at 1.0 - 1.5 U/ml. Separate stock solutions of MBTH and formaldehyde were combined first and incubated 30 minutes at room temperature, to allow for azine formation, before addition of hydrogen peroxide. Absorbance at 630 nm was monitored as a function of time in 1-cm path-length cuvettes except as noted.

^bThis hydrogen peroxide concentration represents the maximum that would be experienced in the initial enzymatic phase of the standard procedure (a) for hydrogen peroxide (50 nmoles H₂O₂ in 0.3 ml).

^cThese absorbances were read in 0.5 cm path-length cuvettes.

of the reagent formulation were considered: absolute concentration and the ratio of azine to free MBTH. As formaldehyde concentration in the initial mixture reached approximately 8.67 mM and MBTH concentration reached 9.13 mM, crystallization occurred and hence concentrations above this level were not further considered. Concerning the ratio of coupling partner to oxidizable substrate (azine to MBTH here), others have suggested a ratio of 50 as necessary (124). In our case the highest absorbances were obtained with ratios of 20 or greater (Table 1, experiments 1, 3-5). However, only slightly lower color yields were observed with ratios down to 3 (experiments 6,7) but it seems clear that ratios of less than 1 (excess of the oxidizable substrate) were unacceptable (experiment 8). At the opposite extreme, where nominal concentration of oxidizable substrate was zero, a slight decrease was noted (experiment 9). The final entry in Table 1 shows that the reagent amounts not greatly in excess of stoichiometric still give appreciable color development.

For the standard procedure we have selected the conditions of experiment 1. As Table 1 stands it would appear that the conditions of experiment 5 would serve equally. However, as it was the intent to quench the reaction mixtures with acetone or 1N hydrochloric acid we

sought conditions in which chromophore development proceeded in an initial 0.3 ml volume prior to dilution to 1.0 ml on quenching. Thus, the peroxide concentrations presented in Table 1 span the range expected for the initial 0.3 ml volumes of the standard procedures. If the MBTH and formaldehyde concentrations in experiment 5 were chosen with hydrogen peroxide at 0.150 mM for the initial enzymic reaction the relative reagent and peroxide concentrations would be similar to those of experiment 10 and thus a loss in color yield would be expected.

Peroxidase concentration was very important when generating the final blue chromophore. As outlined in the experimental section, different amounts of enzyme activity were tested in our assay. Shown in Figure 20 are curves of absorbance (630 nm) versus time at various enzyme levels over a range of peroxide concentrations. It was evident that variation in the amount of enzyme activity dramatically affected the rate of chromophore formation. Less dramatic was the rate of decay of absorbance as a function of enzyme concentration which appeared to increase slightly with decreasing enzyme concentrations. For example, the decay rates for the data in Figures 20A through D are, 2.8 to 1.5, 2.5 to 1.3, 3.5 to 1.8 and 3.3 to 1.7% per minute, respectively, where the percentages decrease with

Figure 20

Influence of Peroxidase Concentration on
Chromophore Formation and Stability

Legend

Runs were formulated as in the standard procedure (a) for hydrogen peroxide except that the reactions were not quenched. Enzyme concentrations of 2.78, 1.67, 0.67 and 0.33 U/ml are represented in panels A through D, respectively. At each enzyme concentration hydrogen peroxide amounts of 146, 97, 73 and 36 μM were taken and are represented by curves (i) through (iv), respectively.

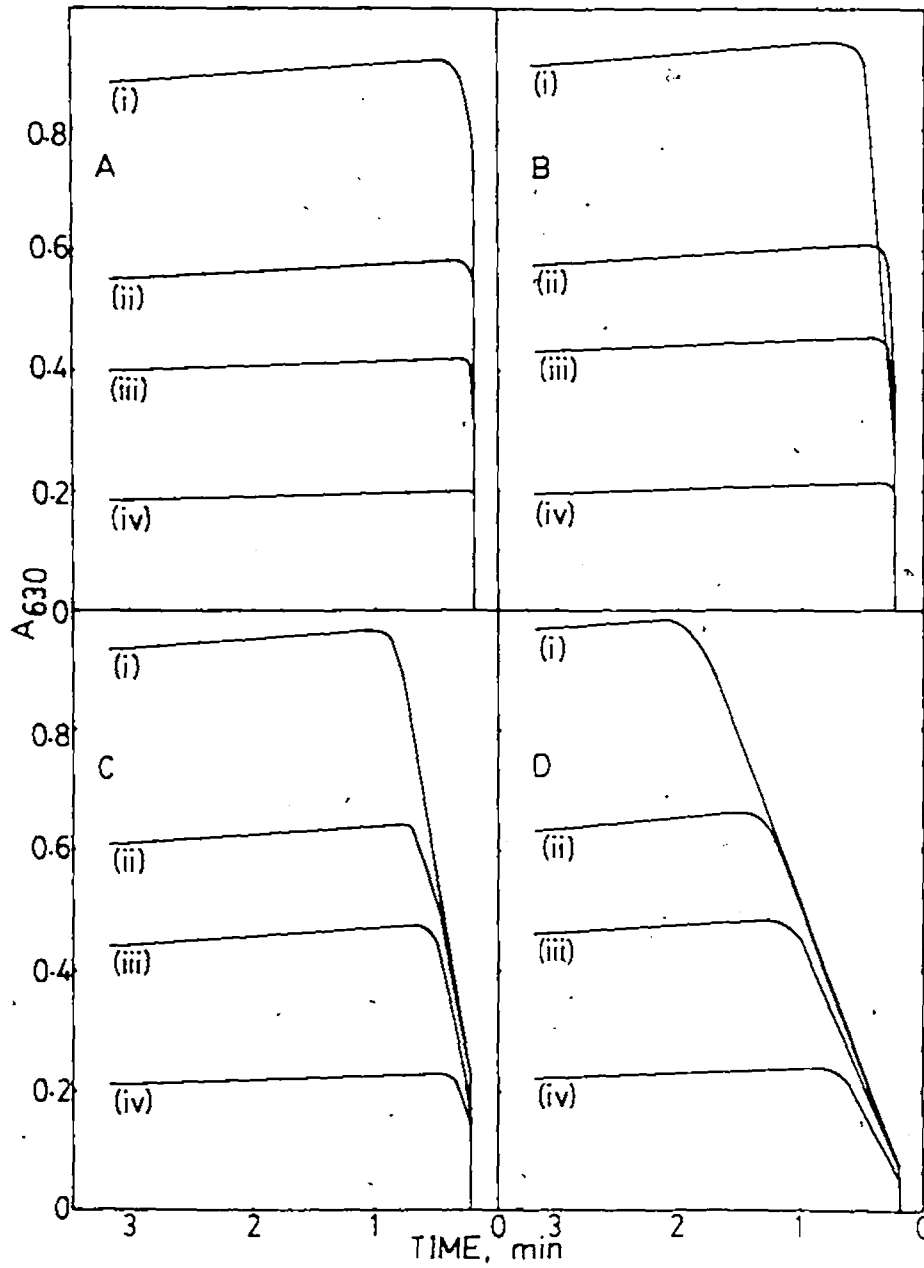


Figure 20

increasing hydrogen peroxide concentration.

The data represented in Figure 20, and more not shown there, were used to calculate extinction coefficients as a function of enzyme level using the maximum absorbances at 630 nm. The results, given in Table 2, show that higher color yields were achieved at lower enzyme concentrations. However, at peroxidase concentrations below 0.67 U/ml the absorbance maxima for a range of peroxide concentrations were reached at widely different times as exemplified by Figure 20D. Thus, for the standard procedure an enzyme level of 1.67 U/ml (0.5 U/0.30 ml), Figure 20B was chosen as giving the best compromise between extinction coefficient and time required to reach the maximum absorbance across the desired range of peroxide concentrations.

The optimization described above was performed in aqueous solutions. The same studies indicated the necessity for quenching and indicated the time window in which it should be carried out for a given enzyme level. Significant stabilization of the chromophore has been observed upon dilution with acetone (198) or upon acidification to pH 1 (199). The data for both quenching methods are shown in Table 3 and plotted in Figure 21. Assuming two moles of peroxide are consumed per mole of chromophore formed the extinction coefficient for this chromophore may be calculated

TABLE 2

Influence of Peroxidase Concentration
on Chromophore Formation^a

| [Enzyme] (U/ml) | Extinction coefficient ^b ($\text{mM}^{-1}\text{cm}^{-1}$) | y-Intercept |
|--------------------|---|--------------------|
| 4.17 | 48.2 \pm 1.3 | -0.241 \pm 0.009 |
| 2.78 | 51.2 \pm 0.6 | -0.199 \pm 0.004 |
| 1.67 | 52.4 \pm 0.4 | -0.161 \pm 0.003 |
| 0.67 | 53.1 \pm 0.3 | -0.085 \pm 0.002 |
| 0.33 | 53.7 \pm 0.4 | -0.067 \pm 0.003 |
| 0.22 | 53.6 \pm 0.6 | -0.058 \pm 0.004 |
| 0.17 | 52.3 \pm 0.7 | -0.054 \pm 0.005 |

^aRuns were formulated as in the standard procedure (a) for hydrogen peroxide with the amounts of hydrogen peroxide shown in Figure 20, except that enzyme concentration was varied and reactions were not quenched. Absorbance at 630 nm was followed as a function of time and the maximum absorbance, $A_{630,\text{max}}$, was determined in each case.

^bLinear regression analysis of the $A_{630,\text{max}}$ versus $[\text{H}_2\text{O}_2]$ data yielded a y-intercept, shown, and a slope from which the extinction coefficient was calculated, assuming 2 equivalents of H_2O_2 per mole of chromophore. Correlation coefficients were greater than 0.998. Error limits shown are root mean square deviations.

TABLE 3

Standard Curve Data for Hydrogen Peroxide^a

| <u>Quenched with 1N HCl</u> | | <u>Quenched with Acetone</u> | |
|-----------------------------|---------------|------------------------------|---------------|
| H_2O_2 (nmol) | A_{630} | H_2O_2 (nmol) | A_{670} |
| 43.5 | 1.156 ± 0.007 | 45.1 | 1.473 ± 0.005 |
| 29.0 | 0.700 ± 0.005 | 30.1 | 1.010 ± 0.006 |
| 21.8 | 0.521 ± 0.000 | 22.6 | 0.718 ± 0.005 |
| 10.9 | 0.258 ± 0.002 | 11.3 | 0.316 ± 0.004 |

^aRuns were formulated in quadruplicate as in the standard procedure (a) for hydrogen peroxide. The uncertainties shown are root mean square deviations.

Figure 21

Standard Curve for Hydrogen Peroxide

Legend

Data from Table 3 are plotted: open circles - acetone quenched, closed circles - 1N HCl quenched. Lines drawn are from linear regression with correlation coefficients greater than 0.997. Equation of the line for the chromophore in acetone is, $A_{670} = (0.6865 \pm 0.00196) (0.05) \text{ (nmoles H}_2\text{O}_2) - (0.056 \pm 0.007)$ and in 1N HCl, $A_{630} = (0.05510 \pm 0.02236) (0.05) \text{ (nmoles H}_2\text{O}_2) - (0.065 \pm 0.008)$.

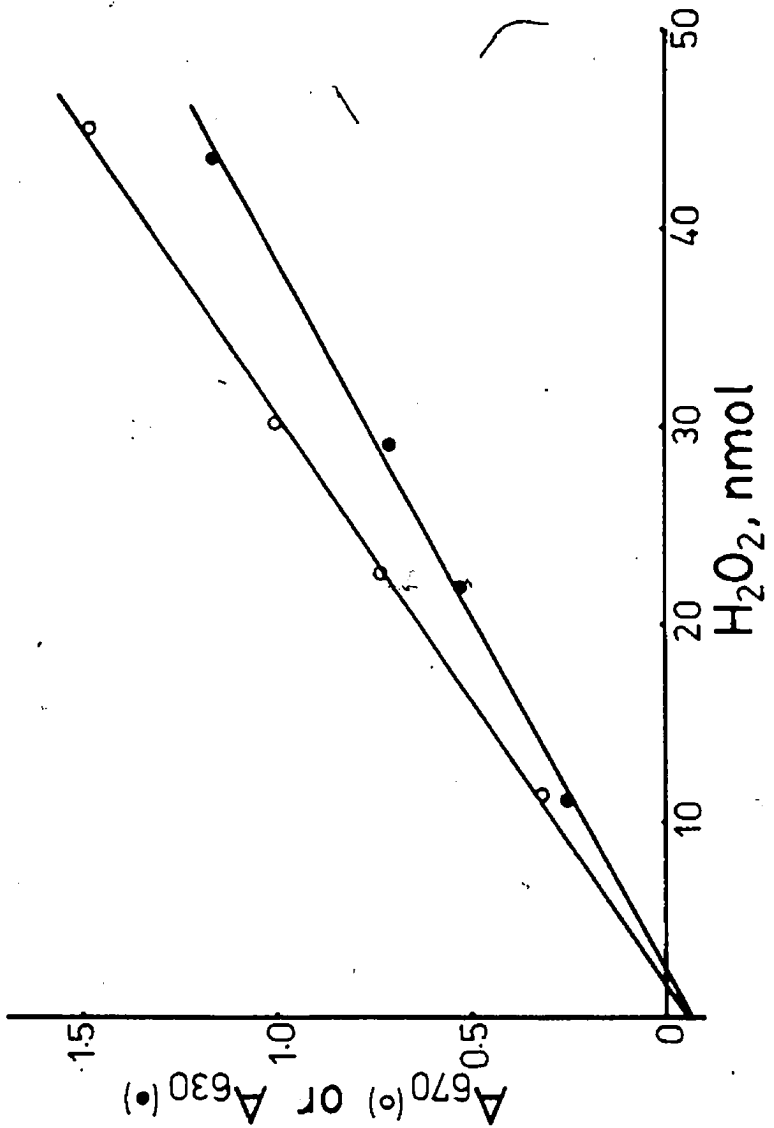


Figure 21

for an aqueous acid medium, $55.1 \pm 2.4 \text{ mM}^{-1}\text{cm}^{-1}$, or in an aqueous organic medium, $68.7 \pm 2.0 \text{ mM}^{-1}\text{cm}^{-1}$. Acetone as a quenching agent clearly gives a superior color yield but has obvious drawbacks with respect to the vessels used.

The foregoing results encouraged us to consider glucose as a potential source of hydrogen peroxide in the presence of glucose oxidase. While this enzyme has optimal activity at pH 5.6, 25% of the maximal activity is shown at pH 3.5 (205). Glucose oxidase, a flavoenzyme, oxidizes D-glucose at the C-1 position to yield a stoichiometric amount of D-gluconic acid and hydrogen peroxide via the D-glucono-1,5-lactone as shown in Figure 22. Thus, we initially concerned ourselves with a coupled enzyme system at pH 3.44. Again the optimal amount of enzyme present in the reaction mixture had to be determined. This was done spectrophotometrically by monitoring the initial reaction as a function of time as previously described. Other authors (119,124) have suggested that glucose oxidase activity exceed that of peroxidase by several fold. In Figure 23 the solid and dotted lines, respectively, show data based on glucose oxidase:peroxidase ratios of 10 and 30. In each case peroxidase activity was maintained at the level (1.67 U/ml) chosen above. The higher ratio (Figure 23, dotted lines) not only resulted in a lower color yield but also apparently

Figure 22

Glucose Oxidase Treatment of D-Glucose

Legend

D-glucose in the presence of glucose oxidase and the coenzyme flavin adenine dinucleotide undergoes oxidation at the C-1 alcohol position yielding D-glucono-1,5-lactone and hydrogen peroxide in stoichiometric amounts. Subsequent hydrolysis of the lactone to D-gluconic acid occurs.

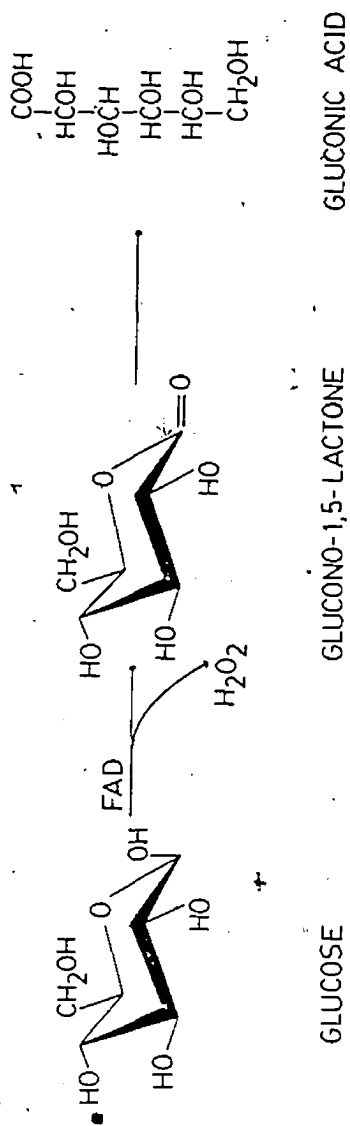


Figure 22

Figure 23

Influence of Glucose Oxidase Concentration on Chromophore Formation and Stability in the Coupled Glucose Oxidase-Peroxidase System

Legend

Glucose oxidase concentrations of 16.7 U/ml, solid lines, and 50 U/ml, broken lines, were included with peroxidase and chromogens as for the standard procedure (a) for hydrogen peroxide except that glucose, 133, 89, 67 and 33 μM was substituted for hydrogen peroxide, lines (i) through (iv), respectively.

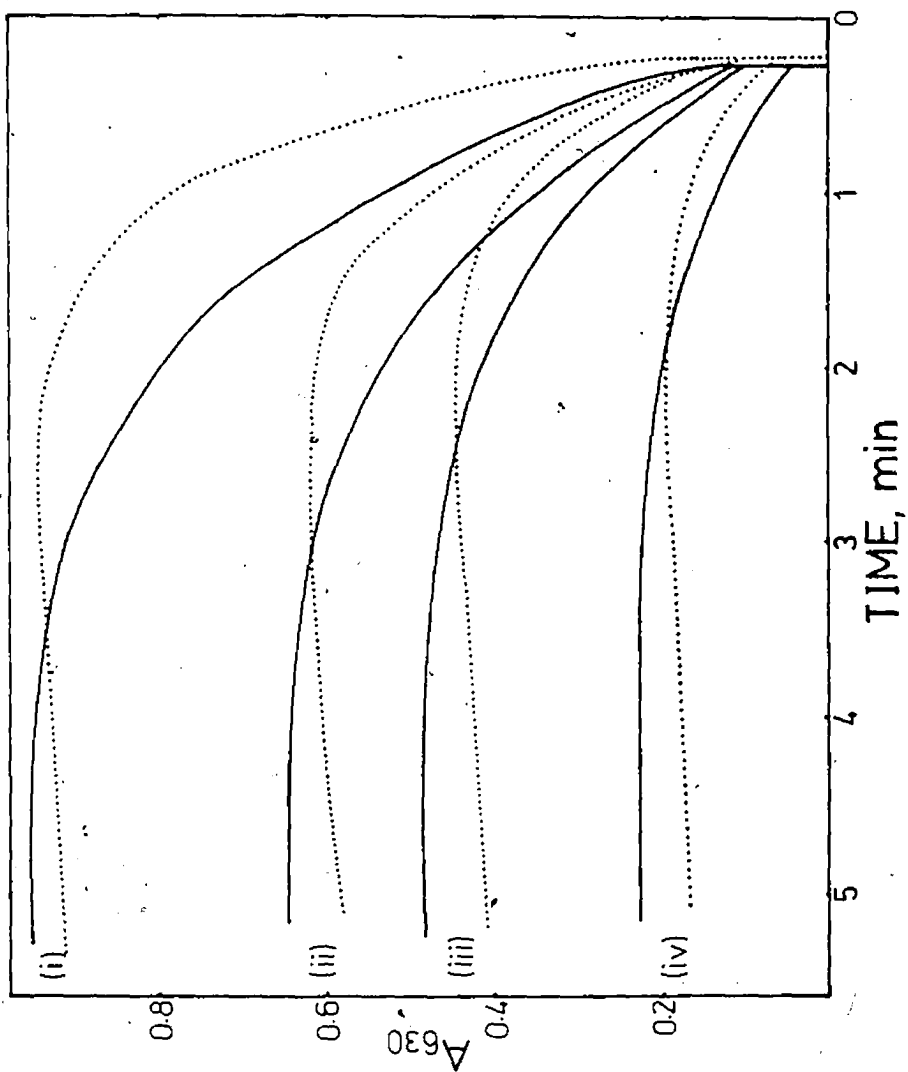


Figure 23

destabilized the chromophore in solution as seen by the rates of decay of absorbance after the maxima have been reached. For example, the decay rates for the data in Figure 23 are less than 0.7 and 2.3 to 1.5% per minute, for the oxidase:peroxidase ratios of 10 and 30, respectively.

The presence of catalase, even in trace amounts, in the glucose oxidase preparation could diminish the available peroxide (206). This problem would be acute if glucose oxidase were used in a stepwise procedure, at pH 3.44 as we do here, or at any other pH at which glucose oxidase is active (205). When glucose and glucose oxidase were incubated for two minutes at that pH before mixture with chromogen plus peroxidase a 40% loss in available hydrogen peroxide was observed. A recent article (206) suggested that certain concentrations of sodium azide selectively inhibit catalase in the presence of peroxidase. The stepwise procedure mentioned above was repeated but 30 μ M sodium azide was included in the first stage. The availability of hydrogen peroxide was 98% of theoretical. However, this concentration of sodium azide at the glucose oxidase stage (or six-fold diluted at the peroxidase stage) was markedly lower than 1-2 mM used by Thompson *et al.* (206). Indeed, when we attempted to use higher azide concentrations, peroxidase showed a large reduction in color yield in the

presence of hydrogen peroxide. For example, color yield was 80% of theoretical when sodium azide was included at 70 μ M at the glucose oxidase stage. It should be noted that the studies of Thompson et al. (206) were at pH 6.85 while our studies were carried out at pH 3.44 and this may account for the apparent discrepancy.

The maximum absorbances seen in Figure 23 (solid lines) represent 55-58% of those expected assuming the same extinction coefficient as for hydrogen peroxide. As a result of the specificity of glucose oxidase for β -D-glucose it was inferred that the rate of mutarotation for D-glucose was limiting under the conditions of our procedure from the following experiment. A reaction was formulated as for the 73.1 μ M curve in Figure 23 (solid line) and allowed to proceed until the absorbance at 630 nm levelled off at 61% of the absorbance expected based on the hydrogen peroxide data of Figure 21 (line for HCl quenched samples). The mixture was boiled, cooled, and an aliquot mixed with fresh enzymes and chromogen as in the standard procedure. The maximum absorbance at 630 nm for this mixture was 20% of the total expected for the original mixture or 61% of that not accounted for at the previous stage.

Figure 24 shows a standard curve for glucose using the enzyme levels discussed above, and acetone quenching as

Figure 24

Standard Curve for Glucose

Legend

The coupled glucose oxidase-peroxidase system at pH 3.44 was used as outlined in the experimental section on quadruplicate samples. Standard deviations on the absorbance readings were 0.005 or less. The line shown is the least squares line (correlation coefficient 0.997):
 $A_{670} = (0.03945 \pm 0.00117) (0.05) \text{ } \mu\text{moles glucose} - (0.048 \pm 0.004).$

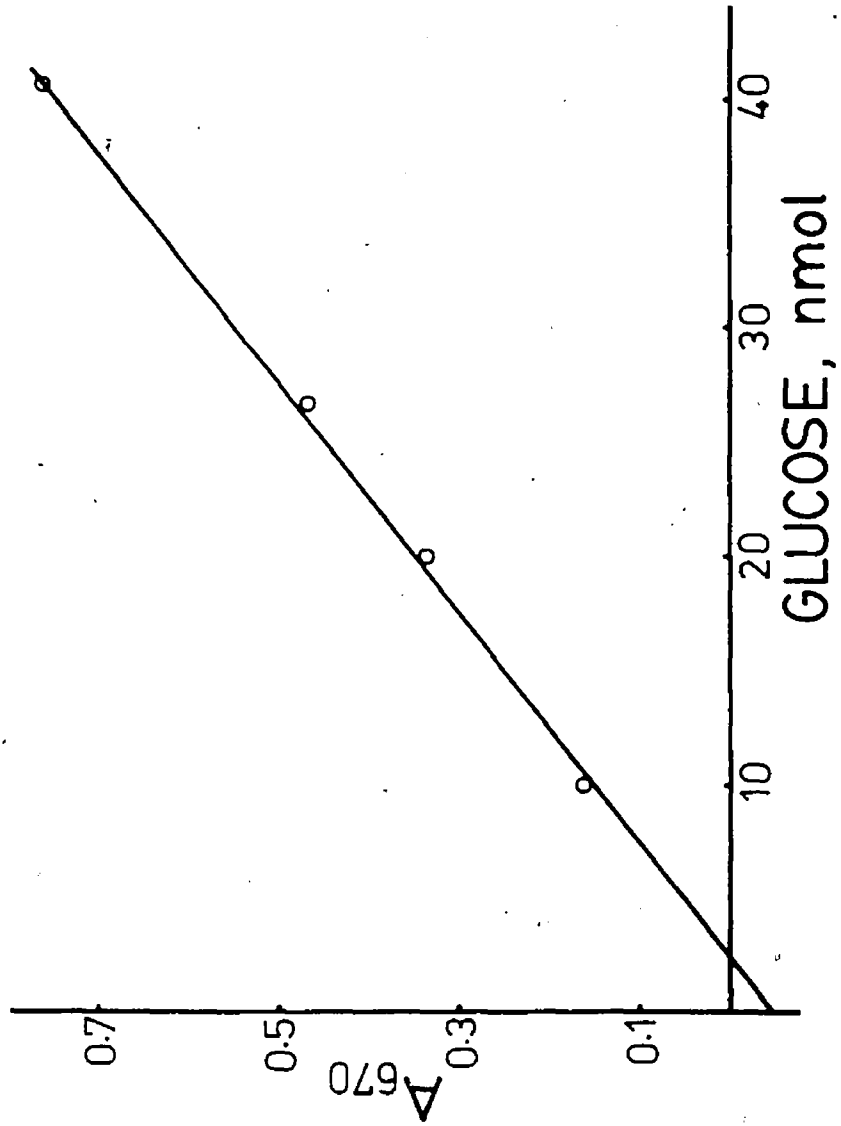


Figure 24

in the standard procedure. From that data an extinction coefficient of $39.5 \pm 1.2 \text{ mM}^{-1} \text{ cm}^{-1}$ may be calculated, which upon prororation for 64% β -D-glucose content becomes $61.7 \pm 1.8 \text{ mM}^{-1} \text{ cm}^{-1}$.

Adaptation of the chromogen system to a choline oxidase-peroxidase coupled reaction for determination of choline required a modification of our experimental design. Due to choline oxidase's pH optimum of 7.8 (120) it was necessary to generate hydrogen peroxide in a separate reaction mixture containing choline and choline oxidase. Choline oxidase oxidizes choline at the alcohol position yielding betaine and liberating two equivalents of hydrogen peroxide as shown in Figure 25. Figure 26 shows color development in the second (peroxidase) stages for aliquots which had been incubated at various times with choline oxidase at 6 U/ml. For the peroxidase stages here slightly better chromophore stability was observed with peroxidase activity of 0.83 U/ml. Figure 27 shows the color development and stability of the chromophore when varying amounts of choline were present with choline oxidase. These choline concentrations are similar to those in the standard procedure.

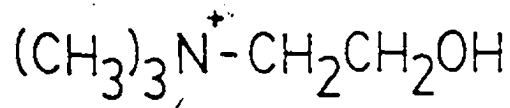
The standard curve for choline, shown in Figure 28, corresponds to an extinction coefficient of $55.6 \pm 1.8 \text{ mM}^{-1} \text{ cm}^{-1}$

Figure 25

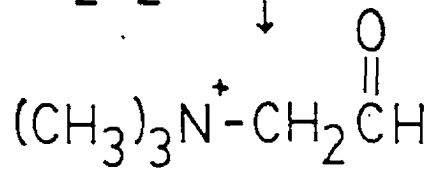
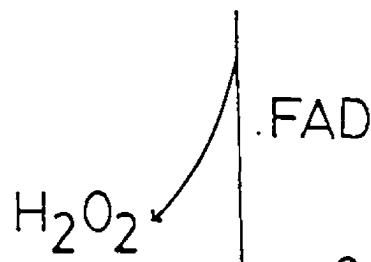
Choline Oxidase Treatment of Choline

Legend

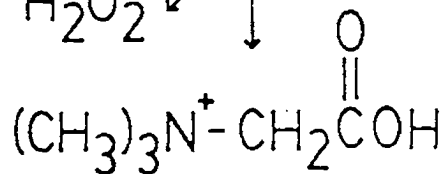
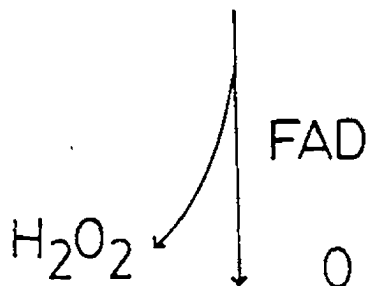
Choline oxidase, a flavoenzyme, in the presence of flavin adenine dinucleotide catalyzes the oxidation of choline at the alcohol position yielding the corresponding carboxylic acid betaine and two equivalents of hydrogen peroxide via the betaine aldehyde.



CHOLINE



BETAINE ALDEHYDE



BETAINE

Figure 25

Figure 26

Chromophore Formation in the Stepwise
Choline Oxidase-Peroxidase Reaction

Legend

Choline (40 nmoles/50 μ l) and choline oxidase were incubated at pH 7.8 as in the standard procedure. At various times 50 μ l aliquots were withdrawn and mixed with chromogens plus peroxidase as in the standard procedure. Reactions were not quenched, but A_{630} was monitored as a function of time.

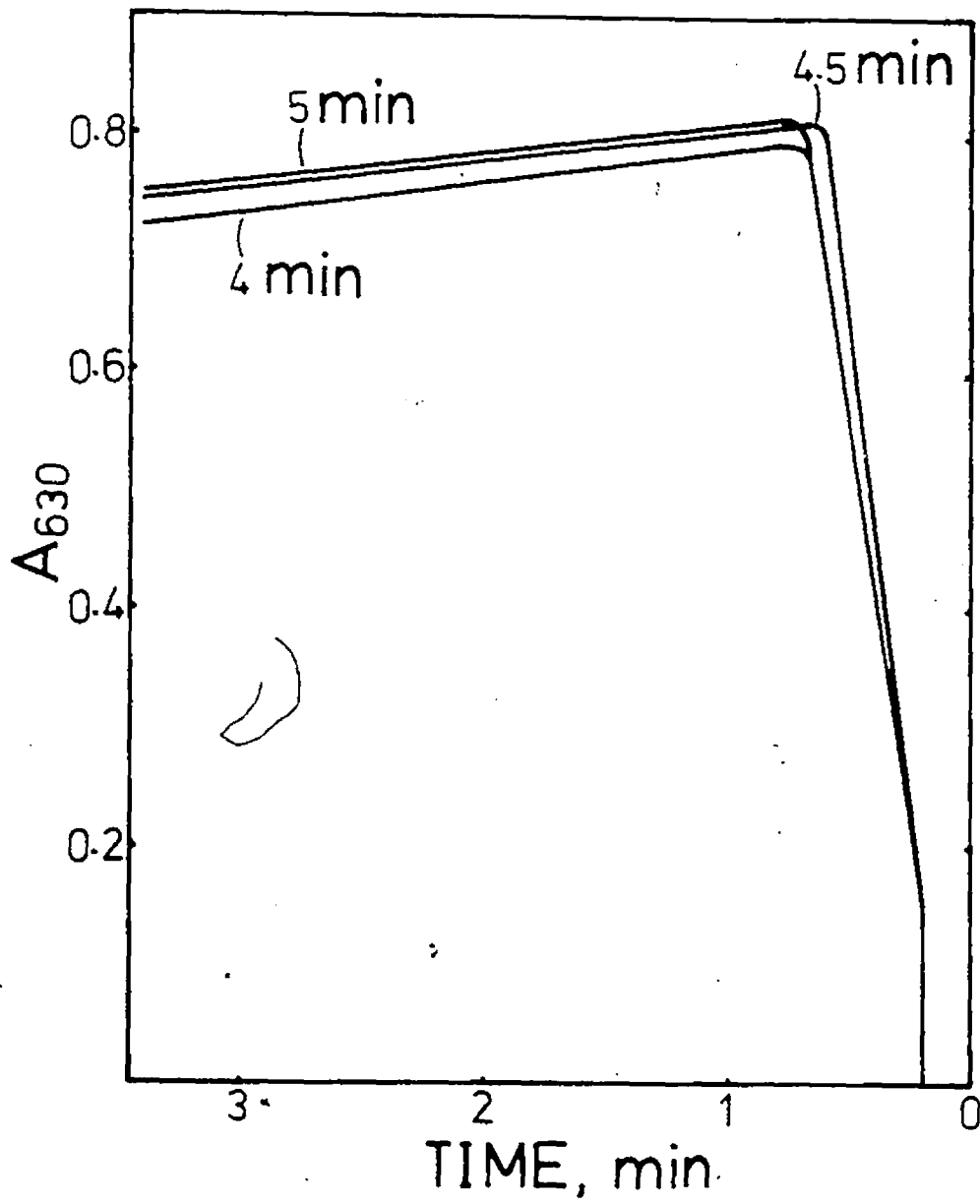


Figure 26

Figure 27

Chromophore Formation and Stability in the Stepwise
Choline Oxidase-Peroxidase System

Legend

Choline (40, 27, 20 and 10 nmoles/50 μ l) and choline oxidase were incubated at pH 7.8 and allowed to react. After 4 minutes 50 μ l aliquots were withdrawn and mixed with chromogens as in the standard procedure. Reactions were not quenched, but A_{630} was monitored as function of time.

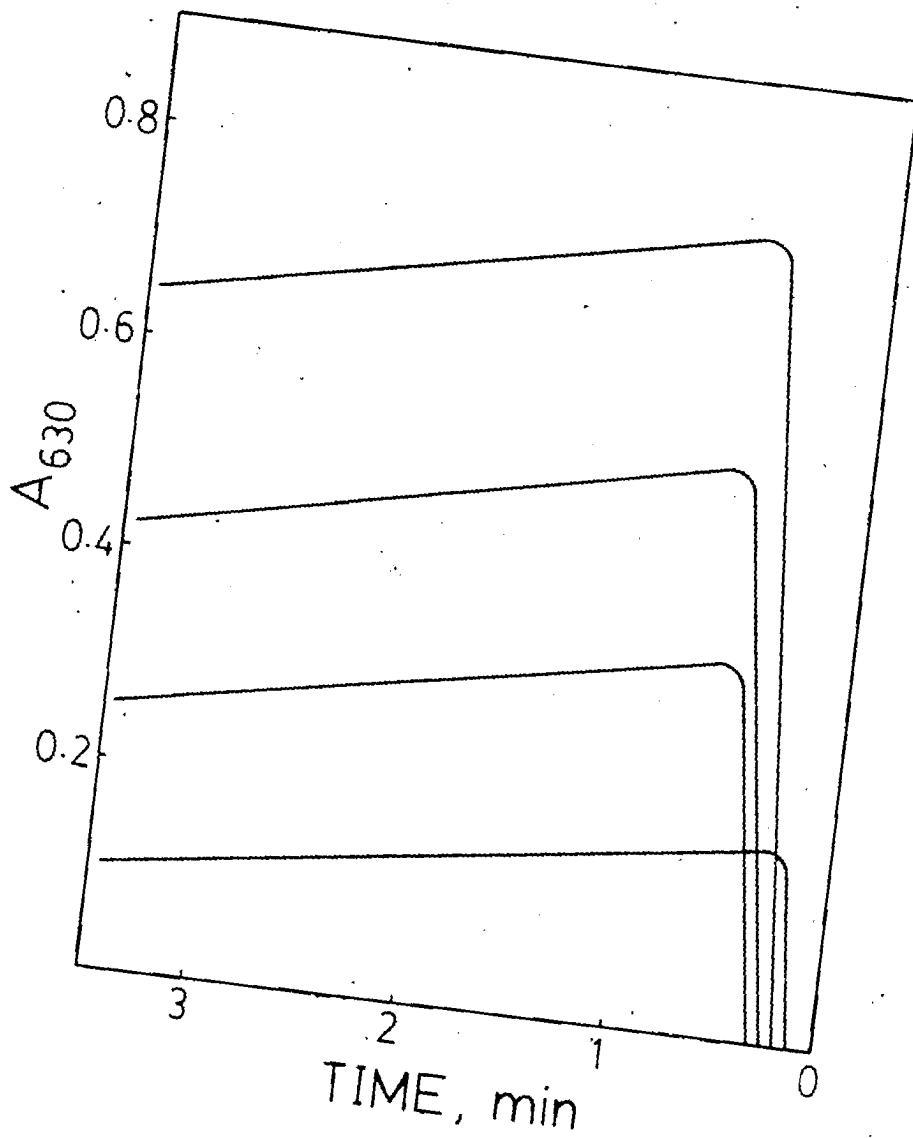


Figure 27

Figure 28

Standard Curve for Choline

Legend

The stepwise choline oxidase-peroxidase system at pH 7.8 was used as outlined in the experimental section on quadruplicate samples. Standard deviations on the absorbance readings were 0.014 or less. The line shown is the least squares line (correlation coefficient 0.997):

$$A_{670} = (0.05562 \pm 0.0018) (\text{nmoles choline}) - (0.071 \pm 0.006).$$

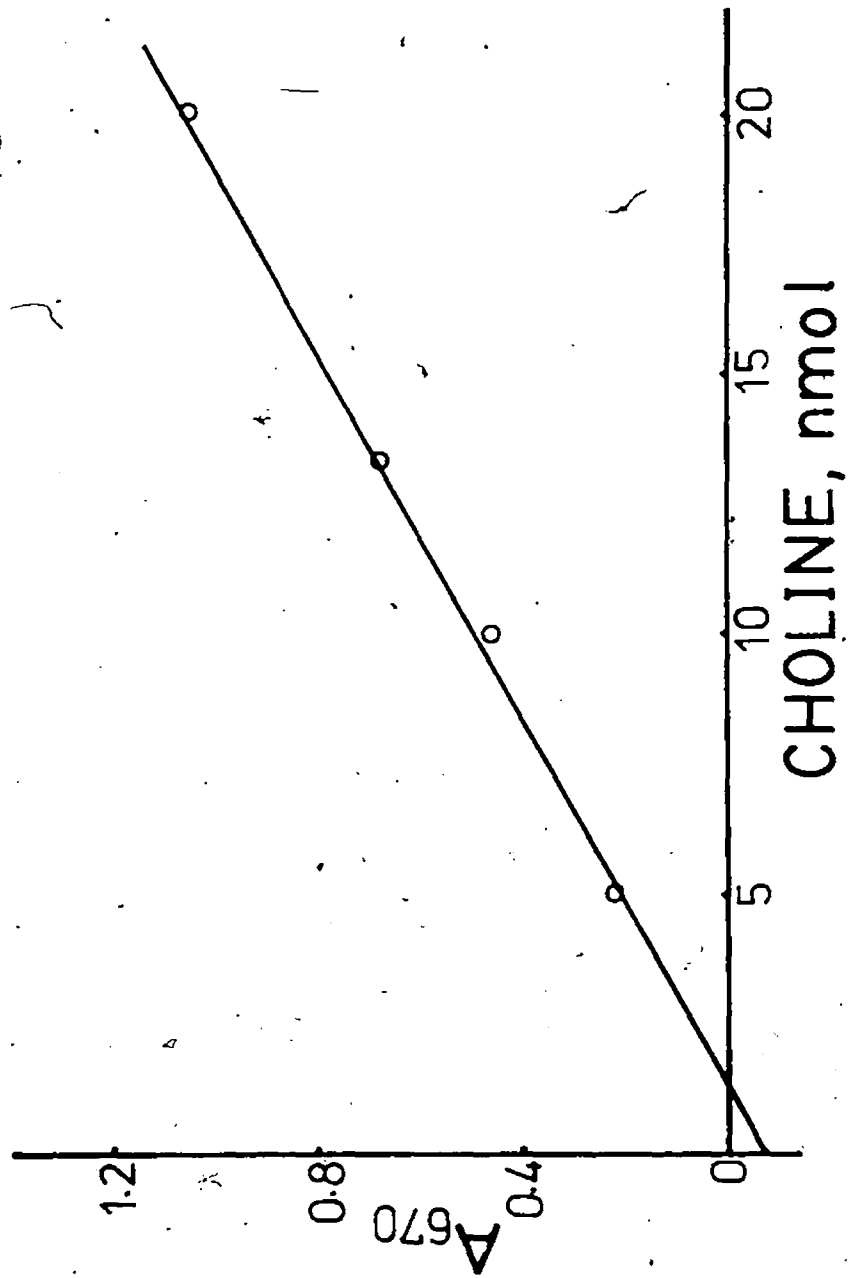


Figure 28

with respect to choline (two equivalents of H_2O_2 formed per mole). The fact that this extinction coefficient is lower than those for glucose or hydrogen peroxide by 5 to $9 \text{ mM}^{-1}\text{cm}^{-1}$, respectively, is probably a result of the stepwise nature of the determination. Color yield is, however, significantly higher for choline due to stoichiometry as noted.

It was of immense interest to quantitate the number of galactosyl or N-acetylgalactosaminyl residues present on erythrocyte membrane glycoconjugates. We attempted to take advantage of the properties of galactose oxidase via the oxidative coupling of MBTH and its corresponding azine in the presence of peroxidase. However, we failed to capture hydrogen peroxide liberated from the action of galactose oxidase on glycoconjugates. Erythrocyte ghosts exposed to hydrogen peroxide were observed to take up the analyte quantitatively within seconds. Possibly hydrogen peroxide is rapidly consumed by membrane-bound glutathione peroxidase (207) or may be involved in other chemical reactions with proteins or with catalase present in the galactose oxidase preparation.

The application of the chromogen system to a galactose oxidase-peroxidase coupled system in determining galactose or N-acetylgalactosamine also required a modification to

the experimental design as for the choline oxidase-peroxidase system. It was necessary to generate hydrogen peroxide in a separate reaction mixture containing galactose and galactose oxidase because of a pH optimum of 7.0 (208) for the oxidase. Color development in the peroxidase step for aliquots which had been incubated at various times with galactose oxidase at 100 U/ml is shown in Figure 29. Peroxidase at this stage was present at 1.7 U/ml. Figure 30 shows the color development and the stability of the chromophore when varying amounts of galactose are present in the reaction mixture.

The galactose standard curve, shown in Figure 31, represents an extinction coefficient of $3.2 \pm 0.14 \text{ mM}^{-1} \text{ cm}^{-1}$ with respect to galactose. The very low extinction coefficient observed for this system is possibly due to the ability of hydrogen peroxide to inactivate galactose oxidase (208) or due to the activity of catalase present in the oxidase preparation.

A. Simplified Procedure for the Determination of Cell Surface Sialic Acid

Membrane bound sialic acid was to be estimated indirectly by determining the formaldehyde liberated as a result of periodate oxidation under conditions specified by Gahmberg and Andersson (32). The focus of this work was to ensure that, firstly, formaldehyde could be determined reliably in

Figure 29

Chromophore Development in the Stepwise Galactose
Oxidase-Peroxidase System

Legend

Galactose (500 nmoles/50 μ l) and galactose oxidase were incubated at pH 7.0 as in the standard procedure for galactose. At various times 50 μ l aliquots were removed and mixed with chromogens plus peroxidase as outlined in the standard procedure. Reactions were not quenched, but A_{630} was monitored as a function of time.

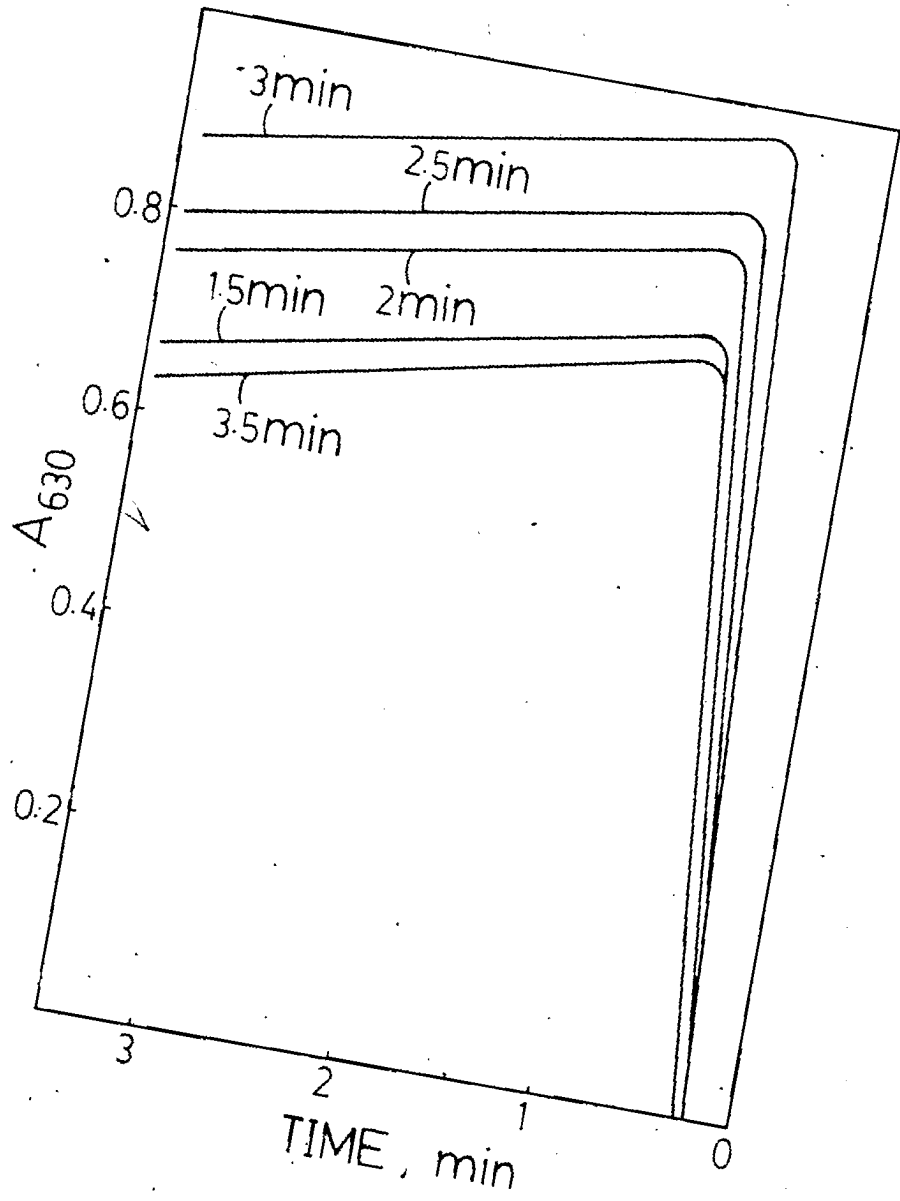


Figure 29

Figure 30

Chromophore Development and Stability in the
Stepwise Galactose Oxidase-Peroxidase System

Legend

Galactose (250, 167, 125 and 63 nmoles/50 μ l) and galactose oxidase were allowed to react in a separate reaction mixture at pH 7.0. After 3 minutes 50 μ l aliquots were removed and mixed with chromogens as in the standard procedure. Reactions were not quenched, but A_{630} was monitored as a function of time.

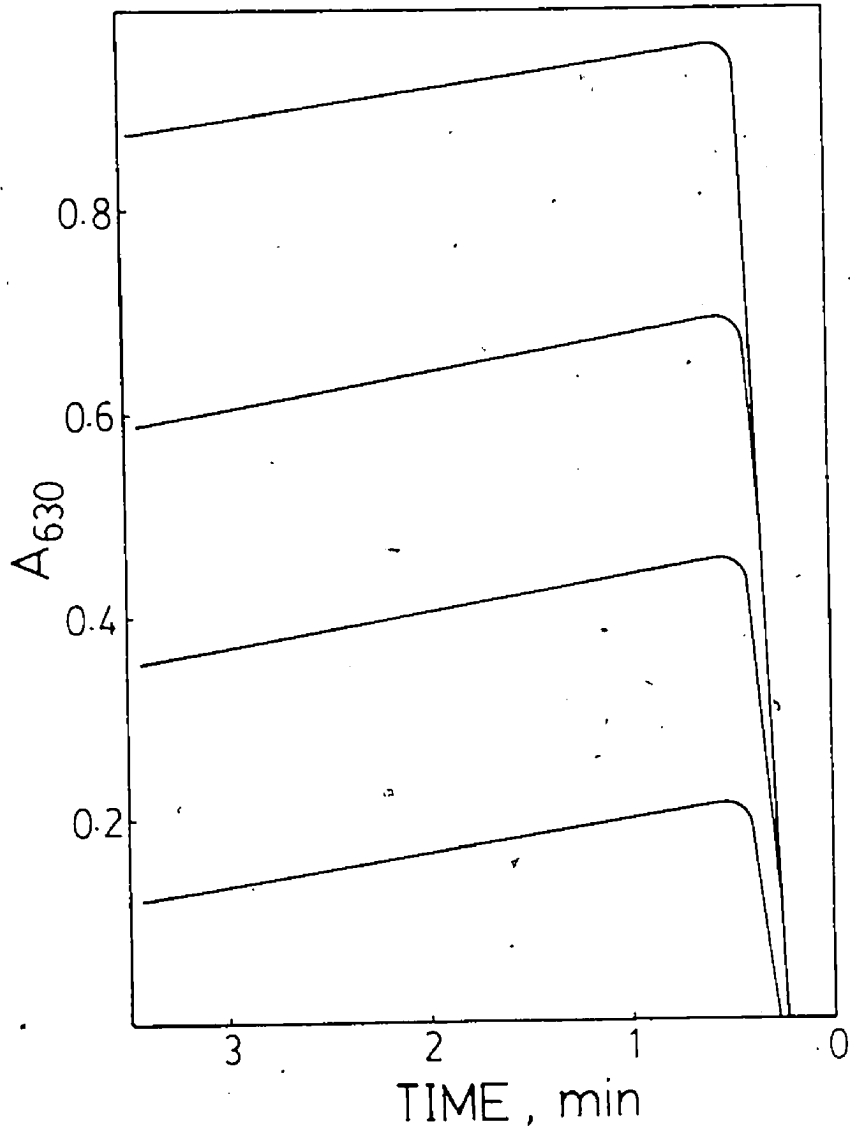


Figure 30

Figure 31

Standard Curve for Galactose

Legend

The stepwise galactose oxidase-peroxidase system at pH 7.0 was employed as for the standard procedure on quadruplicate samples. Standard deviations on the absorbance readings were 0.008 or less. The line shown is the least squares line (correlation coefficient 0.999):

$$A_{670} = (0.00323 \pm 0.00014) (0.5) (\text{nmoles galactose}) + (0.0138 \pm 0.002).$$

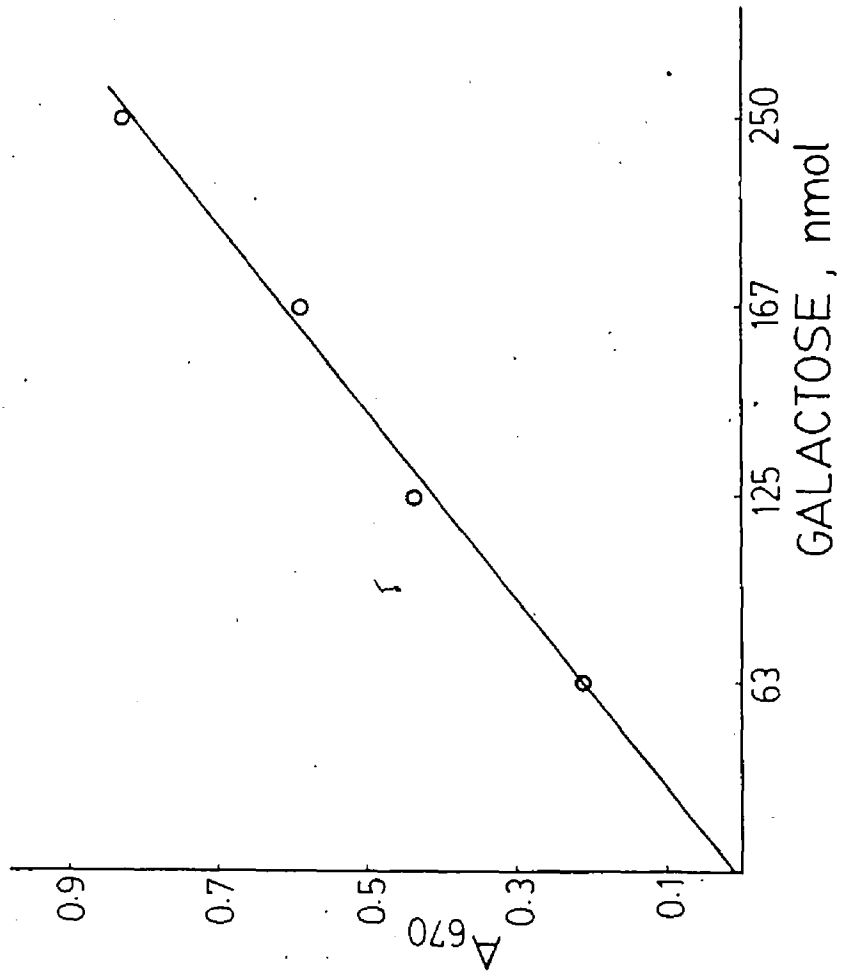


Figure 31

the samples of present interest with the sensitivity achieved by others (77,198) using the chromogen MBTH. Secondly, it was necessary to determine the yield of formaldehyde recovered from cellular samples under the conditions of periodate oxidation.

The formaldehyde procedure used here is an adaptation of the formulation of Sawicki et al. (198) in which ferric chloride is the oxidizing agent and the chromophore is quenched with acetone. From the standard curve for formaldehyde, open circles on Figure 32, an extinction coefficient of $68.5 \text{ mM}^{-1} \text{ cm}^{-1}$ may be calculated which is similar to that determined by Sawicki et al. (198), $65 \text{ mM}^{-1} \text{ cm}^{-1}$, for the same medium (70% acetone) and to that determined by Massamiri et al. (203), $67 \text{ mM}^{-1} \text{ cm}^{-1}$, for wholly aqueous solutions. Next, human erythrocyte ghost suspensions, 20% packed cell volume, were treated with known amounts of formaldehyde under conditions that would have been encountered during periodate oxidation. Supernatant recoveries, represented by closed circles in Figure 32, correspond to an extinction coefficient of $66.8 \text{ mM}^{-1} \text{ cm}^{-1}$ which is 97.5% of that for formaldehyde standards. However, when whole cells at 21% hematocrit, 2.5×10^9 cells per ml, were treated similarly with formaldehyde, recoveries, represented by open triangles in Figure 32, dropped to 56%.

Figure 32

Formaldehyde Determination Using the MBTH Test

Legend

Formaldehyde was determined in quadruplicate by standard procedure (a) or (b) as appropriate. Points without error bars had standard deviations smaller than the symbol. Lines drawn are the least squares lines.

Open circles: formaldehyde standards in PBS (correlation coefficient 0.999): $A_{670} = (0.0685 \pm 0.0001)$ (nmol HCHO) + (0.041 ± 0.025) .

Closed circles: formaldehyde standards incubated in a 20% suspension of erythrocyte ghosts for 10 minutes at 0° before centrifugation and sampling (correlation coefficient 0.999): $A_{670} = (0.0668 \pm 0.005)$ (nmol HCHO) + (0.026 ± 0.008) .

Open triangles: formaldehyde standards incubated in a 21% suspension (2.5×10^9 cells per ml) of whole erythrocytes for 10 minutes at 0° before centrifugation and sampling (correlation coefficient 0.998): $A_{670} = (0.0384 \pm 0.0009)$ (nmol HCHO) + (0.040 ± 0.003) .

Filled triangle, open square and filled square: formaldehyde standard incubated in whole erythrocyte suspensions of 8.0×10^8 , 4.0×10^8 and 2.0×10^8 cells per ml, respectively, for 10 minutes at 0° before centrifugation and sampling.

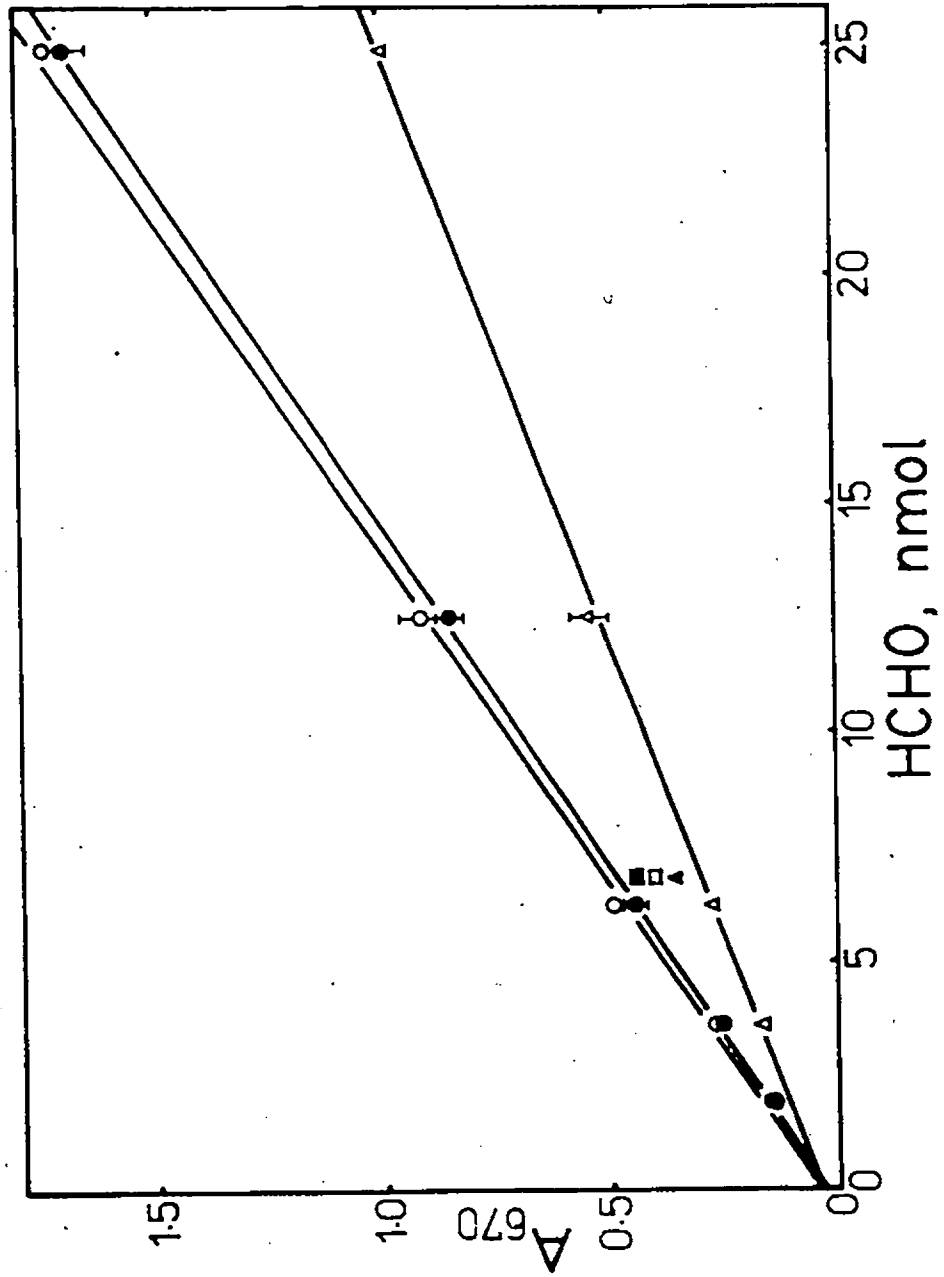


Figure 32

At lower cell densities of 8.0×10^8 (filled triangle), 4.0×10^8 (open square) and 2.0×10^8 (filled square) cells per ml recoveries were 68, 77 and 85%, respectively, based on quadruplicate determinations at a nominal formaldehyde level of 7.8 nmoles/50 μ l.

Further confirmation of decreased recoveries with increasing cell densities was obtained by carrying out paired control experiments as suggested by Massamiri et al. (77). Duplicate whole cell suspensions were treated with periodate and then one was mixed with a known amount of formaldehyde before centrifugation and sampling of the supernatant. The second suspension was centrifuged first and an aliquot of the supernatant was mixed with a proportional amount of formaldehyde before sampling. These samples were compared directly for absorbance in the standard formaldehyde test. At cell densities of 2.0×10^8 , 4.0×10^8 , 8.0×10^8 and 2.5×10^9 cells per ml the A_{670} values for the first control were 93, 74, 53 and 50% of those of the respective second controls. Thus, at low cell densities used by Massamiri et al. (77), approximately 2% hematocrit, our results confirm theirs and indicate that formaldehyde released may be used as a measure of cell surface sialic acid residues. However, as cell density was increased beyond that used by the previous workers (77),

we find that recovery drops proportionally with increasing cell density.

Two possible causes of low formaldehyde recovery were considered: (a) the influence of protein in the extracellular solution and (b) uptake of formaldehyde by the cells and its removal upon centrifugation. To consider the first, aliquots of erythrocyte hemolysate at various dilutions were mixed with formaldehyde standards for the MBTH test. At hemoglobin concentrations below 6 mg/ml the formaldehyde detected was at least 95% of the theoretical amount. Even at a hemoglobin concentration of 25 mg/ml the minimum recovery of formaldehyde across the whole concentration range was 85%. Likewise the formaldehyde standard curve could be generated in the presence of bovine serum albumin at 1.5 mg/ml without diminution of the color yield. These results indicate that protein in the sample medium at such concentrations does not interfere with the detection of formaldehyde either colorimetrically or as a result of competing Schiff base formation. For this reason a deproteinization step was not included in the method described here in contrast to that of Massamiri *et al.* (77), although, at higher protein concentrations tested it was necessary to sediment a flocculent precipitate formed after quenching in acetone.

Formaldehyde uptake by cells under the conditions of periodate oxidation (10 minutes at 0°) was documented as follows. Whole cell suspensions were treated with formaldehyde as for the open triangle data in Figure 32. Supernatants from these contained 54-64% of the expected aldehyde over the whole concentration range. The pellets were rapidly washed once by resuspension, centrifuged and resuspended to the original volume in PBS. After a further 10 minutes at 0° the samples were centrifuged and their supernatants were checked for formaldehyde. On quadruplicates at each concentration recoveries of 15-20% of the original formaldehyde were observed. This result confirms that formaldehyde uptake is rapid and further suggests it is reversible. The main driving force for uptake is probably imine formation with intracellular proteins. Based on the foregoing we would suggest that methods using formaldehyde liberation to monitor oxidation of bound sialic acid may only be used on intact cells at low density, such as 2% hematocrit seen here with erythrocytes.

The present method, when applied to an erythrocyte ghost sample of 1 ml at 20% packed cell volume containing 0.86 mg of protein, indicated a sialic acid content of 111.3 nmoles, or 129 nmol/mg of membrane protein. For comparison, Steck and coworkers reported separate prepara-

tions with 135 and 138 nmol/mg of membrane protein (209, 210) while Massamiri et al. (77) reported preparations of 52.8 and 72.5 nmol/ 10^9 cells. The latter correspond well with our ghost sample from 2.5×10^9 cells.

Preparation of a Novel Photolabile Heterobifunctional Crosslinking Reagent and its Biological Application

Our laboratory has been interested in studying the behaviour and importance of cell surface glycoproteins with various acyl hydrazides (92). The main thrust of this dissertation was the preparation and application of a potential modifier of periodate- or galactose oxidase-generated aldehydic residues on the erythrocyte membrane surface via hydrazone (Schiff base) formation. The reagent, N-(2-nitro-4-azidophenyl)- β -alanine hydrazide (NAPBAH) was easily prepared with readily available techniques as shown in Figure 33. Yield from the known carboxylic acid (193) was 95%. The physical properties of the intermediates and the final product are given in the experimental section.

The extent of photolysis of NAPBAH was monitored spectrophotometrically by photolyzing the reagent (55 μ M) in methanolic or aqueous solutions at 350 nm using a photochemical chamber as described in Figure 16. Figures 34 and 35 illustrate the resultant spectra after photolyses of varying duration. The spectrum for the reagent in

Figure 33

Syntheses of Azido-containing Reagents

Legend

2-Nitro-4-azidofluorobenzene was prepared by the method of Fleet et al. (191). N-(2-Nitro-4-azidophenyl)- β -alanine was prepared according to the procedure of Hosang et al. (193). The carboxylic acid was esterified in methanol and sulfuric acid as described in the experimental. Subsequently, the hydrazide was prepared by treating a methanolic solution of the methyl ester with hydrazine as described in the experimental.

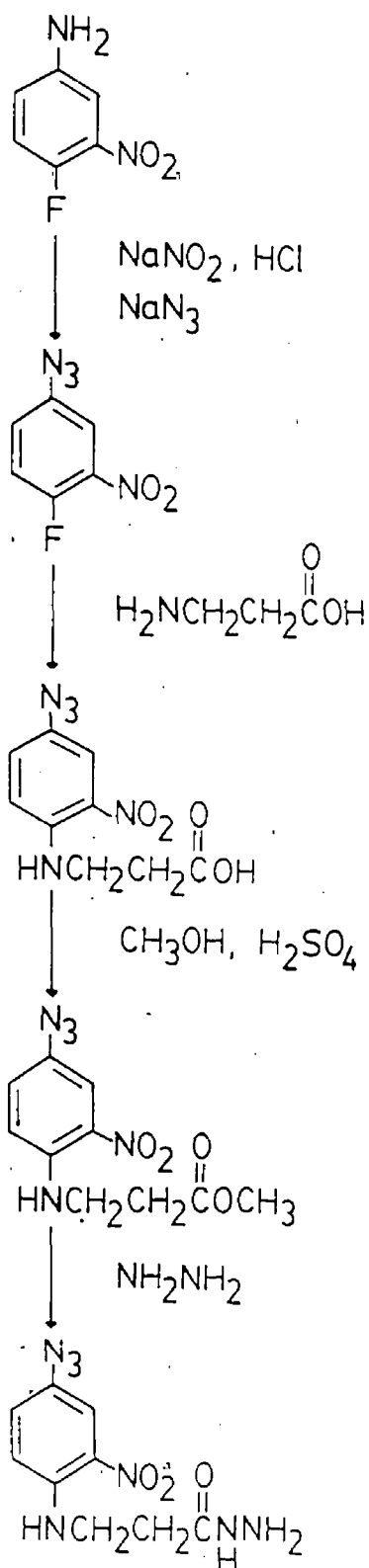


Figure 33

Figure 34

Photolysis of N-(2-Nitro-4-Azidophenyl)- β -Alanine
Hydrazide in Methanol

Legend

A 55 μ M solution of N-(2-nitro-4-azidophenyl)- β -alanine hydrazide in methanol was photolyzed for 0 (—), 30 (· · — · ·), 60 (— — —), 90 (— · · ·) and 150 (· · · · ·) seconds in a Rayonet photochemical reactor equipped with RPR-3500 Å lamps. The absorbance of the solution was measured on a Beckman 35 spectrophotometer.

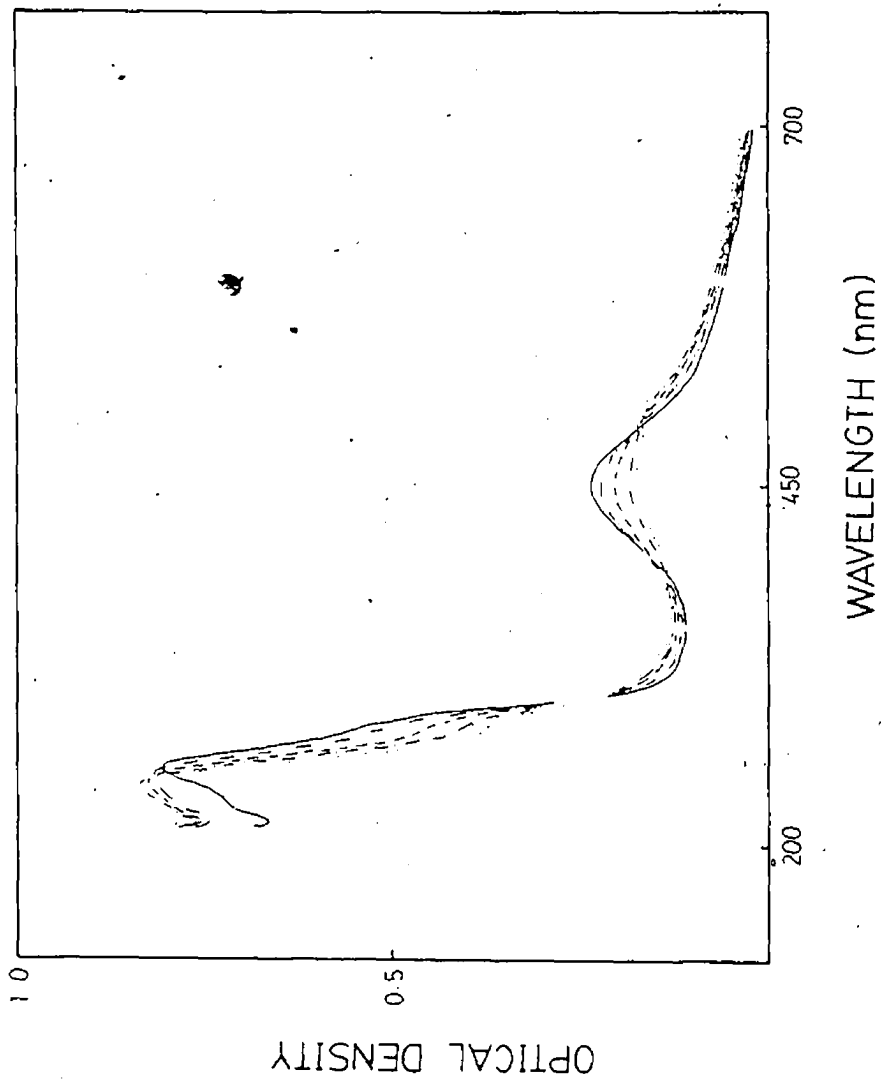


Figure 34

Handwritten mark resembling a stylized 'S' or '2'.

Figure 35

Photolysis of N-(2-Nitro-4-Azidophenyl)- β -Alanine
Hydrazide in Aqueous Buffer

Legend

A 55 μ M solution of N-(2-nitro-4-azidophenyl)- β -alanine hydrazide in aqueous buffer was photolyzed for 0 (—), 30 (—·—·—·), 60 (— — —), 90 (—·—·) and 150 (.....) seconds in a Rayonet photochemical reactor equipped with RPR-3500 Å lamps. The absorbance of the solution was measured on a Beckman 35 spectrophotometer.

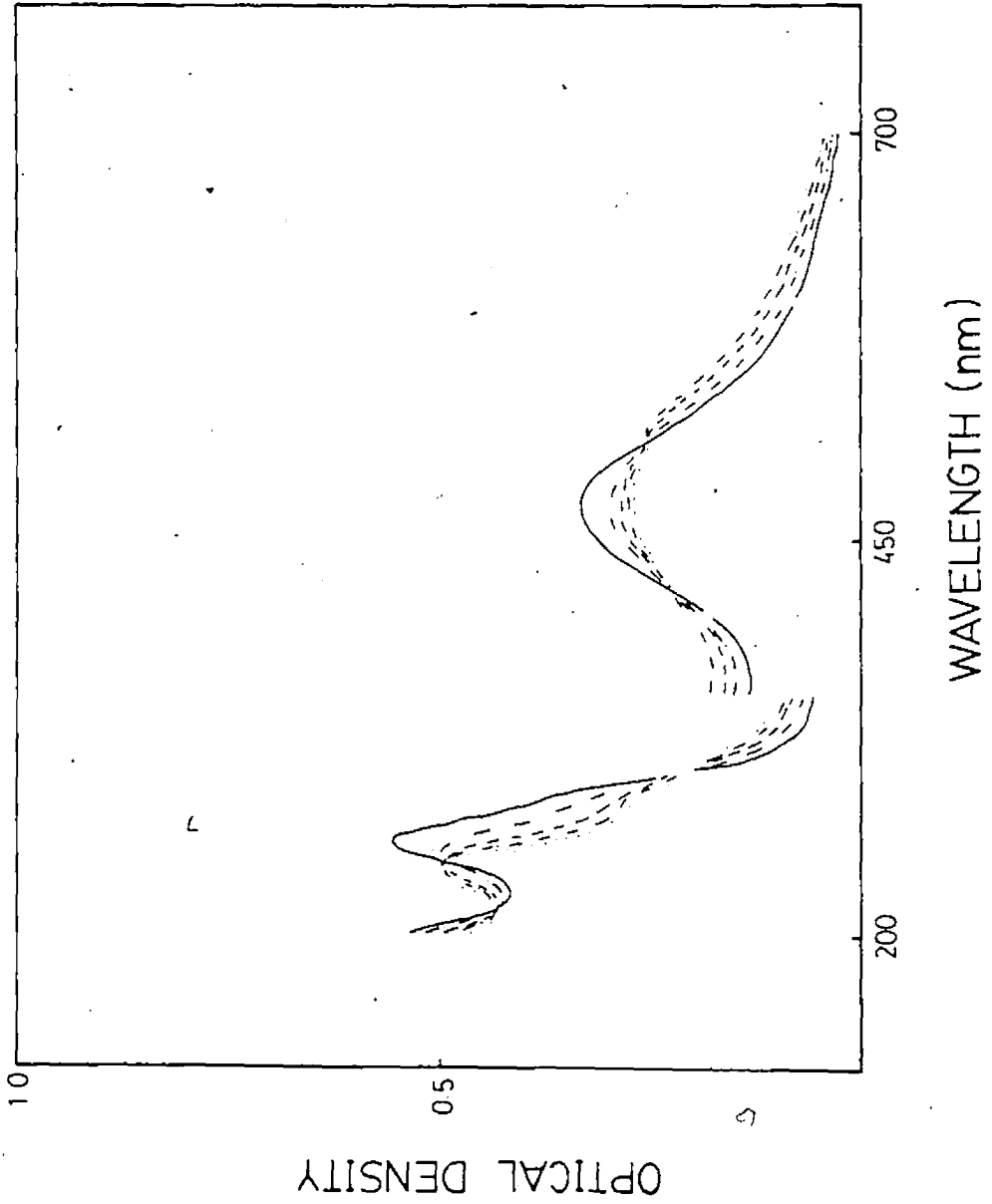


Figure 35

methanol (Figure 34) shows two absorption maxima at 255 nm and 450 nm, with extinction coefficients of $15 \text{ mM}^{-1} \text{ cm}^{-1}$ and $4.5 \text{ mM}^{-1} \text{ cm}^{-1}$, respectively. In aqueous solution (Figure 35) an absorption maximum at 255 nm was also observed with an extinction coefficient of $8.5 \text{ mM}^{-1} \text{ cm}^{-1}$. However, a bathochromic shift to 465 nm for the other absorption maximum was observed with an extinction coefficient of $3.0 \text{ mM}^{-1} \text{ cm}^{-1}$. After 2.5 minutes of photolysis a 50% decrease in the intensity of the long wavelength absorption peak in both solutions was observed. Photolysis times longer than 2.5 minutes (up to six minutes) showed no further diminution in intensity.

To further characterize NAPBAH we elected to derivatize the hydrazide function with acetone in the presence of acetic acid. Typically, 50 mg of the hydrazide was dissolved in a minimal amount of acetone over a steam bath and to it was added two drops of glacial acetic acid. After the reaction was complete (ca. 60 minutes, and confirmed by thin layer chromatography) the solution was evaporated to dryness and dried over phosphorus pentoxide under vacuum for 24 hours. An NMR spectrum was run using deuterated chloroform as the solvent. Two strong singlets at 2.0 and 2.6 ppm were observed as were the other chemical shifts characteristic of NAPBAH. Further, the broad peak at 4.4 ppm present in

the spectrum of NAPBAH due to hydrazide protons was not observable in the spectrum for the hydrazone. An ultraviolet-visible spectrum of a 63 μM solution of the hydrazone in water containing 0.5% ethanol revealed two absorption maxima one at 460 nm and the other at 250 nm with extinction coefficients of $4.0 \text{ mM}^{-1} \text{ cm}^{-1}$ and $18.0 \text{ mM}^{-1} \text{ cm}^{-1}$, respectively. This compound melted at 64-69°C.

The effectiveness of NAPBAH was evaluated with periodate- or galactose oxidase-treated whole erythrocytes or erythrocyte ghosts. This treatment allowed for the generation of sialyl- (32) or galactosyl-aldehydes (114), respectively, on cell surface glycoconjugates. In the presence of NAPBAH these residues were derivatized giving a light-red color to the erythrocyte ghosts which are typically cream-colored. Figures 36 and 37 illustrate proposed routes of reagent incorporation into these exposed aldehydic residues. A similar experiment as described above using whole erythrocytes, in this case, was subjected to hypotonic lysis (19). After thorough washing the packed erythrocyte ghosts were also light-red in color as a result of reagent incorporation. Table 4 outlines the extent of reagent incorporation into periodate-, galactose oxidase- or neuraminidase/galactose oxidase-generated aldehydic residues. The treatment of cell surface glycoconjugates with

Figure 36

Incorporation of N-(2-Nitro-4-Azidophenyl)- β -Alanine
Hydrazide Onto Erythrocyte Membrane
Surface Sialyl Residues

Legend

Periodate-generated sialyl aldehyde residues (32) on erythrocyte membrane surfaces are subsequently modified with N-(2-nitro-4-azidophenyl)- β -alanine hydrazide via hydrazone bond formation.

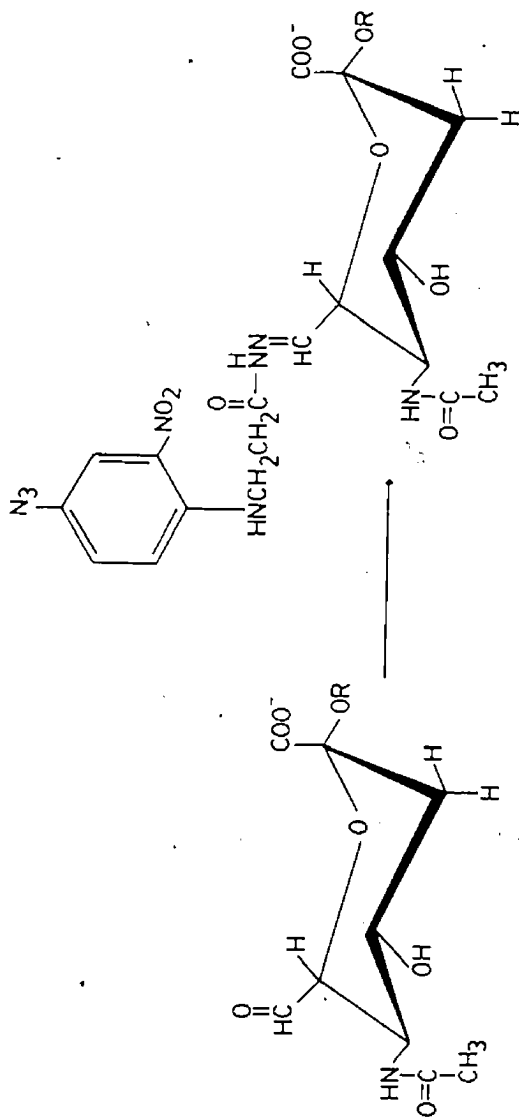


Figure 36

Figure 37

Incorporation of N-(2-Nitro-4-Azidophenyl)- β -Alanine
Hydrazide Onto Erythrocyte Membrane Surface
Galactosyl or N-Acetylgalactosaminyl Residues

Legend

Galactose oxidase-generated galactosyl or N-acetyl-galactosaminyl aldehyde residues (114) on erythrocyte membrane surfaces are derivatized with N-(2-nitro-4-azidophenyl)- β -alanine hydrazide via hydrazone bond formation.

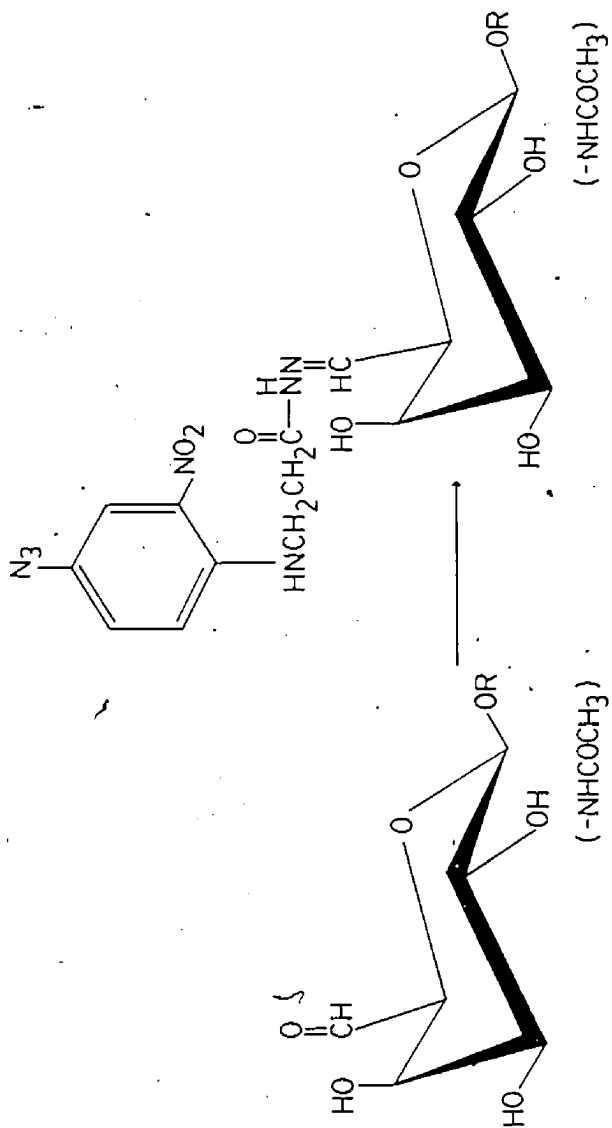


Figure 37

TABLE 4

Extent of Reagent Incorporation onto Erythrocyte Membrane Surfaces of Various Chemical or Enzymic Treatment

| Treatment ^a | A ₄₆₅ | nmol/mg protein ^b | Sites derivatized |
|-------------------------------------|------------------|------------------------------|-------------------|
| periodate | 0.495 | 77 | 60% |
| galactose oxidase | 0.415 | 64 | 70% |
| neuraminidase/ galactose oxidase | 0.580 | 90 | 40% |
| neuraminidase | 0.050 | nil | nil |

^a 400 μ l erythrocyte ghosts were derivatized and subsequently solubilized with 400 μ l 2.5% SDS and the absorbance measured at 465 nm as described in the experimental. Periodate was present at a final concentration of 2 mM. In the enzymic experiments 10 U galactose oxidase and/or 0.2 U neuraminidase were used.

^b According to Steck et al. (209) and Capaldi and Taylor (184) there are approximately 138 and 129 nmol sialic acid per mg of membrane protein, respectively. According to Aminoff et al. (63) there are approximately 47 nmol N-acetylgalactosamine and 43 nmol galactose per mg of membrane protein. Removal of sialic acid by neuraminidase exposes other galactosyl residues increasing the number to 219 nmoles per mg of membrane protein. From the extinction coefficient for the reagent the number of periodate- or galactose oxidase-generated aldehydes derivatized was determined (this assumes no change in extinction coefficient upon formation of the hydrazone).

neuraminidase hydrolyzes sialic acid (63) residues exposing penultimate galactosyl residues as shown in Figure 38. The spectrophotometric technique (184) described above allowed us to determine the number of available sialyl residues for derivatization to be 129 nmoles per mg membrane protein. Thus, the extent of NAPBAH incorporation was calculated to be 77 nmoles sialyl aldehyde per mg membrane protein. Similarly, galactosyl and N-acetyl-galactosaminy l residues were derivatized and shown to incorporate the reagent to a greater degree than for the sialyl residues as shown in Table 4. Assuming the number of available galactose oxidase substrate sites to be 90 nmoles per mg membrane protein (63), 70% of these sites were NAPBAH-derivatized with no prior neuraminidase treatment while 40% derivatization of total sites was achieved when neuraminidase was present prior to galactose oxidase. The treatment of cell surface glycoconjugates with neuraminidase exposes galactosyl residues which were concealed by sialic acid. However, the extent of reagent incorporation did not increase proportionally with this occurrence. As shown in Table 4 there was an increase in the A_{465} suggesting that other galactosyl residues were becoming derivatized when neuraminidase is present prior to galactose oxidase treatment. An explanation for the proportionally low color

Figure 38

Hydrolysis of Glycoconjugate-containing Sialyl
Residues with Neuraminidase

Legend

The treatment of membrane surface glycoconjugates with neuraminidase liberates sialic acid exposing the penultimate R-OH residues (63).

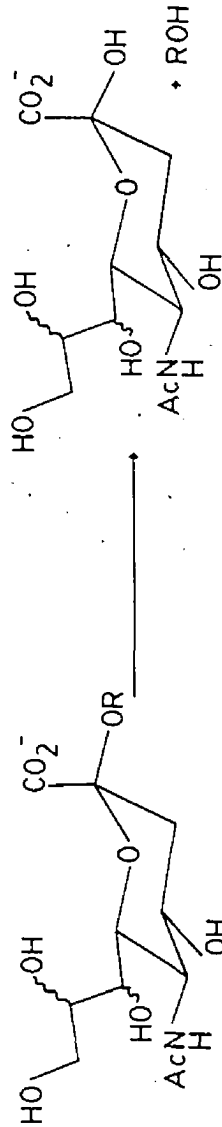


Figure 38

yield is that the amount of galactose oxidase and the time of incubation with the enzyme was not increased even though the theoretical number of galactose substrate sites increased 2.4-fold (i.e., 90 nmoles of galactose residues to 219 nmoles per mg membrane protein) (63). Furthermore, neuraminidase (acylneuraminyl hydrolase; EC 3.2.1.18) may not have exhaustively hydrolyzed sialic acid, although others have shown that more than 95% of the sialic acid present on erythrocyte membranes can be hydrolyzed (211). This residual sialic acid on the cell surface has not been considered in the above calculation. A typical spectrum of derivatized erythrocyte ghosts which were solubilized in 1% sodium dodecyl sulfate is shown in Figure 39. The spectrum shows no effect of the detergent on the absorbance of the bound reagent as no change in wavelength was observed.

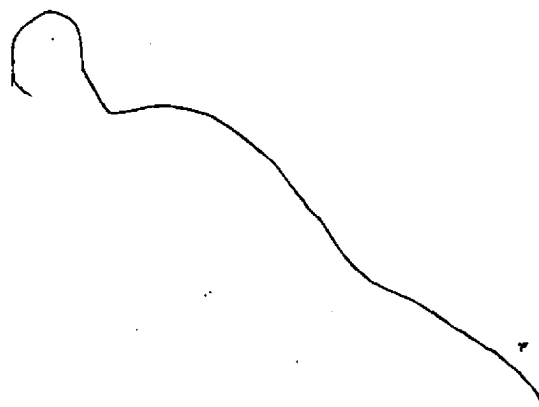
The incorporation of NAPBAH could be reversed by treating the derivatized ghosts with 0.37, 16 and 156 mM hydrazine or 5.33 mM acetic acid hydrazide, Table 5. The former were at 37-fold, 160-fold and 1560-fold molar excess and the latter at 53-fold molar excess over the amount of NAPBAH present on the membrane. To demonstrate this nucleophilic displacement 400 μ l of derivatized packed ghosts were suspended in a solution containing either of the two preceding nucleophiles giving a final volume of

Figure 39

Spectrum of Reagent-Derivatized Erythrocyte Ghosts
Solubilized in Sodium Dodecyl Sulfate

Legend

An 800 μ l aliquot of derivatized erythrocyte ghosts was solubilized in 1% sodium dodecyl sulfate and the absorbance measured as a function of wavelength.



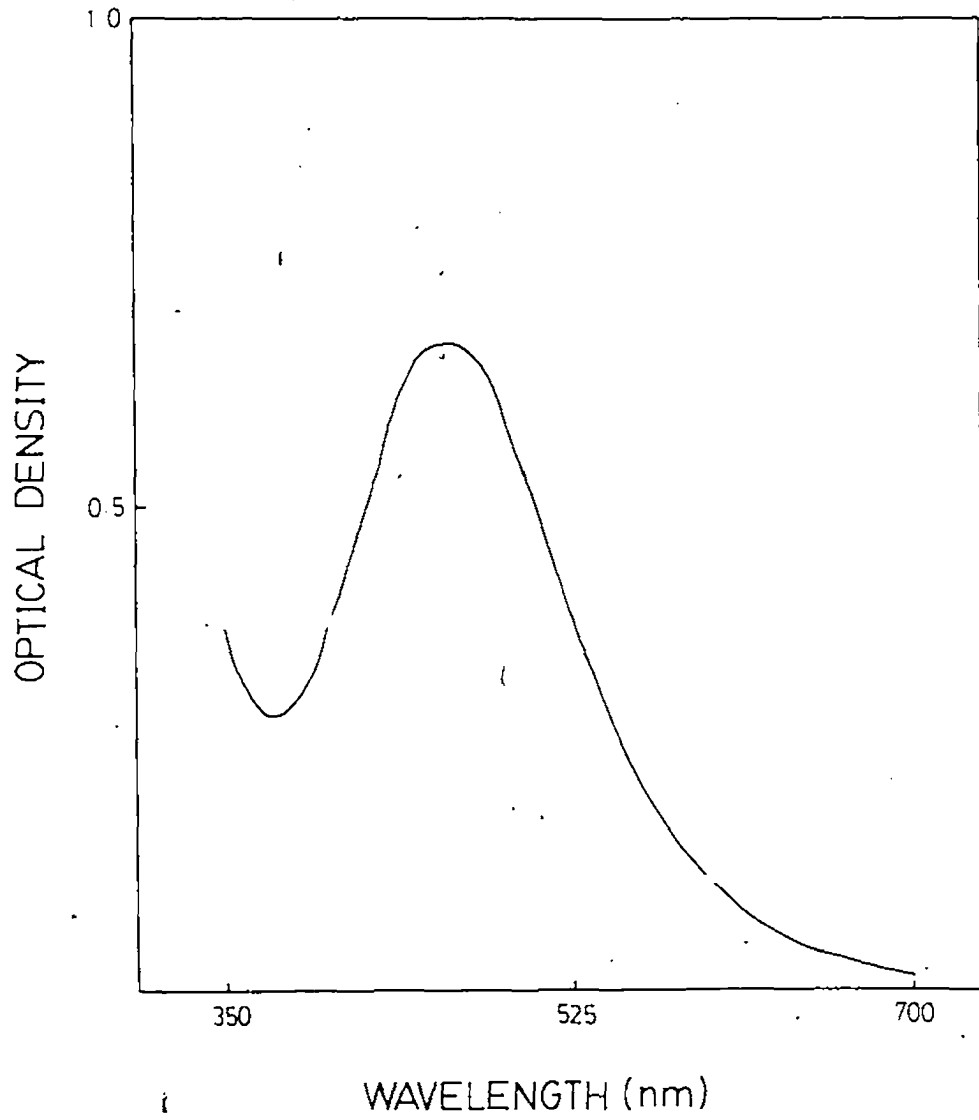


Figure 39

TABLE 5

Extent of Membrane-Bound Reagent
Released by Nucleophiles

| Treatment | Percent Release of Reagent | |
|------------------------------------|-----------------------------------|--------------------------------|
| | No NaBH ₄ ^a | NaBH ₄ ^b |
| hydrazine (0.37 mM) | 51 | 12 |
| (16.0 mM) | 70 | 21 |
| (156.0 mM) ^c | 95 | - |
| acetic acid hydrazide (5.33 mM) | 52 | 8 |

^aTo 400 μ l of derivatized packed ghosts was added 400 μ l of 1.4 and 60 mM hydrazine or 400 μ l of 20 mM acetic acid hydrazide in phosphate wash buffer, diluted to 1.5 ml with the same buffer. These were allowed to react for 1.5 and 2.0 hours, respectively, at room temperature in the dark. The mixture was sedimented (9,000 rpm or 9,750 xg for 5 minutes), supernatant sampled and absorbance at 465 nm measured.

^bThese cells were treated similarly to (a) except that prior to nucleophilic displacement the hydrazone bond was reduced with 50 mM NaBH₄ (96) for 30 minutes at room temperature in the dark. The cells were washed thrice in phosphate wash buffer and sedimented (9,000 rpm or 9,750 xg for 5 minutes).

^cReagent derivatized cells which had been treated with 0.37 mM hydrazine were washed and re-equilibrated with 400 μ l of 312 mM hydrazine for 1 hour at room temperature in the dark. The mixture was sedimented, supernatant sample and absorbance measured as above.

1.5 ml. After a prescribed incubation period the cells were packed and the supernatant sampled for NAPBAH as shown in Table 5. Further, reduction of the hydrazone bond between the aldehydic residue and NAPBAH with sodium borohydride (96) decreased the amount of reagent released via nucleophilic displacement by the two nucleophiles.

To test whether the reagent was photoincorporable into macromolecules such as soluble proteins we attempted to photoincorporate NAPBAH into bovine serum albumin. To 1 ml of a 1 mg/ml BSA (14.5 nmoles BSA) solution in water was added 1 ml of 700 μ M NAPBAH (700 nmoles NAPBAH). This solution was thoroughly mixed and then photolyzed at 350 nm for 6 minutes. To it was added 0.75 ml of 30% trichloroacetic acid and allowed to react for 30 minutes. The mixture was then sedimented on a bench-top centrifuge (3,000 rpm) and the supernatant discarded. The residue was resuspended twice in aqueous solution containing 6% trichloroacetic acid. The residue was then dissolved in 500 μ l of water and the absorbance at 465 nm measured. From the extinction coefficient for NAPBAH the amount of reagent incorporated was determined to be 12.5 nmoles or 1.8% of the hydrazide present originally. This observation confirms reagent incorporation in a light dependent reaction.

To demonstrate the role and importance of oligo-

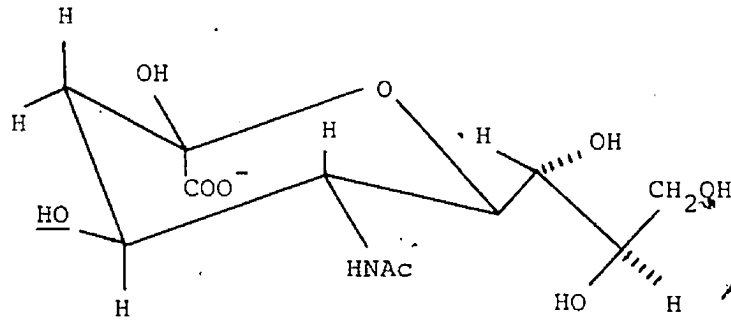
saccharide chains present on glycoproteins we elected to investigate their interaction with sialic acid binding lectins and galactose binding lectins. Recently, glycopeptides containing photoactivable reagents were prepared and used in site-specific labeling of concanavalin-A and castor bean lectins (RCA₆₀ and RCA₁₂₀) (212). Derivatives of monosaccharides have been prepared and used for the investigation of various receptors and their functions (213,214), however, they proved to be poor candidates for those studies because of their limited degree of specificity and relatively poor affinity for the lectins. Conversely, oligosaccharides have a greater degree of specificity and bind more tightly by lectins. By exploiting these properties, regions of lectins involved in binding can be labeled with photolabile glycopeptide probes (212). The importance of specific sugars present on oligosaccharides in intracellular interactions such as agglutination led others to specifically incorporate spin labels to sialyl residues on the membrane surface of erythrocytes (80,91). With this method 40% of the sialic acid residues present on glycoconjugates in the erythrocyte membrane were modified (91). In the presence of various lectins, namely Phaseolus vulgaris phytohaemagglutinin, wheat germ agglutinin and concanavalin-A Feix et al. (91) were able to study the mobility or dynamics of these spin labeled oligosaccharide chains on glycoconjugates. From their observations it was concluded

a conformational change in the glycoprotein receptor occurs when the lectin is bound.

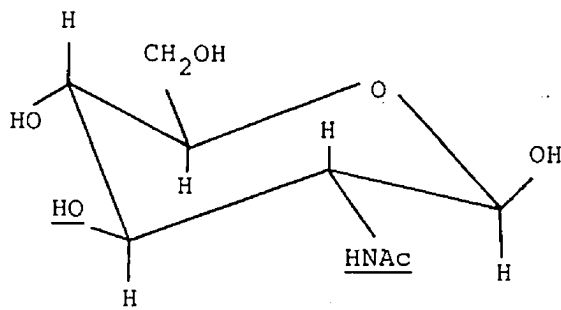
In our studies with sugar binding lectins we initially characterized reagent-derivatized cells with respect to agglutinability in the presence of various lectins. Hemagglutination assays were performed on (i) whole erythrocytes or ghosts regardless of type; (ii) periodate- or galactose oxidase-treated erythrocytes or ghosts; and (iii) oxidized erythrocytes or ghosts which had been modified with NAPBAH. The two sialic acid binding lectins wheat germ agglutinin and limulin were observed to behave quite differently from each other. Wheat germ agglutinin was shown to agglutinate intact erythrocytes as well as periodate-oxidized erythrocytes and derivatized erythrocytes when present at 10 $\mu\text{g/ml}$ (the minimal lectin concentration causing agglutination). Limulin, however, would only agglutinate underivatized erythrocytes, when present at 0.1 $\mu\text{g/ml}$. This lectin concentration is the lowest concentration we studied. There was no apparent agglutination of periodate-oxidized or derivatized erythrocytes by limulin.

Peters et al. (150) identified substituents on the sugars N-acetyl-D-neuraminic acid, N-acetyl-D-glucosamine and N-acetyl-D-galactosamine which were important in the

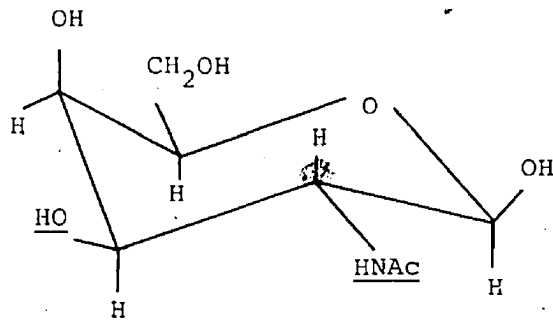
interaction with wheat germ agglutinin as shown below,



α -D-N-acetylneuraminic acid



β -D-N-acetylglucosamine



β -D-N-acetylgalactosamine


The similar reactivities of the above three carbohydrates is explained by their superimposability at the carbon-2 acetamido group and carbon-3 hydroxyl group of the pyranose ring (142) (underlined), as well as the equatorial substituents on carbon-1. Figure 36 illustrates reagent incorporation at the periodate-generated aldehydic group on carbon-7 of sialic acid. This site is well removed from the two substituents indicated above to be critical to the interaction with lectin. This explains the ability of periodate-oxidized or reagent-modified erythrocytes to agglutinate in the presence of wheat germ agglutinin. Limulin, however, probably requires the presence of the carbon-7, -8 and -9 moiety on sialic acid for binding or the NAPBAH hydrazone in that region interferes with sugar binding.

With soluble glycoconjugates such as fetuin, a sialic acid-containing glycoprotein present in fetal calf serum, others were able to show effective inhibition of hemagglutination when it was present in the mixture (142). However, in the presence of the desialyated form of the glycoprotein (asialo-fetuin) a large increase in its concentration was required to achieve the same degree of hemagglutination inhibition. These observations led us to investigate the interaction of wheat germ agglutinin with cell surface sialoglycoconjugates.

The galactose binding lectins used in this study were jequirty bean (Abrus precatorius) lectin and castor bean (Ricinus communis) lectins type 60 and type 120. All three lectins agglutinated intact erythrocytes or ghosts, galactose oxidase-oxidized erythrocytes or ghosts and derivatized erythrocytes or ghosts at lectin concentrations of 0.2 µg/ml and 1.6 µg/ml, respectively.

For initial investigation of the effectiveness of the photolabile hydrazide reagent when present on erythrocyte membrane glycoconjugates we selected wheat germ agglutinin as a potential ligand for photochemical crosslinking. Derivatized membranes were allowed to agglutinate in the presence of wheat germ agglutinin and photolyzed at 350 nm for 6 minutes. To ensure removal of excess lectin the membranes were incubated with 200 mM N-acetylglucosamine, a potent inhibitor of agglutination (147), for 1 hour at room temperature. The membranes were then washed once with buffer containing 200 mM N-acetylglucosamine and twice further with phosphate wash buffer. The membranes were then solubilized and prepared for SDS-PAGE. The Coomassie blue and Periodic acid Schiff stained gels revealed no apparent alteration in the electrophoretic pattern of the membrane proteins and glycoproteins as compared to the profile for derivatized membranes.. The absence of photoincorporation might be explained by the position of

the NAP substituent on the photoreagent being distantly removed from lectin interaction, thus upon photolysis the highly reactive nitrene is unable to covalently insert into the lectin. Initially, from the results of the hemagglutination assays we concluded that the interaction of wheat germ agglutinin with the reagent-derivatized erythrocytes was not significantly affected. Later, we observed that membranes which had been exhaustively derivatized with 350 μ M NAPBAH (i.e., periodate-oxidized membranes incubated with reagent for 16 hours) were unable to become agglutinated in the presence of wheat germ agglutinin. This evidence suggests that the carbon-7, -8 and -9 moiety of sialic acid may be important in the interaction with the lectin. However, Peters *et al.* showed that the sialyl aldehyde (carbon-7) once reduced to the corresponding alcohol was a better inhibitor of hemagglutination (150). An unanswered question is the apparent inability of the lectin to utilize other carbohydrates such as N-acetylglucosamine (149) in the asialoglycoproteins for agglutination. This problem is complex and currently under investigation (149). Both sialic acid and N-acetylglucosamine residues participate in the interaction with wheat germ agglutinin (142, 149), however, the specificity for oligosaccharides remains uncertain. Recently, analogues of the terminal sugar



portion of asparagine-linked glycopeptides (i.e., trisaccharides containing sialic acid, galactose, and glucose or N-acetylglucosamine) were prepared and their affinities for wheat germ agglutinin measured (149). The affinities reported for the interaction of wheat germ agglutinin with these sialyl- and galactosyl-containing analogues are much weaker than those for lectin binding to cells (151,157). This behaviour is explained by the ability of wheat germ agglutinin to interact not only with sialic acid-containing saccharide groups via primary sialic acid binding sites (148) but with other saccharide groups through the use of secondary N-acetylglucosamine binding sites on the lectin (148).

Current interest in determining the mode of interaction of wheat germ agglutinin with specific carbohydrates such as sialic acid on membrane-bound glycoproteins led Lee and Grant (104) and Feix et al. (91) to study these interactions with nitroxide spin labels. With these spin labels they were able to monitor the mobility of the carbohydrates during lectin binding. Both studies demonstrate the importance of sialic acid. Spin labeling provides an elegant tool for the investigation of the relationship between cell-surface binding events to membrane structural-functional interactions. With our reagent NAPBAH

we were unable to provide supportive information on the wheat germ agglutinin binding events with sialic acid residues as others have done (91,104).

The availability of galactose binding lectins allowed further investigation of the effectiveness of NAPBAH in photocrosslinking of cell surface glycoconjugates. Table 4 illustrates the extent of reagent incorporation into galactose oxidase-generated aldehydic residues on cell surface glycoconjugates. The retention of agglutinability of the reagent-derivatized membranes in the presence of either of the following lectins encouraged us to attempt photocrosslinking. After agglutination of these galactosyl-derivatized membranes with jequirty bean lectin, RCA₆₀, RCA₁₂₀ or wheat germ agglutinin the mixtures were photolyzed at 350 nm for 6 minutes. The suspensions were then incubated with 200 mM galactose or N-acetylglucosamine in phosphate wash buffer for 1 hour at room temperature to remove any lectin present on the cell surface (157,158) not involved in photocrosslinking. The lectin conjugated-membrane systems were then washed with the same sugar solution and twice further in excess phosphate was buffer. The hydrazone bond was permanently reduced to the more stable secondary amine with borohydride (96). Samples were then solubilized and prepared for SDS-PAGE following the Laemmli procedure (195). The slab gels were

then stained for protein with Coomassie blue or for glycoproteins employing a silver stain procedure (197). The Coomassie blue stained gels revealed the presence of high and low molecular weight aggregates with an apparent diminution of band 3 protein suggesting remnants of photocrosslinking. Compared to a control consisting of photolyzed, derivatized membranes no aggregates in the 120,000-140,000 dalton or 50,000 dalton region of the gel were observed. Figures 40 and 41, silver and Coomassie blue stained gels, respectively, illustrate typical protein profiles of reagent-derivatized membranes which have undergone photocrosslinking with lectins. The negative image portrayed in Figure 40 reveals the presence of proteins and glycoproteins as clear portions on the gel with a dark background. This observation is contrary to the results of the originators of the method (197), however, others have obtained this negative image on silver-stained electrophoretograms (215). Lane 7 in Figure 40 and lanes 1 and 9 in Figure 41 show the profile of a mixture of standard proteins with myosin being the largest polypeptide with a molecular weight of 205,000 daltons and carbonic anhydrase being the smallest polypeptide with a molecular weight of 29,000 daltons. Using this as a measure of molecular weight a plot of log (molecular weight) versus mobility (R_f) was established from densitometric data taken from Figure 41. From this curve R_f values for these high and

Figure 40

Protein and Glycoprotein Stained Gel.
Via the Silver Stain

Legend

Gel was stained for proteins and glycoproteins according to the procedure of Dubray and Bezar (197) employing the silver stain technique.

To lanes 1 and 2 was added 7.5 μ g of ovalbumin and 7.5 μ g of fetuin, respectively. To lanes 3, 4, 5 and 6 was added 40 μ g of the proceeding photolyzed lectin-membrane systems, i.e., RCA₆₀⁻, RCA₁₂₀⁻, jequirty bean lectin- and wheat germ agglutinin-membrane system, respectively, solubilized in the Fairbanks et al. (19) sample buffer. To lane 7 was added 20 μ g of the standard protein mixture (containing myosin, β -galactosidase, phosphorylase b, bovine albumin, ovalbumin and carbonic anhydrase with molecular weights of 205,000, 116,000, 97,400, 66,000, 45,000 and 29,000 daltons, respectively) solubilized in the Fairbanks et al. (19) sample buffer. Lane 8 contained a similar mixture of proteins solubilized in the Laemmli (195) sample buffer. To lane 9 was added 40 μ g of standard erythrocyte membrane proteins solubilized in the Fairbanks et al. (19) sample buffer.

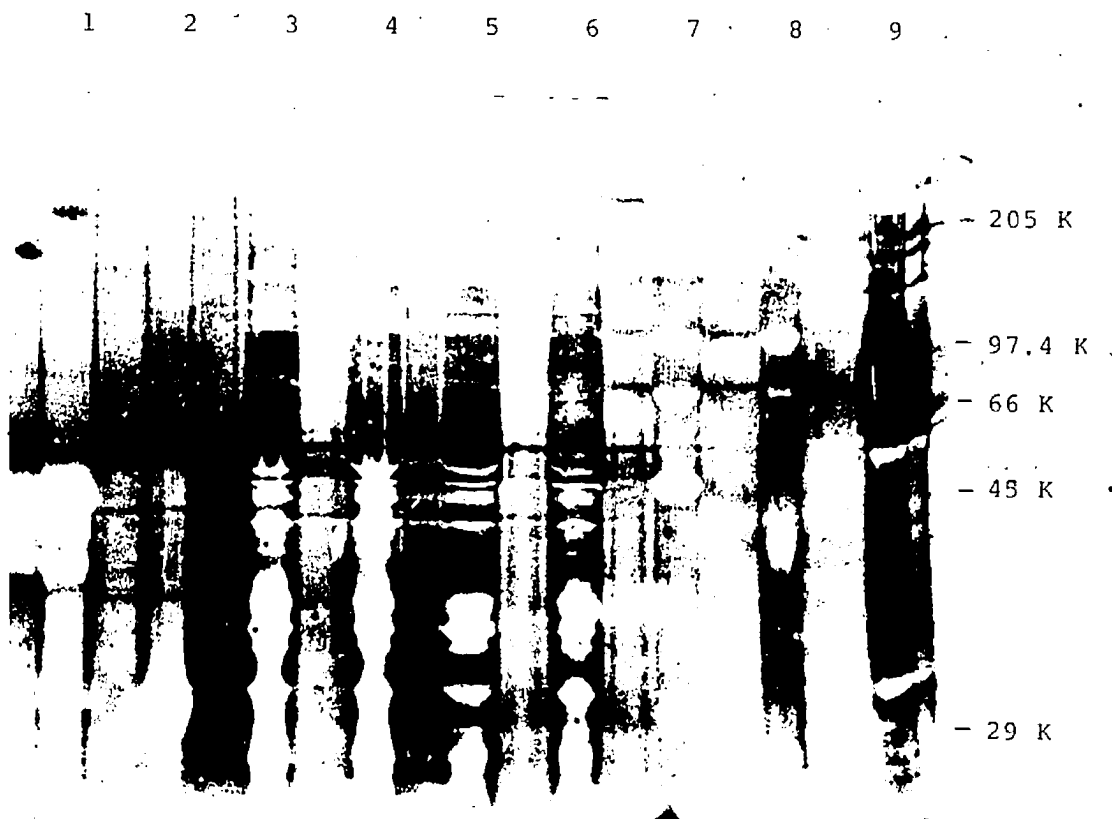


Figure 40

Figure 41

Proteins Stained Via Coomassie Blue

Legend

Gel was stained for proteins with Coomassie blue according to the procedure of Fairbanks *et al.* (19).

To lanes 1 and 9 was added 20 μg and 40 μg of the standard protein mixture (described in Figure 40 and solubilized in the Fairbanks *et al.* (19) sample buffer), respectively. To lanes 2 and 10 was added 40 μg and 5 μg of standard erythrocyte membrane proteins, respectively. The apparent molecular weights for the various bands of membrane proteins are: band 1, 245,000 daltons; band 2, 220,000 daltons; band 3, 84,000 daltons; band 4.5, 55,000 daltons; and band 6, 35,000 daltons. To lanes 3 and 4 was added 15 μg of fetuin and 15 μg of ovalbumin, respectively. To lanes 5, 6, 7 and 8 was added 50 μg of the proceeding photolyzed lectin-membrane systems, i.e., wheat germ agglutinin-, jequirty bean lectin-, RCA₆₀- and RCA₁₂₀- membrane system, respectively. All protein mixtures above were solubilized in the Fairbanks *et al.* (19) sample buffer.

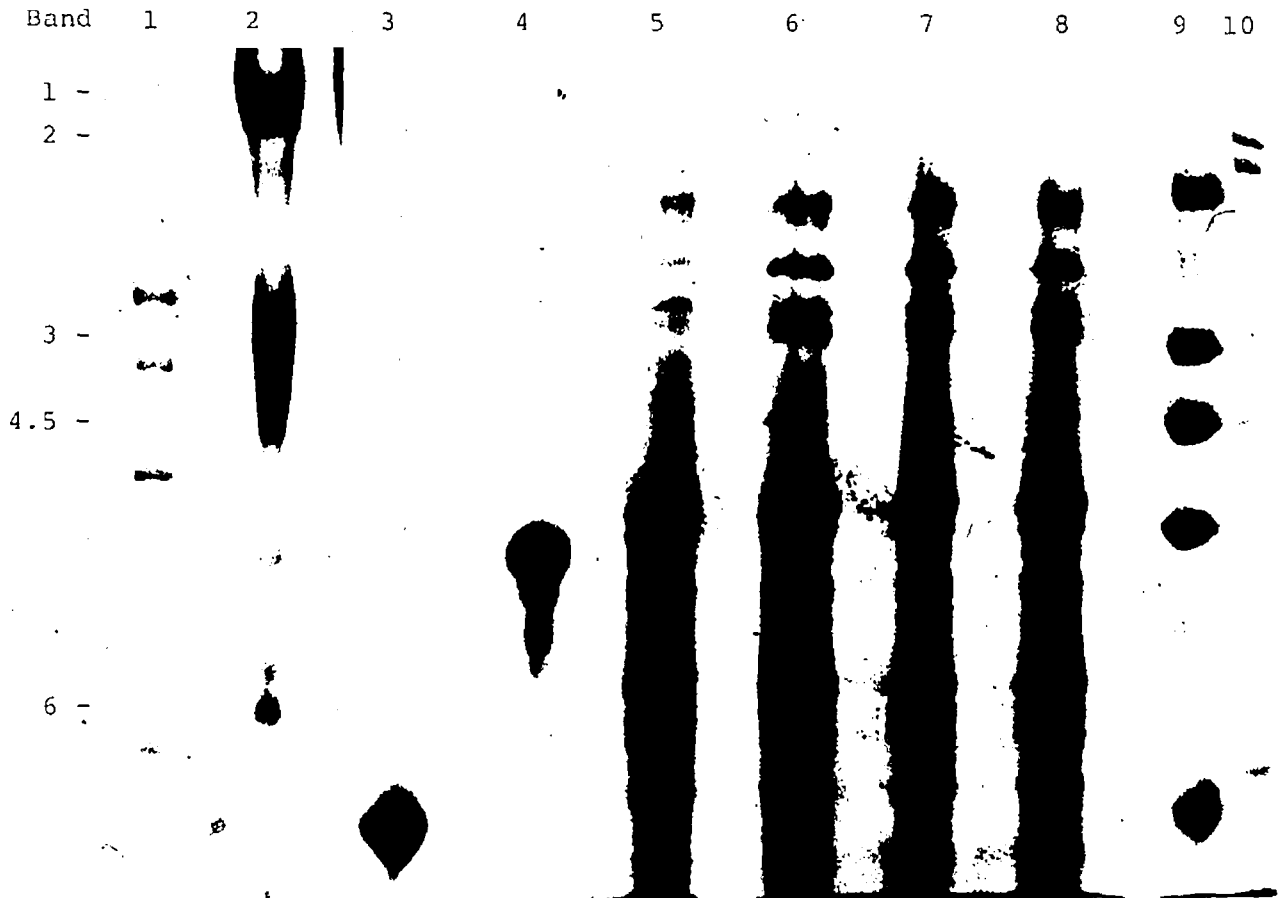


Figure 41

low molecular weight conjugates in lanes 5 to 8 in Figure 41 (lanes 3 to 6 in Figure 40) were used to calculate their apparent molecular weights. The conjugates observed in the jequirty bean lectin (34,000 daltons)-, RCA₆₀ (31,000 daltons)-, RCA₁₂₀ (30,000 daltons)- and wheat germ agglutinin (17,500 daltons)- membrane system represent aggregates of band 3 polypeptides (90,000 daltons), PAS(1)₂ (85,000 daltons) or PAS 1 (42,500 daltons) and the lectins. Figure 42 illustrates the proposed route for photocrosslinking. In principle, conjugates of apparent 124,000, 119,000 and 76,500 daltons for the jequirty bean lectin-membrane system might be expected to form from the available band 3 and glycophorin species as detailed in Table 6. Likewise, 121,000, 116,000 and 73,500 dalton conjugates for the RCA₆₀-membrane system, 120,000 115,000 and 72,500 dalton conjugates for the RCA₁₂₀-membrane system and 108,000, 103,000 and 60,000 dalton conjugates for the wheat germ agglutinin-membrane system might be expected. From the densitometric data obtained from the Coomassie blue stained gel (Figure 41) apparent molecular weights for the various conjugates were determined and are tabulated in Table 6.

To reassure ourselves that the clear images present on the silver stained gel were protein we repeated the electrophoresis and subsequently stained the gel for

Figure 42

Proposed Route of Photoincorporation of
D-Galactosyl-Derivatized Glycoproteins
Into Galactose Binding Lectins

Legend

Glycoproteins modified at galactosyl or N-acetyl-galactosaminyl residues with NAPBAH covalently insert into galactose binding lectins upon photolysis.

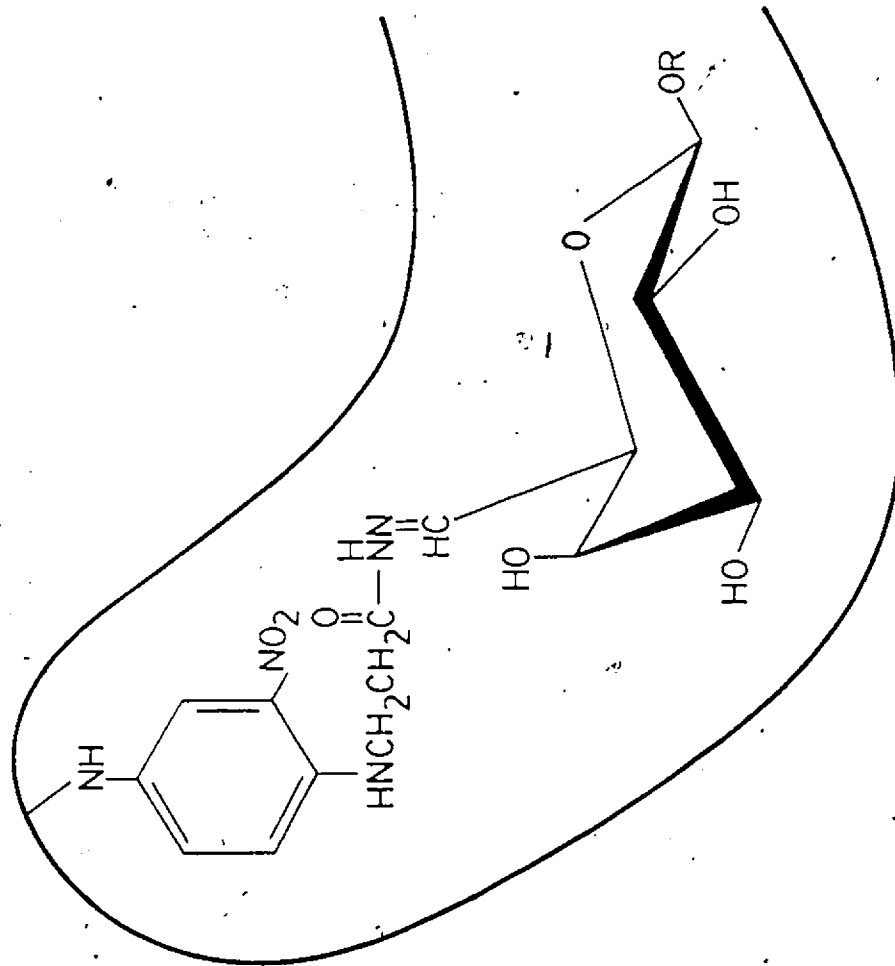


Figure 42

TABLE 6

Theoretical and Observed Apparent Molecular Weights of the Membrane-Lectin Conjugates

| | Jequirry bean lectin | | RCA ₆₀ | | RCA ₁₂₀ | | Wheat germ agglutinin | |
|----------------------|--------------------------|-----------------------|-------------------|----------|--------------------|----------|-----------------------|----------|
| | Theoretical ^a | Observed ^b | Theoretical | Observed | Theoretical | Observed | Theoretical | Observed |
| Band 3 | 124,000 | 133,000 | 121,000 | 136,000 | 120,000 | 130,000 | 108,000 | 120,000 |
| PAS (1) ₂ | 119,000 | 112,000 | 116,000 | 115,000 | 115,000 | 109,000 | 103,000 | 94,000 |
| PAS 1 | 76,500 | 47,000 | 73,500 | 48,000 | 72,500 | 46,000 | 60,000 | 47,000 |

^aThe theoretical molecular weights of the potential conjugates formed upon photolysis were calculated by taking the sum of the molecular weights of band 3 (90,000 daltons), PAS (1)₂ (85,000 daltons) or PAS 1 (42,500 daltons) and jequirry bean lectin (34,000 daltons), RCA₆₀ (31,000 daltons), RCA₁₂₀ (30,000 daltons) or wheat germ agglutinin (17,500 daltons).

^bThe observed apparent molecular weights were determined by translating the R_f values taken from the plot of log (molecular weight) versus mobility (R_f) with the equation of the line $\log (\text{molecular weight}) = (-1.76)(R_f) + (5.52)$ obtained from lane 7 in Figure 41.

protein according to the method of Merrill *et al.* again employing silver (216). Indeed, a positive gel was observed. The positions of proteins and glycoproteins were represented by dark bands, however, the background of the gel was densely stained with silver deposits making photographic reproduction difficult.

We further showed that the high and low molecular weight conjugates observed in Figures 40 and 41 contain carbohydrate such as sialic acid. By exploiting the properties of the fluorescent probe dansyl hydrazine (94,217,218) we were able to label glycoproteins present in the glycoconjugates (218) shown in Figure 43. Fluorescence is observed in the 70,000 dalton region of the gel consisting of the RCA_{60}^- , RCA_{120}^- , jequirty bean lectin - or wheat germ agglutinin-PAS 1 conjugate shown in lanes 5 to 8. High molecular weight conjugates comprising of the above lectins and band 3 or $PAS(1)_2$ were also observed, however, limitations of photographic reproduction of fluorescently labeled gels under ultraviolet light made it difficult to photograph.

The availability of fluorescein isothiocyanate (FITC) labeled lectins such as FITC- RCA_{60} , FITC- RCA_{120} and FITC-wheat germ agglutinin encouraged us to use these lectins in the photoincorporation experiments as it

Figure 43

Sialoglycoproteins Stained Via Dansyl Hydrazine

Legend

Gel was stained for sialoglycoproteins employing dansyl hydrazine according to the method of Eckhardt et al. (218) with slight modifications.

The gel was soaked in a solution of 25% 2-propanol and 10% acetic acid for 12 hours at room temperature then soaked in 10% acetic acid for 30 minutes and incubated in 9.0 mM periodic acid for 1 hour at 4°C in the dark (197). The gel was rinsed with distilled water and treated with 25 mM sodium metabisulfite in 5% acetic acid for 1 hour then in sodium phosphate buffer (1M, pH 7.4) for 1.5 hours with several changes of buffer. Next, the gel was soaked in a 2.0 mM dansyl hydrazine ethanolic solution (265 mg dansyl hydrazine dissolved in 10 ml absolute ethanol diluted to 500 ml with water) for 3 hours at room temperature then placed in a sodium phosphate solution (1M, pH 7.4). The gel was removed and placed on a glass plate on a long-wave (366 nm peak output) ultraviolet lamp (Chromato-vue Transilluminator, Ultraviolet Products, Inc., San Gabriel, CA). Photographs were taken with a Polaroid MP-4 Land camera. Polaroid type 665 (ASA 75) film was used with an exposure time of 5 seconds at f8.0.

Lanes 1 through 8 contain similar protein samples to those described in Figure 41.

1 2 3 4 5 6 7 8

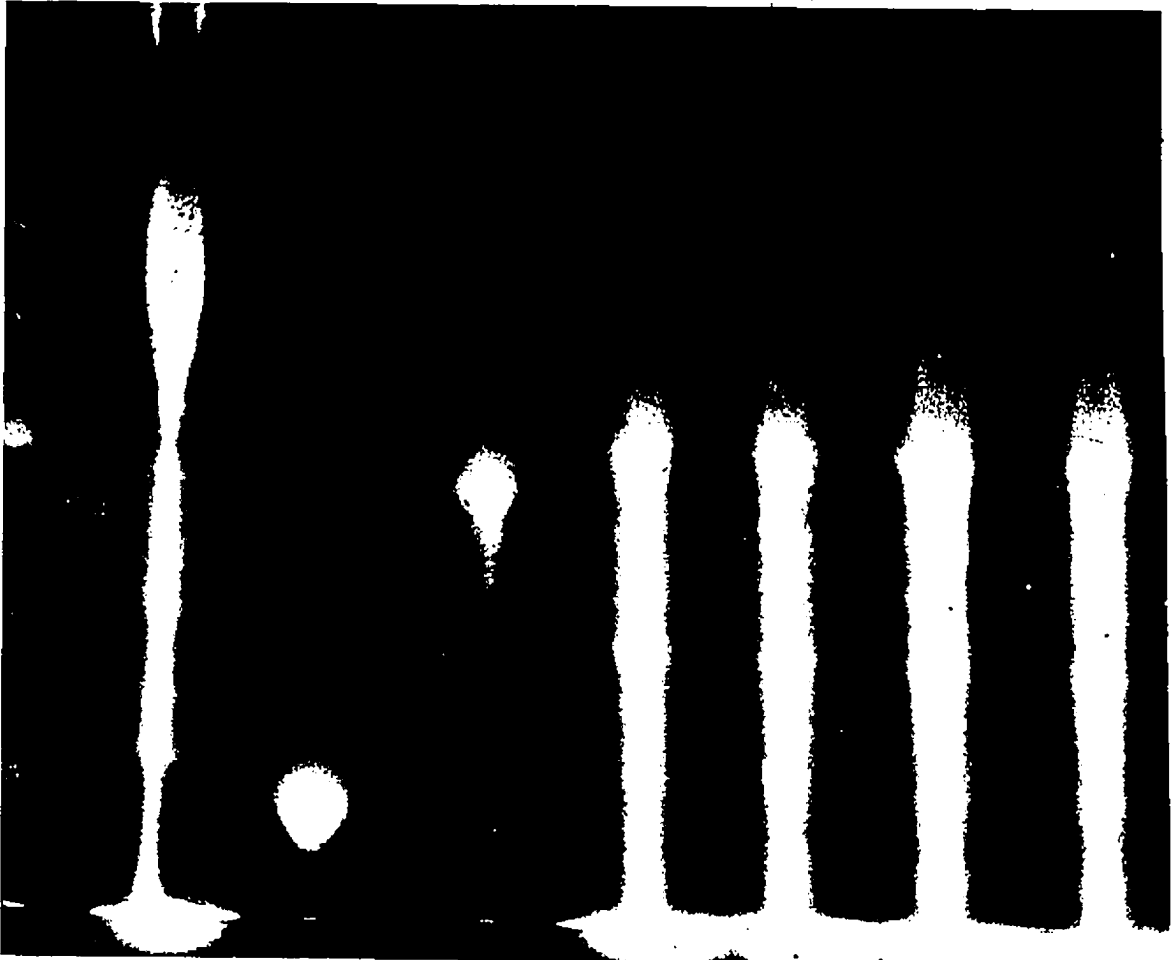


Figure 43

appeared to be an advantageous tool. However, a gel containing electrophoresed samples of photolyzed lectin-membrane systems showed no fluorescence. Samples of FITC-RCA₆₀, FITC-RCA₁₂₀ and FITC-wheat germ agglutinin each containing approximately 15 µg of protein did fluoresce. A similar gel stained for protein with Coomassie blue revealed conjugates in the 120,000-140,000 dalton and 70,000 dalton regions of the gel. Reasons for the absence of fluorescence are two-fold; the degree of FITC sensitivity and the fluorescence photobleaching effect. Firstly, the detectable limit of fluorescein isothiocyanate may have contributed to the problem. As indicated by the intensities of native FITC-labeled lectins on polyacrylamide gels (intensities were not overwhelming) a large amount of lectin (i.e., >2 µg) would have to be present in the band 3-, PAS(1)₂- or PAS 1-lectin conjugates for detection. The fluorescence photobleaching effect seems to be a more likely reason for the absence of fluorescence. Fluorophores in the presence of high energy radiation such as a laser beam or ultraviolet light undergo electronic rearrangement with subsequent loss in fluorescence. Others have used the fluorescence photobleaching recovery technique for studying the mobility of FITC-labeled erythrocyte membrane proteins (219,220) within a lipid bilayer system. By

monitoring fluorescence disappearance in a section of the lipid bilayer caused by laser radiation (i.e., photobleaching) then reappearance of fluorescence to this area in the absence of laser radiation they concluded that lateral movement of FITC-labeled proteins occurs.

The differences in the theoretical and observed apparent molecular weights for the band 3- and PAS(1)₂-lectin conjugates summarized in Table 6 are not significant (i.e., less than 11%), considering the uncertainty in estimating molecular weight from a single gel (19,20,23,24). However, the theoretical molecular weights for the PAS 1-lectin conjugates are considerably larger than the observed apparent molecular weights. This may be due to the unknown migratory ability of the perturbed sialoglycoprotein monomer on SDS-polyacrylamide gels. However, given the magnitude of the discrepancy, it is unlikely that PAS 1-lectin conjugates arise from photocrosslinking. The conjugates of approximately 47,000 dalton apparent molecular weight could be the result of conjugate formation between lectin and reagent-derivatized glycolipids.

CHAPTER IV

CONCLUSIONS

The colorimetric method employing peroxidase presented here has some limitation in its applicability but it is attractive in enzyme-coupled systems which function below pH 4.0 or which can be carried out stepwise without significant loss in hydrogen peroxide. For example, we have shown that the glucose oxidase-peroxidase and the choline oxidase-peroxidase systems function well in generating the chromophore. It is likely that any other enzymes which liberate glucose such as trehalase (119), sucrase (221) and maltase (222) and in addition any other oxidases which tolerate the conditions of the standard procedure such as xanthine oxidase (223) and cholesterol oxidase (224) could be used to advantage with this system.

The colorimetric procedure for the determination of membrane-bound sialic acid residues is simpler to perform than the existing procedures (69,77) without any sacrifice in sensitivity and it has been shown to be quantitative for preparative-scale unsealed erythrocyte ghost suspensions of 20% packed cell volume. For whole cell preparations, however,

quantitative estimation of sialyl residues could only be realized at packed cell volumes of 2% or less due to the rapid uptake of the analyte at higher cell densities.

The new heterobifunctional photolabile crosslinking reagent N-(2-nitro-4-azidophenyl)- β -alanine hydrazide shows much promise as a potential modifier of cell surface glycoproteins via hydrazone bond formation. Furthermore, it can be useful for direct quantification of incorporation due to the absorbance at 465 nm. The extent of N-(2-nitro-4-azidophenyl)- β -alanine hydrazide incorporation was determined to be 77 nmoles sialyl aldehyde per mg membrane protein. The number of galactose oxidase substrate sites (i.e., galactose and N-acetylgalactosamine) derivatized was determined to be 64 nmoles and 90 nmoles per mg membrane protein with no prior neuraminidase treatment and with prior neuraminidase treatment, respectively. The photosensitive azido group allowed us to incorporate reagent-derivatized glycoproteins into carbohydrate-binding glycoproteins wheat germ agglutinin, jequirty bean lectin and castor bean lectins RCA₆₀ and RCA₁₂₀ through covalent attachment.

The availability of the radioactive species of N-(2-nitro-4-azidophenyl)- β -alanine hydrazide containing a carbon-14 label in the amide group or a tritium label in the methylene groups adjacent to the ring amino group could allow identifi-

cation of the amino acids present in the binding site of the lectins upon amino acid sequence analysis of the conjugates. As the importance and function of cell surface glycoproteins as membrane surface recognition sites or receptors is not completely understood the model system presented could be used to advantage for further elucidation of these events.

APPENDIX

Linear Regression Analysis

The linear regression analysis of data points by the least squares method was used. The equation of the line $y = mx + b$ was characterized by the regression constants m , the slope, and b , the y -intercept. Usually, x and y were the concentration and corresponding absorbance, respectively.

$$m = \frac{(\sum x \sum y - N \sum xy)}{((\sum x)^2 - N \sum x^2)}$$

$$b = \frac{(\sum x \sum xy - \sum x^2 \sum y)}{((\sum x)^2 - N \sum x^2)}$$

The coefficient of variation (r^2) was taken to be indicative of how closely the equation fits the experimental data.

$$r^2 = \frac{[\sum xy - \frac{\sum x \sum y}{n}]^2}{[\sum x^2 - \frac{(\sum x)^2}{n}] [\sum y^2 - \frac{(\sum y)^2}{n}]}$$

Determination of Percent Error in Intercepts and Slopes

The following equations (225) were used in calculating the percent error or uncertainties in slope σ_m and intercept σ_b , which are root mean square deviations:

$$\sigma_m = \left[\frac{N}{N\sum x^2 - (\sum x)^2} \right]^{1/2} \sigma_y$$

$$\sigma_b = \left[\frac{\sum x}{N\sum x^2 - (\sum x)^2} \right]^{1/2} \sigma_y$$

where $\sigma_y = \left(\frac{S}{N-1} \right)^{1/2}$, S is equal to $\sum (y_i - \bar{y}_i)^2$, and \bar{y}_i is the best y for given x, $i=1 \text{ --- } N$.

REFERENCES

1. Singer, S. J., and Nicolson, G. L., Science, 175, 720-731 (1972).
2. Danielli, J. F., and Dayson, H., J. Cell. Comp. Physiol., 5, 495-508 (1935).
3. Clark, J. M., and Switzer, R. L., In 'Experimental Biochemistry,' p. 185, W. H. Freeman and Company, San Francisco (1977).
4. Robertson, J. D., Protoplasma, 63, 218-245 (1967).
5. Green, D. E., and Capaldi, R. A., FEBS Lett., 25, 205-209 (1972).
6. Capaldi, R. A., Scientific American, 230, 26-33 (1974).
7. Guidotti, G., Annu. Rev. Biochem., 41, 731-752 (1972).
8. Juliano, R. L., Biochim. Biophys. Acta, 300, 341-378 (1973).
9. Marchesi, V. T., Furthmayr, H., and Tomita, M., Annu. Rev. Biochem., 45, 667-698 (1976).
10. Colley, C. M., Zwaal, R.F.A., Roelofsen, B., and Van Deenen, L.L.M., Biochem. Biophys. Acta, 307, 74-82 (1973).
11. Zwaal, R.F.A., Roelofsen, B., and Colley, C. M., Biochim. Biophys. Acta, 300, 159-182 (1973).
12. Gordesky, S. E., Marinetti, G. V., and Love, R., J. Membr. Biol., 20, 111-132 (1975).
13. Bretscher, M.S., Nature (New Biol.), 236, 11-12 (1972).
14. Marinetti, G. V., and Love, R., Biochem. Biophys. Res. Commun., 61, 30-37 (1974).
15. Nes, W. R., Lipids, 9, 596-612 (1974).
16. Mulder, E., Lamers-Stahlhofen, G.J.M., and van der Molen, H. J., Biochim. Biophys. Acta, 260, 290-297 (1972).
17. Rosenblum, B. B., In 'Erythrocyte Membranes 2: Recent Clinical and Experimental Advances,' Kruckeberg, W., Eaton, J., and Brewer, G., (Editors), pp. 251-265, Alan R. Liss, Inc., New York (1981).

18. Shapiro, A. L., Vinuela, E., and Maizel, J. V., Biochem. Biophys. Res. Commun., 28, 815-820 (1967).
19. Fairbanks, G., Steck, T. L., and Wallach, D.F.H., Biochemistry, 10, 2606-2617 (1971).
20. Neville, D. M., Jr., and Glossmann, H., J. Biol. Chem. 246, 6335-6338 (1971).
21. Gahmberg, C. G., J. Biol. Chem., 251, 510-515 (1976).
22. Mueller, T. J., and Morrison, M., In 'Erythrocyte Membranes 2: Recent Clinical and Experimental Advances', Kruckeberg, W., Eaton, J., and Brewer, G., (Editors), pp. 95-112, Alan R. Liss, Inc., New York (1981).
23. Marchesi, S. L., Steers, E., Marchesi, V. T., and Tillack, T. W., Biochemistry, 9, 50-57 (1970).
24. Clarke, M., Biochem. Biophys. Res. Commun., 45, 1063-1070 (1971).
25. Cabantchik, Z. I., and Rothstein, A., J. Membr. Biol., 15, 207-226 (1974).
26. Tanner, M.J.A., Jenkins, R. E., Anstee, D. J., and Clamp, J. R., Biochem. J., 155, 701-703 (1976).
27. Mueller, T. J., Li, Y-T., and Morrison, M., J. Biol. Chem., 254, 8103-8105 (1979).
28. Tomita, T. J., and Marchesi, V. T., Proc. Natl. Acad. Sci. U.S.A., 72, 2964-2968 (1975).
29. Winzler, R. J., In 'Red Cell Membrane: Structure and Function', Jamieson, G. A., and Greenwalt, T. J., (Editors), p. 57, S. P. Lippincott, Philadelphia (1969).
30. Marchesi, V. T., Tillack, T. W., Jackson, R. L., Segrest, J. P., and Scott, R. E., Proc. Natl. Acad. Sci. U.S.A. 69, 1445-1449 (1972).
31. Harrel, D., and Morrison, M., Arch. Biochem. Biophys., 193, 158-168 (1979).
32. Gahmberg, C. G., and Andersson, L. C., J. Biol. Chem., 252, 5888-5894 (1977).
33. Furthmayr, H., Nature, 271, 519-524 (1978).

34. Furthmayr, H., J. Supramol. Struct., 9, 79-95 (1978).
35. Mueller, T. J., Dow, A. W., and Morrison, M., Biochem. Biophys. Res. Commun., 72, 94-99 (1976).
36. Owens, J. W., Mueller, T. J., and Morrison, M., Arch. Biochem. Biophys., 204, 247-254 (1980).
37. Jackson, R. L., Segrest, J. P., Kahane, I., and Marchesi, V. T., Biochemistry, 12, 3131-3138 (1973).
38. Tanner, M. J., Anstee, D. J., and Mawby, M. J., Biochem. J., 187, 493-500 (1980).
39. Furthmayr, H., Metaxas, M., and Metaxas-Buhla, M., Proc. Natl. Acad. Sci. U.S.A., 78, 631-635 (1981).
40. Blumenfeld, O. O., Gallop, P. M., and Liao, T. J., Biochem. Biophys. Res. Commun., 48, 242-251 (1972).
41. Landsteiner, K., and Levine, P., J. Exp. Med. 47, 757-775 (1928).
42. Wasniowska, K., Dizenick, Z., and Lisowska, E., Biochem. Biophys. Res. Commun., 76, 385-390 (1977).
43. Thomas, D. B., and Winzler, R. J., J. Biol. Chem., 244, 5943-5946 (1969).
44. Javaid, I. J., and Winzler, R. J., Biochemistry, 13, 3635-3638 (1974).
45. Javaid, I. J., and Winzler, R. J., Biochemistry, 13, 3639-3642 (1974).
46. Thomas, D. B., and Winzler, R. J., Biochem. J., 124, 55-59 (1971).
47. Bretscher, M. S., J. Mol. Biol., 98, 831-833 (1975).
48. Cotmore, S. F., Furthmayr, H., and Marchesi, V. T., J. Mol. Biol., 113, 539-553 (1977).
49. Nicolson, G. L., and Painter, R. G., J. Cell Biol., 59, 395-406 (1973).
50. Kornfeld, R., and Kornfeld, S., Annu. Rev. Biochem., 45, 217-237 (1976).

51. Lisowska, E., Duk, M., and Dahr, W., Carbohydr. Res., 79, 103-113 (1980).
52. Anstee, D. J., Mawby, W. J., Parsons, S. F., Tanner, M. J. A., and Giles, C. M., J. Immunogenet., 9, 51-55 (1982).
53. Gahmberg, C. G., Myllyla, G., Leikola, J., Pirkola, A., and Nordling, S., J. Biol. Chem., 251, 6108-6116 (1976).
54. Dahr, W., Uhlenbruck, G., Leikola, J., Pirkola, A., and Landfried, K., J. Immunogenet. 3, 329-346 (1976).
55. Tanner, M.J.A., and Anstee, D. J., Biochem. J., 153, 271-277 (1976).
56. Langley, J. W., Issitt, P. D., Anstee, D. J., McMahon, M., Smith, N., Pavone, B. G., Tessel, J. A., and Carlin, M. A., Transfusion, 21, 15-24 (1981).
57. Jansson, S-E., Gripenberg, J., Hekali, R., and Gahmberg, C. G., Biochem. J., 195, 123-128 (1981).
58. Jokinen, M., and Gahmberg, C. G., Biochim. Biophys. Acta, 554, 114-124 (1979).
59. Van Meer, G., Gahmberg, C. G., Op den Kamp, J.A.F., and Van Deenen, L.L.M., FEBS Lett., 135, 53-55 (1981).
60. Gattegno, L., Perret, G., Fabia, F., and Cornillot, P., Mech. Ageing Develop., 16, 205-219 (1981).
61. Bocci, V., Brit. J. Haematol., 48, 515-522 (1981).
62. Kuster, J. M., and Schauer, R., Hoppe Seyler's Z. Physiol. Chem., 362, 1507-1514 (1981).
63. Aminoff, D., Ghalambor, M. A., and Henrich, C. J., In 'Erythrocyte Membranes 2: Recent Clinical and Experimental Advances', Kruckeberg, W., Eaton, J., and Brewer, G., (Editors), pp. 269-278, Alan R. Liss, Inc., New York (1981).
64. Schauer, R., Meth. Enzymol., 50, 64-89 (1978).
65. Buscher, H. P., Casals-Stenzel, J., and Schauer, R., Eur. J. Biochem., 50, 71-82 (1974).

66. Atkinson, P. H., and Hakimi, J., In 'The Biochemistry of Glycoproteins and Proteoglycans', Lennarz, W. J., (editor), pp. 191-228, Plenum Press, New York (1980).
67. Buscher, H. P., Casals-Stenzel, J., Schauer, R., and Mestres-Ventura, P., Eur. J. Biochem., 77, 297-310 (1977).
68. Corfield, A. P., Ferreira do Amaral, C., Wember, M., and Schauer, R., Eur. J. Biochem., 68, 597-610 (1976).
69. Warren, L., J. Biol. Chem., 234, 1971-1975 (1959).
70. Aminoff, D., Biochem. J., 81, 384-392 (1961).
71. Horgan, I. E., Clin. Chim. Acta, 116, 409-415 (1981).
72. Hammond, K. S., and Papermaster, D. S., Anal. Biochem., 74, 292-297 (1976).
73. Sugahara, K., Sugimoto, K., Nomura, O., and Usui, T., Clin. Chim. Acta, 108, 493-498 (1980).
74. Shukla, A. K., and Schauer, R., Hoppe Seyler's Z. Physiol. Chem., 363, 255-262 (1982).
75. Belman, S., Anal. Chim. Acta, 29, 120-126 (1963).
76. Nash, T., Biochem. J., 55, 416-421 (1953).
77. Massimitti, Y., Durand, G., Richard, A., Feger, J., and Agneray, J., Anal. Biochem., 97, 346-351 (1979).
78. Capaldi, D. J., and Taylor, K. E., Anal. Biochem., 129, 329-336 (1983).
79. Mawby, W. J., Anstee, D. J., and Tanner, M.J.A., Nature, 291, 161-162 (1981).
80. Feix, J. B., and Butterfield, D. A., FEBS Lett., 115, 185-188 (1980).
81. Prohaska, R., Koerner, T.A.W., Armitage, I. M., and Furthmayr, H., J. Biol. Chem., 256, 5781-5791 (1981).
82. Wells, E., and Findlay, J.B.C., Biochem. J., 179, 265-272 (1979).

83. Sadler, J. E., Paulson, J. C., and Hill, R. L., J. Biol. Chem., 254, 2112-2-19 (1979).
84. Neufeld, E. F., and Ashwell, G., In 'The Biochemistry of Glycoproteins and Proteoglycans', Lennarz, W. G., (editor), pp. 241-262, Plenum Press, New York (1980).
85. Grefarth, S. P., and Reynolds, J. A., Proc. Natl. Acad. Sci. U.S.A., 71, 3913-3916 (1974).
86. Macdonald, R. I., and Macdonald, R. C., J. Biol. Chem., 250, 9206-9214 (1975).
87. Silverberg, M., Furthmayr, H., and Marchesi, V. T., Biochemistry, 15, 1448-1454 (1976).
88. Lau, A.L.Y., and Cowburn, D., Biophys. Chem. 14, 267-276 (1981).
89. Liao, T. H., Gallop, P. M., and Blumenfeld, O. O., J. Biol. Chem., 248, 8247-8253 (1973).
90. Cruz, T. F., and Gurd, J. W., Anal. Biochem., 108, 139-145 (1980).
91. Feix, J. B., Green, L. L., and Butterfield, D. A., Life Sciences, 31, 1001-1009 (1982).
92. Taylor, K. E., and Wu, Y-C., Biochem. Intl., 1, 353-358 (1980).
93. Rando, R. R., and Bangerter, F. W., Biochim. Biophys. Acta, 557, 354-362 (1979).
94. Abraham, G., and Low, P. S., Biochim. Biophys. Acta, 597, 285-291 (1980).
95. Rotman, A., Linder, S., and Pribluda, V., FEBS Lett., 120, 85-88 (1980).
96. Jentoft, N., and Dearborn, D. G., J. Biol. Chem., 254, 4359-4365 (1979).
97. Itaya, K., Gahmberg, C. G., and Hakomori, S-I., Biochem. Biophys. Res. Commun., 64, 1028-1035 (1975).
98. Wilchek, M., Spiegel, S., and Spiegel, Y., Biochem. Biophys. Res. Commun., 92, 1215-1222 (1980).

99. Low, P. S., Cramer, W. A., Abraham, G., Bone, R., and Ferguson-Segall, M., Arch. Biochem. Biophys., 214, 675-680 (1982).
100. Wynne, D., Wilchek, M., and Novogrodsky, A., Biochem. Biophys. Res. Commun., 68, 730-739 (1976).
101. Ravid, A., Novogrodsky, A., and Wilchek, M., Eur. J. Immunol., 8, 289-294 (1976).
102. Roffman, E., Spiegel, Y., and Wilchek, M., Biochem. Biophys. Res. Commun., 97, 1192-1198 (1980).
103. Heitzmann, H., and Richards, F. M., Proc. Natl. Acad. Sci. U.S.A., 71, 3537-3541 (1974).
104. Lee, P. M., and Grant, C.W.M., Biochem. Biophys. Res. Commun., 90, 856-863 (1979).
105. Lee, P. M., and Grant, C.W.M., Can. J. Biochem., 58, 1197-1205 (1979).
106. Lee, P. M., and Grant, C.W.M., Biochem. Biophys. Res. Commun., 95, 1299-1305 (1980).
107. Orr, G. A., and Rando, R. R., Nature, 272, 722-725 (1978).
108. Rando, R. R., Orr, G. A., and Bangerter, F. W., J. Biol. Chem., 254, 8318-8323 (1979).
109. Sempere, J. M., Gancedo, C., and Asensio, C., Anal. Biochem., 12, 509-515 (1965).
110. Steck, T. L., and Dawson, G., J. Biol. Chem., 240, 2135-2142 (1974).
111. Gahmberg, C. G., and Hakomori, S., Biochem. Biophys. Res. Commun., 59, 283-291 (1974).
112. Roth, H., Segal, S., and Bertoli, D., Anal. Biochem., 10, 32-52 (1965).
113. Roberts, G. P., and Gupta, S. K., Nature, 207, 425-426 (1965).
114. Gahmberg, C. G., and Hakomori, S., J. Biol. Chem., 248, 4311-4317 (1973).

115. Ito, Y., Tonogai, Y., Suzuki, H., Ogawa, S., Yokoyama, T., Santo, H., Tanka, K-I., Nishigaki, K., and Iwaida, M., J. Assoc. Off. Anal. Chem., 64, 1448-1452 (1981).
116. Grillo, F., Izzo, C., Mazzotti, G., and Murader, E., Clin. Chem., 27, 375-379 (1981).
117. Graf, E., and Penniston, J. T., Clin. Chem., 26, 658-660 (1980).
118. Fossati, P., Principe, L., and Berti, G., Clin. Chem., 26, 227-231 (1980).
119. Chan, A. H., and Cotter, D. A., Microbios. Lett., 15, 7-15 (1980).
120. Artiss, J. D., Thibert, R. J., McIntosh, J. M., and Zak, B., Microchem. J., 26, 487-505 (1981).
121. Artiss, J. D., Draisey, T. F., Thibert, R. J., Zak, B., and Taylor, K. E., Microchem. J., 25, 153-158 (1980).
122. Carey, R. N., Feldruegge, D., and Westgard, J. O., Clin. Chem., 5, 595-602 (1972).
123. Gochman, N., and Schmitz, J. M., Clin. Chem., 18, 943-950 (1972).
124. Ngo, T. T., and Lenhoff, H. M., Anal. Biochem., 105, 389-397 (1980).
125. Hughes, R. C., In 'Membrane Glycoproteins: A Review of Structure and Function', Butterworths, London (1976).
126. Albersheim, P., and Anderson-Prouty, A. J., Annu. Rev. Plant Physiol., 26, 31-52 (1975).
127. Rasmussen, H., Lake, W., and Allan, J. E., Biochim. Biophys. Acta, 411, 63-73 (1975).
128. Huestis, W. H., and McConnell, H. M., Biochem. Biophys. Res. Commun., 57, 726-732 (1974).
129. Nelson, M. J., Ferrell, J. E., and Huestis, W. H., Biochim. Biophys. Acta, 588, 136-140 (1979).
130. Rubin, M. S., Swislocki, N. I., and Sonenberg, M., Arch. Biochem. Biophys., 157, 252-259 (1973)

131. Feller, M., Richardson, C., Behnke, M. D., and Gruenstein, E., Biochem. Biophys. Res. Commun., 76, 1027-1035 (1977).
132. Spiegel, S., and Wilchek, M., J. Immunol., 127, 572-575 (1981).
133. Boyd, W. C., and Slapeigh, E., Science, 119, 419 (1954).
134. Goldstein, I. J., and Hayes, C. E., Adv. Carbohydr. Chem. Biochem., 35, 127-340 (1978).
135. Herzberg, V., Boughter, J. M., Carlisle, S., and Hill, D. E., Nature, 286, 279-281 (1980).
136. Ji, T. H., and Nicolson, G. L., Proc. Natl. Acad. Sci. U.S.A., 71, 2212-2216 (1974).
137. Mishkind, M., Raikhel, N. V., Palevitz, B. A., and Keegstra, K., J. Cell. Biol., 92, 753-754 (1982).
138. Barondes, S. H., Annu. Rev. Biochem., 50, 207-231 (1981).
139. Wilson, I. A., Skehl, J. J., and Wiley, D. C., Nature, 289, 366-373 (1981).
140. Sequeira, L., Annu. Rev. Physiol., 16, 453-481 (1978).
141. Schmidt, E. L., Annu. Rev. Microbiol., 33, 355-376 (1979).
142. Bhavanadan, V. P., and Katlic, A. W., J. Biol. Chem., 254, 4000-4008 (1979).
143. Nicolson, G. L., Blaustein, J., and Etzler, M. E., Biochemistry, 13, 196-294 (1974).
144. Poretz, R. D., and Goldstein, I. J., Carbohydr. Res., 4, 471-477 (1967).
145. Ebisu, S., Shankarlyer, P. N., and Goldstein, I. J., Carbohydr. Res., 61, 129-138 (1978).
146. Lis, H., Sela, B-A., Sachs, L., and Sharon, N., Biochim. Biophys. Acta, 211, 582-585 (1970).
147. Janzen, D. H., Juster, H. B., and Liener, I. E., Science, 192, 795-796 (1976).

148. Wright, C. S., J. Mol. Biol., 141, 267-291 (1980).
149. Kromis, K. A., and Carver, J. P., Biochemistry, 21, 3050-3057 (1982).
150. Peters, B. P., Ebisu, S., Goldstein, I. J., and Flasher, M., Biochemistry, 18; 5505-5511 (1979).
151. Monsigny, M., Roche, A. C., Sens, C., Maget-Dana, R., and Delmotte, F., Eur. J. Biochem., 104, 147-153 (1980).
152. Ganguly, P., and Fossett, N. G., Biochem. Biophys. Res. Commun., 89, 1154-1160 (1979).
153. Marchalonis, J. J., and Edelman, G. M., J. Mol. Biol. 32, 453-465 (1968).
154. Bishayee, S., and Dorai, D. T., Biochim. Biophys. Acta. 623, 89-97 (1980).
155. Van der Wall, J., Campbell, P. A., and Abel, C. A., Develop. Comp. Immunol. 5, 679-684 (1981).
156. Miller, R. L., J. Invert. Pathol. 39, 210-214 (1982).
157. Adair, W. L., and Kornfeld, S., J. Biol. Chem., 249, 4696-4704 (1974).
158. Olsnes, S., Saltvedt, F., and Pihl, A., J. Biol. Chem., 249, 803-810 (1974).
159. Irimura, T., Kawaguchi, T., Terao, T., and Osawa, T., Carbohydr. Res., 39, 317-327 (1975).
160. Lotan, R., Skutelsky, E., Danon, D., and Sharon, N., J. Biol. Chem., 250, 8518-8523 (1975).
161. Sharon, N., and Lis, H., Meth. Membr. Biol., 3, 148-200 (1975).
162. Lotan, R., and Nicolson, G. L., Biochim. Biophys. Acta, 559, 329-376 (1979).
163. Rando, R. R., Acc. Chem. Res., 9, 281-288 (1975)
164. Sato, S., and Nakao, M., J. Biochem., 90, 1177-1185 (1981).
165. Wang, K., and Richards, F. M., Isr. J. Chem., 12, 375-389 (1974).

166. Habeeb, A.F.S.A., Biochim. Biophys. Acta, 673, 527-538 (1981).
167. Kitagawa, T., Shimozone, T., Aikawa, T., Yoshida, T., and Nishimura, H., Chem. Pharm. Bull., 29, 1130-1135 (1981).
168. Ji, T. H., Biochim. Biophys. Acta, 559, 39-69 (1979).
169. Mikkelsen, R. B., and Wallach, D.F.H., J. Biol. Chem. 251, 7413-7416 (1976).
170. Dentler, W. L., Pratt, M. M., and Stephens, R. E., J. Cell Biol., 84, 381-403 (1980).
171. Ngo, T. T., Yam, C. F., Lenhoff, H. M., and Ivy, J., J. Biol. Chem., 256, 11313-11318 (1981).
172. Friebel, K., Huth, H., Jany, K. D., and Trommer, W. E., Hoppe Seyler's Z. Physiol. Chem., 362, 421-428 (1981).
173. Bayley, H., and Knowles, J. R., Meth. Enzymol., 46, 69-114 (1977).
174. Chowdhry, V., and Westheimer, F. H., Annu. Rev. Biochem., 48, 293-325 (1977).
175. Jori, G., and Spikes, J. D., Photochem. Photobiol. Rev., 3, 193-275 (1978).
176. Chong, P.C.S., and Hodges, R. S., J. Biol. Chem. 256, 5064-5070 (1981).
177. DeTraglia, M. C., Brand, J. S., and Tometsko, A. M., Ann. New York Acad. Sci., 19, 59-77 (1980).
178. Staros, J. V., Trends Biochem. Sci., 5, 320-322 (1980).
179. Lwowski, W., In 'Nitrenes', Wiley Interscience, New York (1970).
180. Lwowski, W., Ann. New York Acad. Sci., 19, 491-500 (1980).
181. Turro, N. J., Ann. New York Acad. Sci., 19, 1-17 (1980).
182. Brunner, J., Trends Biochem. Sci., 6, 44-46 (1981).
183. Nielsen, P. E., and Burchard, O., Photochem. Photobiol. 35, 317-323 (1982).

184. Capaldi, D. J., and Taylor, K. E., Microchem. J., in press (1983).
185. Kolthoff, I. M., Sandell, E. B., Meehan, E. J., and Bruckenstein, S., In 'Quantitative Chemical Analysis', 4th edition, p. 854, MacMillan Company, New York (1969).
186. Frisell, W. R., and Mackenzie, C. G., In 'Methods of Biochemical Analysis', Vol. 6, Glick, D., (Editor), pp. 63-57, Interscience, New York (1958).
187. Peterson, G. L., Anal. Biochem., 83, 346-356 (1977).
188. Hünig, S., Angew. Chem. Int. Ed. Engl., 1, 640-646 (1962).
189. Haver, V. M., and Gear, A.R.L., J. Lab. Clin. Med., 97, 187-204 (1981).
190. Bell, W. C., Levy, G. N., Williams, R., and Aminoff, D., Proc. Natl. Acad. Sci. U.S.A., 74, 4205-4209 (1977).
191. Gold, E., Vox Sang., 15, 222-231 (1968).
192. Fleet, G.W.G., Knowles, J. R., and Porter, R. R., Biochem. J., 128, 499-508 (1972).
193. Jeng, S. J., and Guillory, R. J., J. Supramol. Struct., 3, 448-468 (1975).
194. Hosang, H., Vasella, A., and Semenza, G., Biochemistry, 20, 5844-5854 (1981).
195. Laemmli, U. K., Nature, 277, 680-685 (1970).
196. Oakley, B. R., Kirsch, D. R., and Morris, N. R., Anal. Biochem., 105, 361-363 (1980).
197. Dubray, G., and Bezard, G., Anal. Biochem., 119, 325-329 (1982).
198. Sawicki, E., Hauser, T. R., Stanley, T. W., and Elbert, W., Anal. Chem., 33, 93-96 (1961).
199. Paz, M. A. Blumenfeld, O. O., Rojkind, M., Henson, E., Furfine, C., and Gallop, P. M., Arch. Biochem. Biophys., 109, 548-559 (1965).

200. Hauser, T. R., and Cummins, R. L., Anal. Chem., 36, 679-681 (1964).
201. Hünig, S., and Fritsch, K. H., Justus Liebigs Ann. Chem. 609, 172-180 (1957).
202. Sawicki, E., Schumacher, R., and Engel, C. R., Microchem. J., 12, 377-395 (1967).
203. Massimiri, Y., Beljean, M., Durand, G., Feger, J., Pays, M., and Agneray, J., Anal. Biochem., 91, 618-625 (1978).
204. Honda, S., Nishimura, Y., Chilsa, H., and Kakehi, K., Anal. Chim. Acta, 131, 293-296 (1981).
205. Bright, H. J., and Appleby, M., J. Biol. Chem., 244, 3625-3634 (1969).
206. Thompson, R. Q., Patton, C. J., and Crouch, S. R., Clin. Chem., 28, 556-557 (1982).
207. Mills, G. C., J. Biol. Chem., 229, 189-197 (1957).
208. Avigad, G., Amaral, D., Asensio, C., and Horecker, B. L., J. Biol. Chem., 237, 2736-2743 (1962).
209. Steck, T. L., and Yu, J., J. Supramol. Struct., 1, 220-232 (1973).
210. Yu, J., Fischman, D. A., and Steck, T. L., J. Supramol. Struct., 1, 233-248 (1973).
211. Aminoff, D., Bell, W. C., Fulton, I., and Ingebrigtsen, N., Am. J. Hematol., 1, 419-432 (1976).
212. Baenziger, J. U., and Fiete, D., J. Biol. Chem., 257, 4421-4425 (1982).
213. Beppu, M., Terao, T., and Osawa, T., J. Biochem., 78, 1013-1019 (1975).
214. Fraser, A. R., Hemperly, J. J., Wang, J. L., and Edelman, G. M., Proc. Natl. Acad. Sci. U.S.A., 73, 790-794 (1976).
215. Merril, C. R., Dunau, M. L., and Goldman, D., Anal. Biochem., 110, 201-207 (1981).

216. Merril, C. R., Goldman, D., and Van Keuren, M. L., Electrophoresis, 3, 17-23 (1982).
217. Alpenfels, W. F., Anal. Biochem., 114, 153-157 (1981).
218. Eckhardt, A. L., Hayes, C. E., and Goldstein, I. J., Anal. Biochem., 73, 192-197 (1976).
219. Chang, C. H., Takeuchi, H., Ito, T., Machida, K., and Ohnishi, S. I., J. Biochem., 90, 997-1004 (1981).
220. Koppel, D. E., Axelrod, D., Schlessinger, J., Elson, E., and Webb, W. W., Biophys. J., 16, 1055-1069 (1976).
221. Edelman, J., Biochem. J., 57, 22-33 (1954).
222. Palmer, T. N., Biochem. J., 124, 701-724 (1971).
223. Westerfeld, W. W., Richert, D. A., and Higgins, E. S., J. Biol. Chem., 234, 1897-1900 (1959).
224. Allain, C. C., Poon, L. S., Chan, C.S.G., Richmond W., and Fue, P. C., Clin. Chem., 20, 470-475 (1974).
225. Margenau, H., and Murphy, G. M., In "The Mathematics of Physics and Chemistry," pp. 467-516, D. Van Nostrand Co., Inc., New York (1959).

VITA AUCTORIS

- Born : September 4, 1957, Windsor, Ontario, Canada.
- Primary Education : Anderdon Public School, Anderdon, Ontario, Canada, 1962-1971.
- Awards : Anderdon Public School, Grade 4, Scholastic Award, 1962.
Anderdon Public School, Grade 8, Industrial Arts Award, 1971.
- Secondary Education : General Amherst High School, Amherstburg, Ontario, Canada, 1971-1976.
- Awards : General Amherst High School, Year II, III, IV, and V, Honour Roll, 1973-1976.
Ontario Scholar, Year V, 1976.
Valedictorian, Year V, 1976.
- University Education : University of Windsor, Windsor, Ontario, Canada, Honours Bachelor of Science in Biology and Chemistry, 1976-1980.
University of Windsor, Windsor, Ontario, Canada, Doctoral Program, 1980-1983.
- Awards : Society of Chemical Industry Gold Medal, 1980
University of Windsor Postgraduate Scholarship, 1982.
University of Windsor Postgraduate Scholarship, 1983.
- Professional Affiliations : American Association for the Advancement of Science (A.A.A.S.).
American Association for Clinical Chemistry (A.A.C.C.).
American Chemical Society (A.C.S).
Canadian Biochemical Society (C.B.S.).
Chemical Institute of Canada (C.I.C.).
Society of Chemical Industry (S.C.I.).

Publications:

Capaldi, D. J., and Taylor, K. E., A New Peroxidase Color Reaction: Oxidative Coupling of 3-Methyl-2-Benzothiazolinone Hydrazone (MBTH) with its Formaldehyde Azine. Application to Glucose and Choline Oxidases, Analytical Biochemistry, 129, 329-336 (1983).

Capaldi, D. J., and Taylor, K. E., On the Use of 3-Methyl-2-Benzothiazolinone Hydrazone to Determine Cell Surface Sialic Acid: A Simplified Procedure and a Caution, Microchemical Journal, in press (1983).